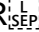


**UNIVERSITY OF NAPLES “FEDERICO II”**

**PhD Program in  
Biology  
XXXII Cycle**



***“Molecular mechanisms underlying epidermal defects  
and inflammation in AEC syndrome”***

SUPERVISOR   
Prof. Missero Caterina

CANDIDATE  
Dr. Stefano Sol

PhD COORDINATOR  
Prof. Salvatore Cozzolino

Academic Year 2019-2020

***“Molecular mechanisms underlying epidermal defects  
and inflammation in AEC syndrome”***

# TABLE OF CONTENTS

<b>LIST OF ABBREVIATIONS</b>	5
<b>LIST OF PUBLICATIONS</b>	7
<b>ABSTRACT</b>	9
<b>1. BACKGROUND</b>	10
1.1 The skin: structure and function	10
1.2 p63, the master regulator of epidermal gene expression	12
1.3 p63-deficient mice	15
1.4 p63-associated disorders	17
1.5 AEC syndrome	20
1.6 AEC mouse model	21
1.7 The role of Thymic stromal lymphopoietin (Tslp) in skin immune function	23
1.8 Signaling pathways involved in Tslp regulation	25
1.9 Regulation of KLKs activity in the epidermis	26
1.10 Protein aggregation of p63 in AEC syndrome	28
1.11 Quality control of unfolded proteins	29
<b>2. AIM OF THE STUDY</b>	33
<b>3. MATERIALS AND METHODS</b>	34
3.1 Generation of conditional p63 <sup>+/<i>Flox</i>L514F</sup> mouse model	34
3.2 Mouse genotyping	34
3.3 RNA isolation and RT-qPCR	35
3.4 Primary keratinocytes and cell cultures	36
3.5 Skin permeability assay	37
3.6 Preparation of CEs	38
3.7 Detection of TEWL	38
3.8 Serum Na and Cl detection assay	38
3.9 RNA-seq analysis	39
3.10 Histology and Immunostaining	39
3.11 Retroviral preparation	40
3.12 Retroviral infection	40
3.13 ELISA	41
3.14 Luciferase reporter assay	41
3.15 BN-PAGE, SDS-PAGE and Western Blot	41

3.16 CHX degradation assay	42
3.17 Differentiation and PRIMA-1-Met treatment of human epidermal keratinocytes	43
<b>4. RESULTS</b>	<b>44</b>
4.1 Epidermal-specific expression of L514F mutation results in severe postnatal epidermal barrier defects	44
4.2 Dysregulated epidermal differentiation markers and defective adhesion molecules in AEC mice	49
4.3 Inflammation in AEC mouse model	55
4.4 KIKs/PAR2/NFAT pathway regulates Tslp expression in AEC syndrome	59
4.5 KLK6 activates TSLP expression through NFAT and NF- $\kappa$ B signaling in human keratinocytes	62
4.6 Generation of AEC conditional mouse model in a Tslp null background	65
4.7 AEC-associated p63 mutants interact with specific molecular chaperones involved in protein disaggregation	67
4.8 p63 aggregation is not reduced by PRIMA-1 <sup>MET</sup>	70
4.9 Doxorubicin and epirubicin rescue mutp63 transactivation function	72
<b>5. DISCUSSION</b>	<b>73</b>
<b>6. REFERENCES</b>	<b>82</b>

## LIST OF ABBREVIATIONS

**AEC syndrome** Ankyloblepharon- Ectodermal defects- Cleft lip/palate syndrome

**WT** Wild Type

**+/-L** K14-Cre; p63<sup>+/-FloxL514F</sup>

**L514F** K14-Cre; p63<sup>FloxL514F/FloxL514F</sup>

**L514F; Tslp eKO** K14-Cre; p63<sup>floxL514F/floxL514F</sup>; Tslp<sup>FloxL2/FloxL2</sup>

**EEC** Ectrodactyly Ectodermal defects Cleft lip/palate syndrome

**LMS** Limb Mammary Syndrome

**ADULT** Acro Demato Ungual Lacrimal Tooth Syndrome

**RHS** Rapp Hodgkin Syndrome

**E17.5** Embryonic day 17.5

**P0** Post-natal day 0

**P3** Post-natal day 3

**P5** Post-natal day 5

**P7** Post-natal day 7

**P8** Post-natal day 8

**P10** Post-natal day 10

**P15** Post-natal day 15

**P50** Post-natal day 50

**AER** Apical Ectodermal Region

**Krt1** Keratin 1

**Krt5** Keratin 5

**Krt6** Keratin 6

**Krt10** Keratin 10

**Krt14** Keratin 14

**Krt15** Keratin 15

**Krt16** Keratin 16

**Krt17** Keratin 17

**Lor** Loricrin

**Ivl** Involucrin

**Flg** Filaggrin

**Dsg1** Desmoglein 1

**Dsc3** Desmocollin 3

**Dsp** Desmoplakin

**DBD** DNA binding domain

**SAM** Sterile- $\alpha$ -Motif  
**PS** Post-SAM domain  
**KCs** Keratinocytes  
**ECs** Epithelial Cells  
**ED** Ectodermal Dysplasia  
**H&E** Haematoxylin and Eosin  
**TEM** Tissue-electron microscopy  
**qRT-PCR** quantitative Real Time-Polymerase Chain Reaction  
**Tslp** Thymic Stromal Lymphopoietin  
**AMPs** Anti Microbial Peptides  
**LC** Langerhans Cells  
**DCs** Dendritic cells  
**DDCs** Dermal Dendritic cells  
**NK** Natural killer cells  
**DETCs** Dendritic Epidermal T cells  
**DAMPs** Danger-Associated molecular patterns  
**TH** T helper cells  
**APCs** Antigen-Presenting Cells  
**TNF- $\alpha$**  Tumor Necrosis Factor- $\alpha$   
**TLRs** Toll-like receptors  
**HMGB1** High Mobility Group Box 1  
**PAR2** Protease Activated Receptor 2  
**AD** Atopic Dermatitis  
**NS** Netherton Syndrome  
**Klk5** Kallikrein 5  
**Klk6** Kallikrein 6  
**Klk7** Kallikrein 7  
**Klk9** Kallikrein 9  
**Klk10** Kallikrein 10  
**NFAT** Nuclear Factor of Activated T cells

## LIST OF PUBLICATIONS

This thesis is based on the following articles

***Improvement of epidermal covering on AEC patients with severe skin erosions by PRIMA-1MET/APR-246.*** Aberdam E, Roux LN, Secrétan PH, Boralevi F, Schlatter J, Morice-Picard F, **Sol S**, Bodemer C, Missero C, Cisternino S, Aberdam D, Hadj-Rabia S. *Cell Death Dis.* 2020 Jan 16;11(1):30. doi: 10.1038/s41419-020-2223-8.

***Isolation and Enrichment of Newborn and Adult Skin Stem Cells of the Interfollicular Epidermis.*** Sol S, Antonini D, Missero C. *Methods Mol Biol.* 2018 Mar 27. doi: 10.1007/7651\_2018\_131.

***Suppression of KLK6/TSLP signaling leads to an amelioration of the cutaneous and systemic inflammation in AEC syndrome.*** Sol S, Mollo MR, Cirillo L, Johnson JL, Polishchuk E, Scalia G, Polishchuk R, Pampalakis G, Furio L, Hovnanian A, Sotiropoulou G, Antonini D, Missero C. (In preparation)

Publications by the author not included in this thesis:

***Disruption of the Lotus japonicus transporter LjNPF2.9 increases shoot biomass and nitrate content without affecting symbiotic performances.*** Sol S, Valkov VT, Rogato A, Noguero M, Gargiulo L, Mele G, Lacombe B, Chiurazzi M. *BMC Plant Biol.* 2019 Aug 30;19(1):380. doi: 10.1186/s12870-019-1978-5.

***The Nitrate Transporter Family Protein LjNPF8.6 Controls the N-Fixing Nodule Activity.*** Valkov VT, Rogato A, Alves LM, Sol S, Noguero M, Lérán S, Lacombe B, Chiurazzi M. *Plant Physiol.* 2017 Nov;175(3):1269-1282. doi: 10.1104/pp.17.01187. Epub 2017 Sep 20.



## ABSTRACT

AEC syndrome (OMIM #106260) is a severe genetic disorder caused by mutation in the p63 gene, encoding a master regulator of epidermis. AEC syndrome is characterized by congenital erythroderma and severe skin erosions that severely affect the quality of life of patients and are life-threatening. We generated a conditional knock-in mouse model carrying an inducible AEC mutant in p63 (L514F), which similarly exhibits focal skin erosions, reduced resilience to mechanical stress and premature death.

At the molecular level, reduced mechanical stress resilience is accompanied with a progressive skin inflammation. Clear signs of severe inflammation are preceded by strongly elevated levels of Thymic stromal lymphopoietin (Tslp), an IL-7 like cytokine. The epidermal-derived Tslp is released in the blood circulation, causing a dramatic expansion of immature B-cells in the bone marrow and giving rise to an autoimmune lymphoproliferative disorder. Genetic ablation of Tslp in the epidermis significantly reduces skin inflammation and increases body weight and survival in AEC mutant mice. In AEC epidermis Tslp induction is accompanied by strong upregulation of the Klk6 protease, whose gene is directly repressed by functional p63. Klk6 treatment or overexpression of its effector NFAT induce Tslp in keratinocytes. *In vitro* co-treatment of primary keratinocytes with an active form of recombinant human Klk6 and a combination of inhibitors of NFAT- and NF- $\kappa$ B signaling show a significant reduction of Tslp expression level. Collectively these data indicate that extensive skin erosions in AEC syndrome can cause systemic inflammation and an autoimmune lymphoproliferative disorder due to excessive Tslp production, and point to novel therapeutic targets for AEC syndrome.

In addition, it has recently demonstrated that AEC syndrome is a protein aggregation disorder as AEC-associated p63 mutations lead to protein misfolding, aggregation and impairment of transcriptional activity. Based on this knowledge, I tested potential therapeutic approaches to treat AEC syndrome based on preventing aggregation and/or enforcing the endogenous protein disaggregation machinery either by an unbiased high-throughput screening of small molecules that may be able to restore the correct folding of the mutant protein or by genetic manipulations of specific chaperons.

# BACKGROUND

## 1.1 The skin: Structure and function

The skin is the largest multilayered organ of the body with an extensive surface area of approximately 1.8 m<sup>2</sup>. The skin is the first line of defense against the environment, performing many important functions: protect us from trauma, ultraviolet radiation, microorganisms and chemicals agents. Prevents the loss of liquid; participates in the mechanism of thermoregulation, increasing (vasodilatation) or slowing down (vasoconstriction) the dispersion of heat.

It is composed of three layers, the epidermis, dermis, and the hypodermis (subcutaneous layer), all three of which vary significantly in their anatomy and function.

This barrier function is mediated by the epidermis, a stratified squamous epithelium consisting of an outermost cornified layer, a number of differentiated layers, and the basal stem cell layer anchored to the basement membrane (BM), rich in extracellular matrix, which separate it and its appendages, including the hair follicles and sweat glands from the underlying dermis. It has a thickness comprised between 50 µm and 1.5 µm. The layers of the epidermis include the stratum basal (the deepest portion of the epidermis), stratum spinosum, stratum granulosum, stratum lucidum, and stratum corneum (the most superficial portion of the epidermis) (Fig. 1).

The stratified squamous epithelium of the epidermis is maintained by cell division within the basal layer, composed primarily of keratinocytes, an undifferentiated proliferative cell, that traverse apically as they undergo terminal differentiation. During this process, the cells undergo a complex series of morphological and biochemical changes that result in the production of the stratum corneum, the highly cornified outermost layer of the tissue composed by cornified cell envelopes (CE) assembled by cross-linking of structural proteins and lipids. More in detail, stem and progenitor cells within the basal layer must balance self-renewing cell divisions and BM adhesion with differentiation and concomitant departure to the suprabasal layers. The attachment to underlying matrix is allowed thanks to a series of adhesion molecules such as hemidesmosomes, laminin and anchoring fibrils. Some of their daughter keratinocytes enter the spinous layer through asymmetric mitoses, where

they exit the cell cycle, grow larger and establish robust intercellular connections (Simpson et al, 2011). This process is marked by distinct shifts in gene expression, including a shift from Keratins 5 and 14 (Krt5, Krt14) to Keratins 1 and 10 (Krt1/Krt10) intermediate filament expression and the expression of genes required for the synthesis of the CE, including the many members of the small proline-rich repeat (SPRR), late cornified envelope (LCE), and S100A families (Fuchs & Green, 1980; Brettmann et al, 2018). Defects in the Krt5/Krt14 network cause basal keratinocyte fragility and account for their rupture upon mechanical stress. Similarly, dominant negative mutations in Krt10/Krt1 cause suprabasal keratinocyte fragility (Coulombe and Lee, 2012), highlighting the role of keratins in the mechanical stability of the epidermis and the basal layer as a hotspot of mechanical stresses between the stiff BM and the suprabasal layers. In addition, other keratins are also expressed suprabasally, as Keratin6 (Krt6), Keratin16 (Krt16) and Keratin17 (Krt17), but only in hyperproliferative condition such as wound healing. Interspersed among the keratinocytes of spinous layer is a type of dendritic cell called the Langerhans cell, which functions as a macrophage by engulfing bacteria, foreign particles, and damaged cells that occur in this layer. Above the spinous layer, keratinocytes contain numerous keratohyalin granules packed with the protein profilaggrin in their cytoplasm, hence the name “stratum granulosum”. Cells in the granular layer flatten and assemble a water-impermeable cornified envelope underlying the plasma membrane and express filaggrin (Flg) and loricrin (Lor) as markers. In addition, cornified envelope proteins, which are rich in glutamine and lysine residues, are synthesized and deposited under the plasma membrane of the granular cells. As response to the increased permeability to the calcium, the cells activate transglutaminase, generating  $\gamma$ -glutamyl  $\epsilon$ -lysine crosslinks to create an indestructible barrier. Finally, stratum corneum keratinocytes release lysosomal enzymes to degrade major organelles, including the nucleus. The final steps of terminal differentiation involve also the extrusion of lipid bilayers, packaged in lamellar granules, onto the scaffold of the cornified envelope. The dead stratum corneum cells create an impenetrable layer that is continually replaced (Fuchs, 2007).

Keratinocytes move from the proliferative basal layer through the granular layer and continually replaced the cells of the outward layers. Indeed, as the body's outer frontier, the epidermis is subject to repeated trauma that must be repaired after wounding (Shen et al, 2013). Within this layer, epidermal stem cells divide to self-

renew and produce transient amplifying (TA) cells, which are able of a more limited proliferative capacity. Transit amplifying cells constitute the major cell type in the basal layer of the developing and mature epidermis and after few rounds of cell division they exit from the cell cycle, and initiate a terminal differentiation program, as they migrate outward toward the tissue surface.

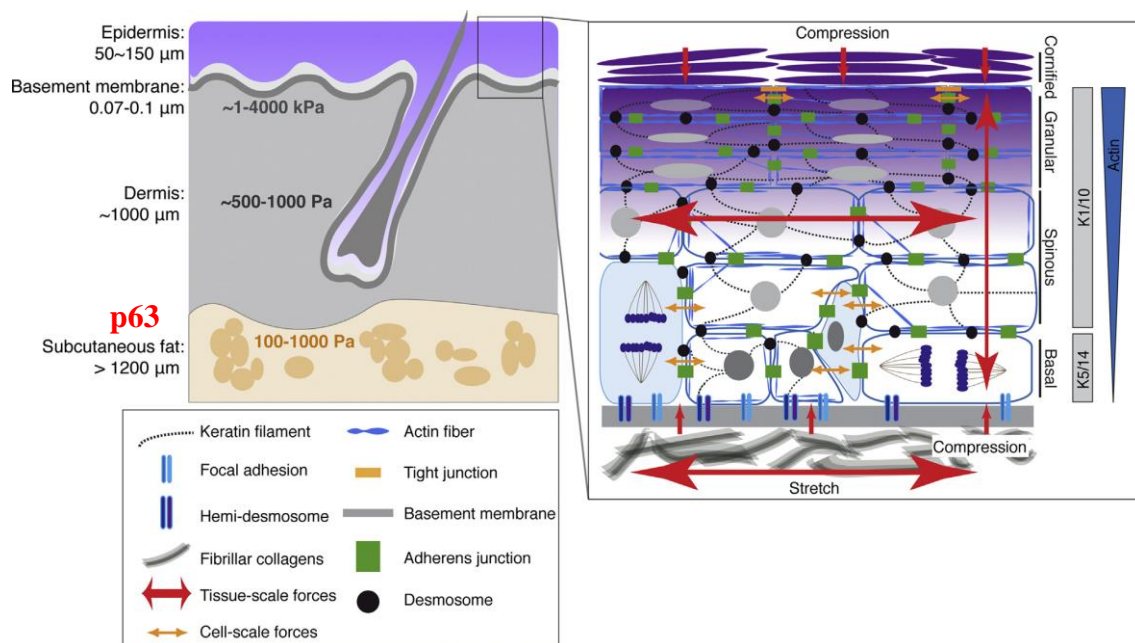


**Figure 1: Mechanical properties and force coupling in the skin.** The skin consists of the epidermis, dermis, and subcutaneous fat, with compartment-specific mechanical properties and the basement membrane representing the stiffest structure (left panel). The epidermis (right panel) is a load-bearing element subjected to large-scale forces including compression and stretch (red arrows), which are transmitted within and across layers (red arrows). The epidermis consists mainly of keratinocytes connected via actin-linked adherens junctions and keratin-linked desmosomes. The basal layer adheres to the basement membrane via integrins that form actin-linked focal adhesions and keratin-linked hemidesmosomes. Tight junctions are formed only in the last viable layer through mechanotransduction by high-tension adherens junctions. Differentiating cells depart from the basal layer through perpendicular cell divisions and delamination. Cell shape changes, divisions, and movement within the layers generate forces between cells (orange arrows), modulating cell fate and position. K, keratin (adapted from Biggset al., 2019).

## 1.2 p63, the master regulator of epidermal gene expression

p63 belongs to the p53 gene family consisting of three genes, p53, p63, and p73, that show significant homology (Fig. 2) (Yang et al, 2002). Similarly to its family

members p53 and p73, p63 is a zinc-finger tetrameric transcription factor, with three functional domains: an N-terminal transactivation domain which shares 25% homology with N-terminal part of p53, a central DNA binding domain (DBD) which shares 65% of homology with the corresponding p53 domain and C-terminal oligomerization domain, essential for tetramerization, which shares 35% of homology with the oligomerization domain (OD) of p53 (Yang et al., 2002). At the N-terminal, two classes of proteins are made, the TAp63 and the DNp63, due to the presence of two independent promoters. TAp63 isoforms contain an acidic N-terminal transactivation domain similar to the one found in the canonical full-length p53. It is expressed in female germ cells where it is essential in DNA damage-induced oocyte death (Suh et al., 2006). The first 26 amino acids of the N-terminal region in DNp63 are required for its transcriptional activity (Dohn et al., 2001; Ghioni et al., 2002; Helton et al., 2006). At the 3' region of the p63 gene alternative splicing events result in at least three isoforms, alpha, beta or gamma ends (Yang et al., 1998). DNp63alpha is highly abundant in the basal regenerative layer of the epidermis and other stratified epithelia, and it is virtually absent in other tissues (Yang et al., 1998). DNp63alpha plays multiple essential roles in epidermal development and stratification, keratinocyte proliferation and differentiation, controlling expression of several epidermal genes including itself and other transcription factors (Yang et al., 1998; Antonini et al., 2006; Laurikkala et al., 2006; Nguyen et al., 2006; Truong et al., 2006; Koster et al., 2007; Moretti et al., 2010; Thomason et al., 2010; Vanbokhoven et al., 2011; Romano et al., 2012). Identification of direct p63 target genes has been greatly facilitated by several high-throughput gene expression profiling and ChIP-seq studies performed in human or mouse keratinocytes (Truong et al., 2006; Vigano et al., 2006; Della Gatta et al., 2008; Kouwenhoven et al., 2010; McDade et al., 2012), revealing that p63 controls a large number of basal and suprabasal genes, thereby regulating the entire differentiation program.

The C-terminal end of p63 include a SAM domain and a post-SAM domain (PS) absent in the other isoforms and in p53 (Yang et al., 1998) (Fig. 2). SAM domains are found in several proteins and have diverse functions, they can interact with themselves, bind to other SAM domains, bind to non-SAM domain proteins, or to RNA (Qiao and Bowie, 2005). The SAM domain in p63 is unable to form homodimers (Chi et al., 1999; McGrath et al., 2001), and its function remains

uncovered. The PS domain include a transcriptional inhibitory domain (TID), which interacts with the TA domain of another TAp63 molecule, forming a closed and inactive dimer that can be activated by phosphorylation, resulting in an active tetramer (Su et al., 2010; Deutsch et al., 2011). Its functional role in the context of the DNp63alpha that lacks the TA domain, is poorly understood. The most C-terminal subdomain contains a sumoylation site involved in the regulation of the p63 intracellular concentration (Straub et al., 2010), and nonsense mutations in this subdomain are causative of SHFM (Split Hand and Foot Malformations) (van Bokhoven and Brunner, 2002).

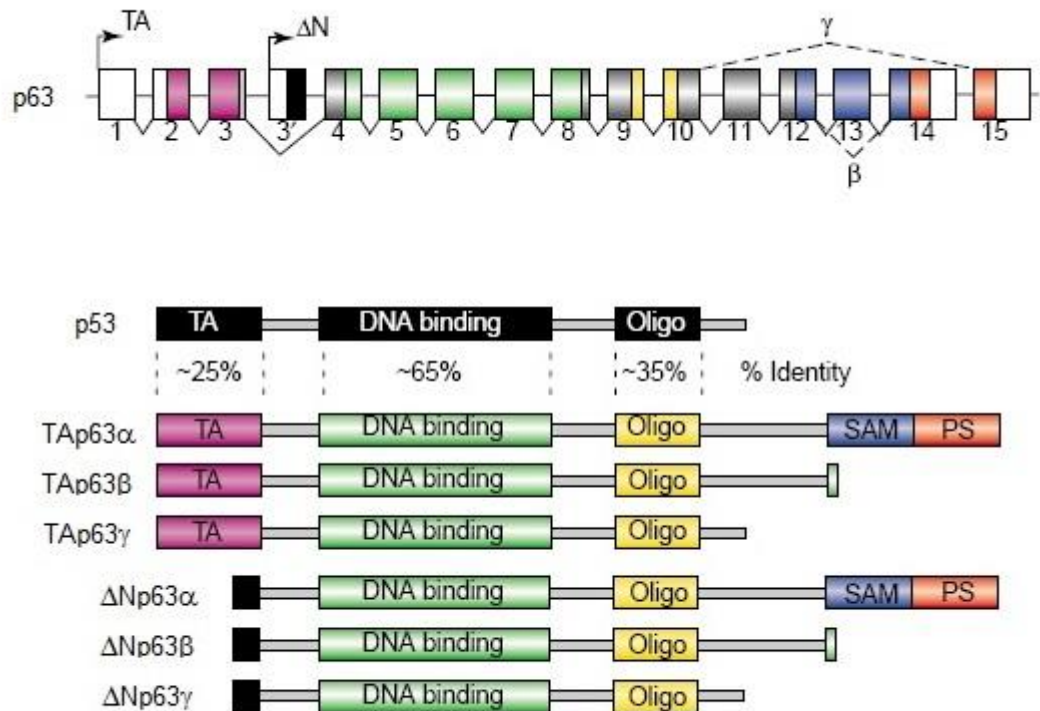


**Figure 2: Functional domains and isoforms of the p53 family proteins.** Comparison between p53 and p63 proteins. Schematic representation of p63 gene structure and isoforms. Two alternative promoters give rise to TAp63 or DNp63 transcripts, whereas at the 3' end alternative splicing events generate  $\alpha$ ,  $\beta$  or  $\gamma$  isoforms. In the lower panel, protein domains conserved in p53 family are shown: Transactivation domain (TA), DNA binding domain, Oligomerization domain. SAM and PS domains in p63  $\alpha$  isoforms are absent in p53 full-length gene. The percentage of identity between p53 and p63 conserved domains are indicated (adapted from Yang et al., 2002).

### 1.3 p63-deficient mice

In the 1999, two independent groups obtained a p63-deficient mouse model. Using these models, they could explore the unique roles of p63 in development of ectodermal derived tissues. p63<sup>-/-</sup> mice die for dehydration soon after birth and display severe defects of all stratified epithelia and their derivatives, facial clefting and impaired limb formation, suggesting that p63 plays a pivotal role in these tissues (Mills et al, 1999; Yang et al, 1999). Defects in the surface epithelium of p63<sup>-/-</sup> mice have been ascribed to loss of proliferative potential of keratinocyte stem cells (Senoo et al, 2007; Yang et al, 1999), and/or altered epidermal stratification and cell differentiation associated with reduced expression levels of Krt5/Krt14 and Krt1/Krt10 (Koster & Roop, 2004; Mills et al, 1999; Romano et al, 2009). p63-deficient newborns show striking limb defects. The fore limbs were truncated and hind limbs were completely absent and the structures dependent upon epidermal-mesenchymal interactions during embryonic development, such as hair follicles, teeth and mammary glands, are absent. Phalanges and carpals were absent in both the p63-homozygous mutant, whereas more proximal forelimb structures were slightly heterogeneous in the extent of the truncation in the two models. The femur and all distal skeletal elements were also absent. These defects are caused by a failure of the apical ectodermal ridge (AER) to differentiate. The lack of a proper AER limb buds in p63 null mice results from a failure of the ectoderm to undergo growth and differentiation that give rise to this stratified epithelium. Indeed, several genes that are important in limb-bud outgrowth are not expressed, such as Fgfr8, a marker of the AER, and Msx-1 which expression in the mesenchyme depends on an ectodermal signal, or abnormally expressed, such as Lmx-1, a marker of the dorsal limb mesenchyme (Mills et al, 1999; Yang et al, 1999).

The skin in the knock-out mouse model generated by McKeon's group lacks expression of the basal layer markers as Krt5 and Krt14 and also spinous layer markers Krt1 and Krt10. Even though, isolated patch of the epidermis showed the expression of late differentiation markers such as Loricrin, Involucrin and Filaggrin. The authors prove that p63 is required for the initial development and continued regeneration of the epidermis and that the loss of p63 in the tissues failed to maintain the proliferative potential of stem cells in skin (Fig. 3) (Yang et al, 1999). In addition, to reinforce this hypothesis the same authors in another study demonstrate

that p63 is fundamental to maintain the proliferative potential of epithelia stem cells of both thymus and epidermis (Senoo et al, 2007).

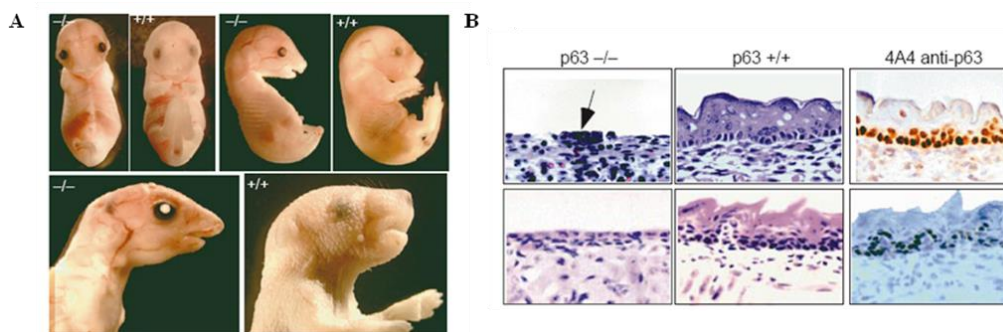


**Figure 3: Phenotype of p63 knockout mice.** A) The newborn p63 null mice show defects in limb formation and craniofacial defects associated with skin and appendages aberrant development for lack of stratification and differentiation. B) H&E staining of the epidermis at E17 display p63<sup>-/-</sup> mice lacking squamous stratification in the epidermis. Middle, wild-type H&E control mice showing extensive stratification. In the right the basal staining with anti-p63 antibody to show the endogenous expression of p63 in the epidermis (adapted from Yang et al., 1999).

The p63 knock out mice generated by Mills and colleagues developed aberrant skin and appendages due to lack of stratification and differentiation (Fig. 4) (Mills et al, 1999). The authors showed that in p63 null mice all structures that required the ectodermal mesenchymal signal were compromised because the ectoderm failed to receive the signal. They showed that the skin of p63 null mice were covered by a single disorganized layer of ectodermal cells or flattened epidermal cells in which they did not detect the expression of any early or late differentiation markers. Their results suggested that p63 is the determining factor of stratification, and supported the hypothesis that p63 is required for simple epithelial cells to commit to a stratified epithelial lineage during development (Mills et al, 1999).



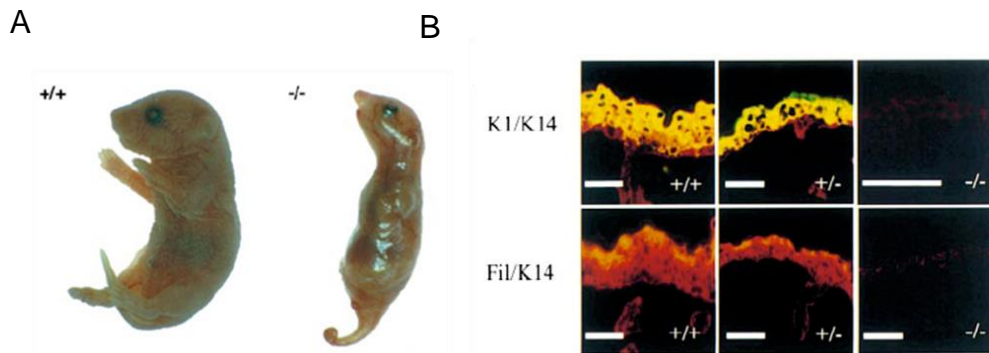


**Figure 4: The phenotype of p63-deficient newborn mice generated by Mills's group.** A) p63 null mice show severe limb and skin defects. B) Expression of different markers in the epidermis of p63 null mice: staining for Krt14 in red and Krt1 and Filaggrin (Fil) in green. Krt14 is weakly express in p63 null mice, whereas Krt1 and Fil are not detectable in the epidermis (Adapted from Mills et al., 1999).

#### 1.4 p63-associated disorders

The crucial role of the transcription factor p63 in the formation of the epidermis and other stratifying epithelia is demonstrated by two lines of evidence. First, p63-deficient mice have no epidermis and aberrant squamous epithelia, and are also devoid of epithelial appendages, such as hair follicles and teeth. Second, heterozygous mutations in the human p63 gene are responsible for several ectodermal dysplasia (ED) syndromes, which are congenital disorders characterized by abnormalities of two or more ectodermal structures, such as hair, nails, sweat glands and digits. p63 expression is highest in the proliferative basal cell layer where epithelial progenitor cells are thought to reside in a range of stratified epithelia, including skin, in particular in the nuclei of basal cells of the skin, cervix, tongue, esophagus, mammary glands, prostate and urothelium (Carroll et al, 2007). In humans heterozygous mutations in p63 (TP63) give rise to five rare ED-related syndromes with overlapping features including ectodermal dysplasia, cleft lip/palate, and limb malformations, namely Ectrodactyly, Ectodermal Dysplasia, and Cleft lip/palate syndrome (EEC, OMIM 604292), Ankyloblepharon-Ectodermal defects-Cleft lip/palate (AEC, OMIM 106260), Limb Mammary Syndrome (LMS, OMIM 603543), Acro-Dermato- Ungual-Lacrimal-Tooth syndrome (ADULT, 103285), and Rapp–Hodgkin Syndrome (RHS, OMIM 129400) (reviewed in (Rinne et al., 2009)). In addition, some p63 mutations are causative of a non-syndromic

form of Split Hand/Foot Malformation (SHFM4, OMIM 605289). The mutation patterns in the p63 gene is associated with different p63 clinical conditions displaying a clear genotype-phenotype association. Usually, mutations clustered in the DNA binding domain are causative of EEC syndrome, whereas mutations clustered in C-terminal domain are often causative of AEC syndrome.

EEC syndrome is mainly caused by point mutation in the DNA binding domain (DBD) of the p63 gene. EEC syndrome comprises limb malformation, ectodermal dysplasia and orofacial clefting. Representative limb malformation are ectrodactyly and syndactyly (Rinne et al, 2007). Ectodermal dysplasia is seen as lightly colored, sparse hair and can be observed absence of eyelashes, eyebrows and alopecia. Skin is thin and dry, sometimes resembling dermatitis.

LMS was the first p63 syndrome linked to chromosome region 3q27. Mutations in LMS are located in the N- and C-terminus of the p63 gene. LMS phenotype comprises malformations of the hands and/or feet and hypoplastic nipples and/or mammary glands. Ectodermal defects are much less prominent than in EEC syndrome, but mammary gland hypoplasia or aplasia is more frequent in LMS than in EEC.

ADULT syndrome phenotype is most similar to LMS syndrome, although clear differences can be seen when observing larger families or patient population. The main difference is the absence of orofacial clefting and the presence of hair and skin defects in the ADULT syndrome. Nevertheless, teeth, skin, nail, hair and lacrimal duct defects are constantly present in ADULT syndrome (100, 91, 100%, 53% and 67%, respectively). A point mutation in exon 8, changing R298 in the DNA binding domain into either a glutamine or a glycine has been found. While EEC syndrome mutations in the DNA binding domain impair the binding of p63 protein to DNA (Celli et al, 1999), arginine 298 is not located close to the DNA-binding interface, and mutation of this arginine does not affect DNA binding (Duijf et al, 2002). Two other mutations are located in the N-terminus.

RHS was first described in 1968 by Rapp and Hodgkin in three individuals from one family with sparse eyebrows, slow-growing wiry scalp hair, nail dystrophy, hypodontia, clefting, hypohidrosis, and characteristic facies. RHS share most

features with AEC but is differentially classified because of the lack of skin erosions and the absence of ankyloblepharon. Other ED symptoms, such as orofacial clefting and the absence of limb malformations are similar to AEC. In both syndromes clefting in lip and/or palate is equally frequent. The strong overlap between AEC and RHS suggest that they are variable manifestations of the same clinical entity (Bertola et al, 2004; Rinne et al, 2007). AEC and RHS mutations are located in the C-terminus of the p63 protein. They are either point mutations in the SAM domain or deletions in the SAM or PS domains (Barrow et al, 2002; Celli et al, 1999; Kantaputra et al, 2003; McGrath et al, 2001; van Bokhoven & Brunner, 2002). In 2001, heterozygous missense mutations in the TP63 gene were identified as the molecular basis for AEC syndrome and, in 2003, the first TP63 gene mutation was reported in RHS.

SHFM is a pure limb malformation (ectrodactyly and syndactyly) condition, without orofacial clefting or ectodermal dysplasia. The non-syndromic SHFM4 is caused by several mutations, which are dispersed throughout the p63 gene and probably it is caused by altered protein degradation, even though different degradation routes are involved (Rinne et al, 2007). A non-syndromic orofacial clefting type was also linked to p63 gene, R313G is the first mutation discovered (Leoyklang et al, 2006).

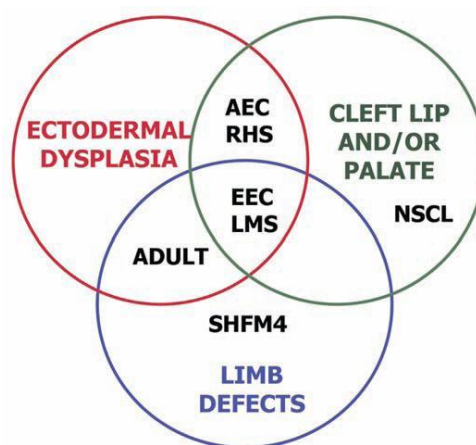


**Figure 5: Various combinations of ectodermal dysplasia, orofacial clefting and limb malformations are the hallmark of p63-associated syndromes.** EEC syndrome is the prototype of these syndromes and together with LMS shows all three hallmarks. ADULT syndrome patients never show orofacial clefting, whereas AEC and RHS never show limb defects. Non-syndromic limb defect condition (SHFM4) and non-syndromic cleft lip/palate (NSCL) are also caused by mutations in the p63 gene. (From Hans van Bokhoven et al, 2007)

## 1.5 AEC syndrome

Ankyloblepharon-Ectodermal defects Cleft lip/palate syndrome (AEC), also known as Hay–Wells syndrome, was first reported by Hay and Wells in 1976 (Hay & Wells, 1976). It is a rare autosomal dominant disorder, characterized by congenital fusion of the eyelids (ankyloblepharon), ectodermal dysplasia with severe involvement of the skin, and cleft palate with or without cleft lip. Clinical manifestations have different penetrance: about 75% of patients have severe skin erosions at birth, with some AEC patients reported to have up to 70% denuded skin. By 4 – 5 years age erosions could disappear, except for the head and auricular region. Clefting occurs approximately in 80% of AEC patients. The ankyloblepharon occurs only in 44% of AEC cases (Fig. 6a-b-c-d). Hearing loss has been reported in about 40% of the patients. AEC patients have nails and teeth defects in about 75–80% of cases (Fig. 6a-b-c-d).

Among the p63-related disorders, AEC syndrome is characterized by the most severe skin symptoms, including congenital erythroderma, skin fragility, blistering and extensive erosions in 80% of the patients (Hay and Wells, 1976; McGrath et al., 2001). Dermatologic findings include also, skin atrophy, scaling, atopic dermatitis and palmoplantar hyperkeratosis (Dishop et al., 2009; Julapalli et al., 2009). At or after birth, patients may present manifestations such as erosive lesions and collodion membrane, leading to an initial suspicion of epidermolysis bullosa (EB), a group of rare disorder characterized by skin blistering. Skin erosions are often accompanied by crusting, granulation tissue, and secondary infections and resolve in several months or even years. Healing results in scarring alopecia. The biological mechanisms underlying the skin erosions remain unveiled, and treatment is limited to gentle wound care and antibiotic treatment to prevent or cure infections. Healing is slow and recurrent breakdown is typical. In addition to skin defects, AEC and EEC patients may develop corneal abnormalities leading to substantial pain and photophobia (Di Iorio et al., 2012). Corneal limbal stem cell failure results in recurrent corneal ulceration, neovascularization and scarring and ultimately irreversible blindness. The standard care for both skin erosions and corneal ulcerations consists in minimizing trauma and preventing infections.

Most mutations causative of AEC syndrome is clustered in the C-terminal domain

of the p63alpha isoform, and are either missense mutations found predominantly in the SAM domain, or frame-shift mutations in the PS domain that cause elongation of the amino acid sequence (Rinne et al, 2009). An interesting genotype-to-phenotype correlation exists among the syndromes.

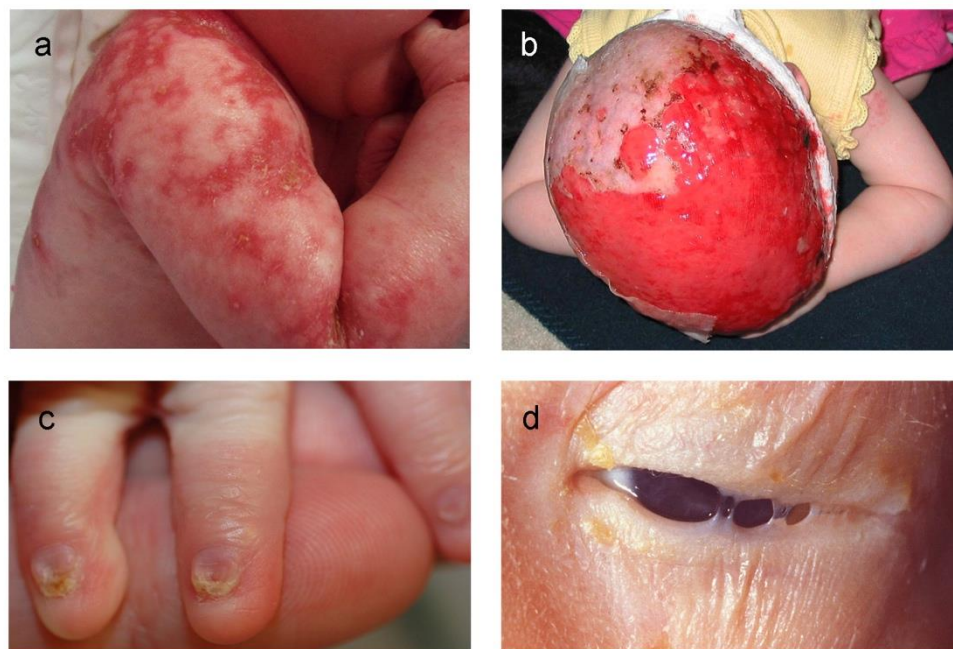


**Figure 6: Clinical appearance of a child affected by AEC syndrome.** a) A close up of reticulated scarring that is typically seen in AEC patients as the results of skin erosions healing processes. b) Scalp erosions with hemorrhagic crusting, granulation tissue and secondary infection. c) Dystrophic fingernails of AEC patients characterized by small nails with partial loss/absence and distal fraying of the nail plate. d) Focal fusion of the eyelids (ankyloblepharon) (Adapted from Ferone et al., 2015).

## 1.6 AEC mouse models

To study the functional activity of mutant p63 in AEC syndrome a first knock-in mouse model (p63<sup>+/L514F</sup>) was generated in our laboratory (Ferone et al, 2012). This model carries a phenylalanine substitution in position 514 (L514F) and closely resembles the human disease (Ferone et al, 2012). This mutation falls in the first helix of the SAM domain and disrupts the folding of the protein. Among the AEC causative mutations we decided to focus our attention on L514 amino acids for three reasons: first of all, this amino acid is mutated in three different amino acids (phenylalanine, valine or serine); this mutation affects an amino acid that is

predicted to be buried inside the protein and has a small solvent accessible surface, so any mutation in this region is likely to affect the overall structure and stability of the protein by altering the packing of the helices, and moreover the substitution of a leucine with a phenylalanine probably cause a severe steric clash between two phenylalanine rings that are located close to each other (McGrath et al, 2001; Rinne et al, 2007).

*p63<sup>+L514F</sup>* mice showed a lethal phenotype due to a severe cleft of the secondary palate which is lethal in mice but not in humans. *p63<sup>+L514F</sup>* skin displayed an overall reduction in skin thickness and fragility, accompanied by a significant epidermal atrophy and hair follicle hypoplasia, thus recapitulating the defects observed in AEC syndrome (Fig. 7). At molecular level, several known p63 target genes are downregulated in AEC mutant epidermis including desmosomal genes (desmoglein 1 (Dsg1), desmocollin 3 (Dsc3), desmoplakin (Dsp), and crucial regulators of epidermal cell proliferation such as Fgfr2 and Fgfr3 (Ferone et al., 2012; Ferone et al., 2013). Ferone et al., 2012, found that skin fragility observed in the constitutive mouse model was caused by a strong reduction of desmosomes, whereas epidermal hypoplasia and cleft palate are associated with a transient reduction in epithelial cell proliferation during development. These defects closely resemble those observed in the Fgfr2b<sup>-/-</sup> mice (Candi et al, 2006; De Moerlooze et al, 2000; Petiot et al, 2003; Rice et al, 2004; van Bokhoven et al, 2001). Since p63 transcriptionally controls the Fibroblast growth factor receptors Fgfr2 and Fgfr3 and their expression, they found that impaired FGF signaling downstream of p63 is likely an important determinant of reduced ectodermal cell proliferation and defective self-renewing compartment in AEC syndrome.

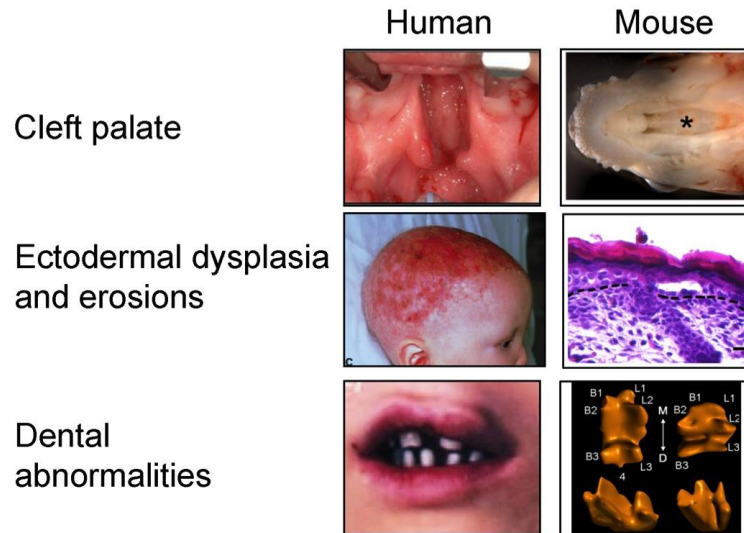


**Figure 7: Child affected by AEC syndrome compared to the constitutive AEC mouse model.** Comparison between AEC syndrome phenotype and constitutive AEC mouse model indicated that the mouse model faithfully recapitulated some human features, as cleft palate, skin erosions and dental abnormalities.

### 1.7 The role of Thymic stromal lymphopoietin (Tslp) in skin immune function

Skin integrity is maintained by the intimate interaction between epidermal keratinocytes and resident immune cells that supports recovery from a number of insults such as barrier disruption and bacterial or viral infection. Failure of the immune system to maintain tolerance or re-establish homeostasis after keratinocyte perturbation can cause autoimmune and chronic pro-inflammatory disorders that can give rise to skin neoplasia. Central to a productive interaction between keratinocytes and resident immune cells is an array of immune-regulatory factors that are either constitutively expressed or induced in keratinocytes or immune cells following insult.

One of the cytokines that is rapidly induced in keratinocytes under stress is TSLP. Thymic stromal lymphopoietin (TSLP) belongs to the interleukin (IL)-2 cytokine family, specifically it is a paralog of IL-7 (Leonard, 2002) (Friend et al, 1994). TSLP is involved in several immunoregulatory functions, but in particular it is able to stimulate thymocytes to induce the production of TH lymphocytes and the consequently differentiation of TH2 cells and the relative production of IL4 and IL13.

TSLP, as IL-7, promotes the differentiation of B-cells and it is also able to evoke itch in atopic dermatitis patients (Wilson et al, 2013). It is also implicated in the pathogenesis of asthma, as the agent sensitizing the lung to allergens (Fig. 8) (Demehri et al, 2009a).

Human and murine TSLP are very similar, in fact they share a high degree of homology (Reche et al, 2001) (Sims et al, 2000). During allergic inflammation, the primary producers of TSLP are epithelial cells, such as keratinocytes, and stromal cells although recent data have demonstrated that both dendritic cells (DCs) and mast cells are capable of TSLP production (Soumelis et al, 2002) (Watanabe et al, 2004) (Ying et al, 2005) (Kashyap et al, 2011) (Moon et al, 2011).

Several kinds of cells, such as T cells, B cells, natural killer (NK) cells, monocytes, basophils, eosinophils and DCs, and non-hematopoietic cell lineages such as epithelial cells respond to the TSLP regulation and express the TSLP Receptor (TSLPR) (Fig. 8). TSLPR is constituted by two units: the former, the TSLPR subunit and the latter, the IL-7R $\alpha$  chain both in humans and mice (Ziegler & Artis, 2010) (Reardon et al, 2011).

The early studies characterizing TSLP showed that TSLP could support B-cell development (Friend et al, 1994) (Levin et al, 1999). Several groups demonstrated the association of TSLPR mutations with a subtype of B cell leukemia confirming that altered TSLP expression can have a significant impact on B cells (Chapiro et al, 2010, Roll and Reuther, 2010, Tasian and Loh, 2011). In addition, elevated systemic levels of TSLP has been demonstrated to lead to aberrant B-cell lymphopoiesis, with direct actions on B cell development and indirect effects leading to autoimmune diseases (Astrakhan et al, 2007 and Iseki et al, 2012). Indeed, Demehri et al proved that in Notch1; Notch2 conditional knock out mice high systemic levels of Tslp caused the insurgence of a B-lymphoproliferative disorder, an autoimmune condition associated to Tslp (Demehri et al, 2008).



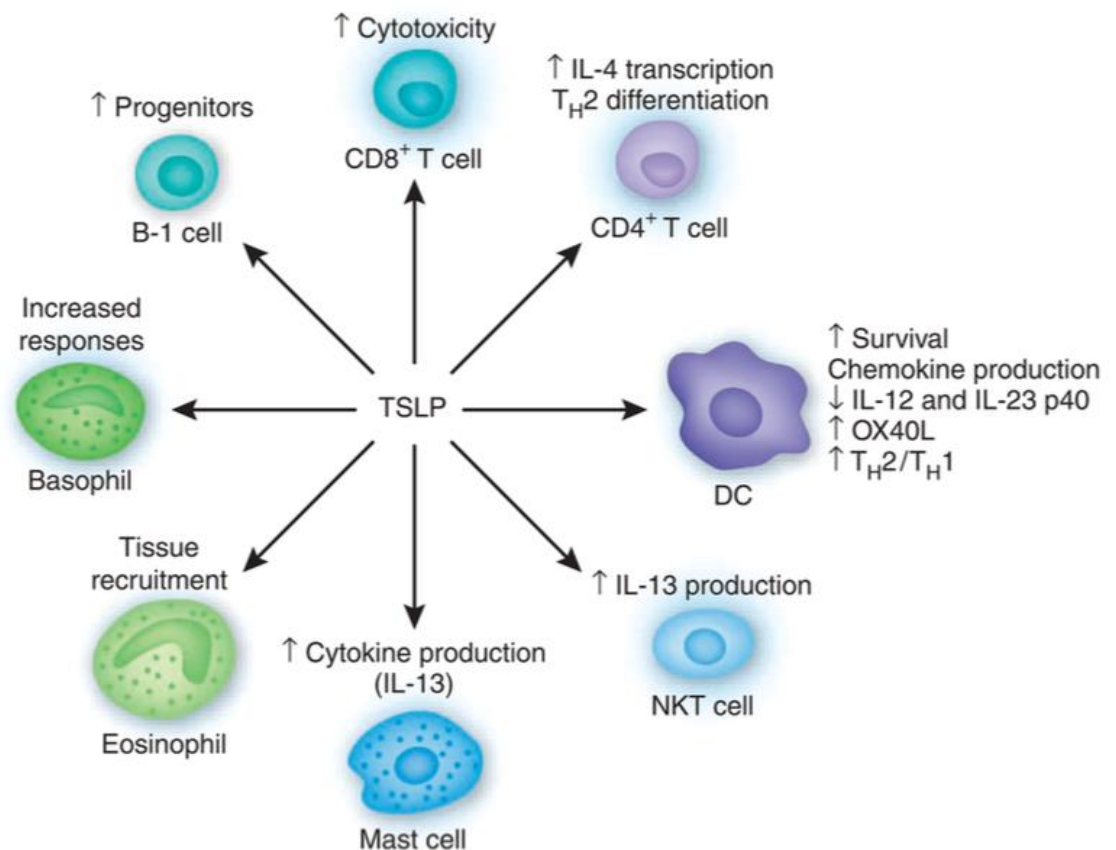


**Figure 8: Tslp cellular targets.** Tslp acts on several cellular targets such as lymphocytes (B and T-cells), granulocytes, DCs, natural killer T cells (NKT), mast cells, eosinophils, and basophils.

### 1.8 Signaling pathway involved in Tslp regulation

Nowadays, the mechanism of action of Tslp has not yet been defined. Several research groups are still working in this field. So far, Murthy et al have demonstrated that ADAM17 is involved in the basal Notch activation and it triggers Notch signaling to regulate c-Fos activation, monitoring so epidermal barrier homeostasis. Loss of this control induces the production of cytokines or alarmins, such as Tslp and IL33, which trigger immune responses. Independent studies have demonstrated that the loss of Notch, deregulation of AP-1 signaling pathway, or elevated production of epithelial TSLP results in inflammatory skin disease (Demehri et al, 2009a) (Dumortier et al, 2010).

Moreover, Wilson et al showed a new role covered by TSLP. They demonstrated that it might evoke itch behaviors directly by activating sensory neurons, and

indirectly by activating immune cells, which secrete inflammatory mediators that target sensory neurons, or both. Indeed, keratinocytes may directly communicate with sensory neurons via neuromodulators (Ikoma et al, 2006). The release of TSLP by keratinocytes has been demonstrated that is correlated to the GPCR protease-activated receptor 2 (PAR2) and to  $Ca^{2+}$  influx that activates the NFAT/calcineurin pathway which triggers the activation of Tslp transcription (Wilson et al, 2013). TSLP secretion has been demonstrated to be calcium dependent. Epithelial cells such as keratinocytes express  $Ca^{2+}$  channels on their surface like ORAI1, ORAI2. In keratinocytes, the ORAI1 signaling pathway connects PAR2 to TSLP release. The activation of PAR2 allows the release of  $Ca^{2+}$  from endoplasmic reticulum and the activation of ORAI1 regulator, called STIM1 (STromal Interaction Molecule 1) that opens ORAI1 channels to promote  $Ca^{2+}$  influx.  $Ca^{2+}$  activates calcineurin, a phosphatase involved in the NFAT dephosphorylation. NFAT dephosphorylated translocates from the cytoplasm to the nucleus and induces the transcription of TSLP. Wilson and colleagues found that TSLP is released by keratinocytes under  $Ca^{2+}$  influx and it activates sensory neurons directly to evoke itch behaviors. In addition, they identify the ORAI1/NFAT signaling pathway as a key regulator of PAR2-mediated TSLP secretion by epithelial cells. Instead, Furio and coworkers (Furio et al, 2015) showed that patients affected by Netherton syndrome (NS) presented elevated systemic levels of Tslp. They demonstrated that the overproduction of Tslp in NS syndrome is related to the activation of PAR2-NF- $\kappa$ B axis by kallikrein 5 (KLK5) activity. NS is a disorder characterized by severe skin inflammation, scaling and atopy for which physicians and scientists do not have a complete understanding. In NS patients, an intrinsic mechanism takes place in keratinocytes and leads to increased expression of TSLP, TNF- $\alpha$ , IL-8 and ICAM-1 as a result of PAR2 activation by active KLK5. Overall, the mechanisms underlying Tslp action are tricky and involve several pathways. It will take some time for scientists to understand the pawn genes involved in this mechanism.

### **1.9 Regulation of KLKs activity in the epidermis**

Kallikreins (KLKs) or kallikrein related peptidases are a subgroup of extracellular serine proteases differently expressed in many tissues and exist as a subgroup of 15 serine proteases encoded by a tightly clustered multigene family on chromosome

19q13.4 (Yousef et al., 2002). The epidermal KLKs are predominantly localized in the upper stratum granulosum and stratum corneum at different levels of expression: KLK1, KLK4, KLK5, KLK6, KLK7, KLK8, KLK10, KLK11, KLK12, KLK13, and KLK14 (Komatsu et al., 2015 and Williams et al., 2016). These proteases are synthesized as pre- pro-enzymes (precursor or zymogene) transported separately by lamellar granules in the granular layer (Ishida-Yamamoto et al., 2003). After secretion into the intercellular space, pre-KLKs are activated by removal of an NH<sub>2</sub>-terminus signal peptide by themselves and other proteases (Eissa et al., 2008). KLKs thus play essential roles in the physical and biochemical barrier functions of the stratum corneum and are involved in some age- and sex-associated changes to the skin barrier. They are involved in three main functions: 1) promotion of skin desquamation and/or keratinocyte proliferation, regulating skin renewal and barrier thickness; 2) regulation of lipid metabolism by controlling lipid-processing enzymes and the activation of PAR2; 3) processing of pro-cytokines and antimicrobial peptides involved in innate immune responses.

The activity of a KLK is typically controlled by itself or other KLKs in the proteolytic activation cascade. Briefly, KLK5, also known as stratum corneum tryptic enzyme (SCTE), is thought to initiate the cascade reaction through auto-activation (Fig. 9). KLK5 activates other KLKs, like KLK7 also called as stratum corneum chymotryptic enzyme (SCCE) and KLK14. Moreover, the activated KLK14 can then activate pro-KLK5 via positive feedback. These KLKs are secreted by keratinocytes into stratum corneum and after secretion they participate in a proteolytic cascade. KLK5 also activates KLK8. The activated KLK8 can process pro-KLK1 and pro-KLK11 in vitro (Eissa et al., 2010). KLK6 is capable of activating KLK5 and KLK11. Until now, the place of some KLKs such as KLK11 and KLK13 in the activation cascade has remained unclear. After the activation, KLK5 and KLK7 cleave corneodesmosomes, which are composed by DSG1, DSC1 and corneodesmosin, starting the skin desquamation process or shedding of SC corneocyte cells. Matriptase, an activator of serine-protease and the lympho-epithelial Kazal type inhibitor (LEKTI), which is a protease inhibitor, regulate KLK activity both in normal and pathologic condition.

KLK5, KLK6 and KLK14 are able to activate the keratinocyte-expressed proteinase-activated receptor 2 (PAR2), beginning an inflammation process mediated by NFAT/calcineurin/Tslp signaling pathway (Wilson et al, 2013).

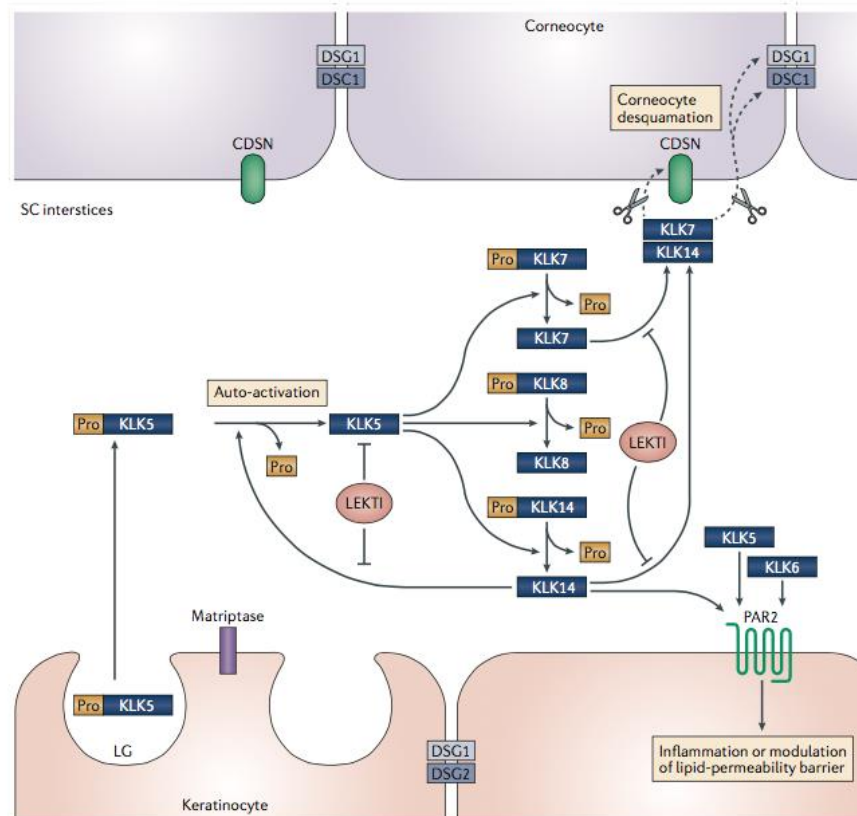


**Figure 9: The proteolytic cascade of kallikreins in skin epidermis.** KLKs in the epidermis are secreted by lamellar granules (LG) of keratinocytes in the stratum granulosum into the stratum corneum (SC). Upon secretion it starts their activation and the related proteolytic cascade (Adapted from Prassas et al, 2015).

### 1.10 Protein aggregation of the p63 in AEC syndrome

Among the p63-associated disorders, AEC syndrome is uniquely characterized by long-lasting and life-threatening skin erosions. Despite the severity of the symptoms, molecular studies have been hampered by the paucity of human biological material, and the poor understanding of the molecular mechanisms underlying the disorder. Our laboratory has recently demonstrated that AEC associated mutations cause protein misfolding and aggregation due to either introduction of aggregation-prone regions in the case of aberrant protein elongation, or by conformational changes that expose peptides with a natural high aggregation propensity (Russo et al., 2018). The latter is equivalent to the well-known gain-of-function mutations of p53 in cancer (e.g., R175H).

Mutant p63 in AEC keratinocytes exhibits aberrant aggregation and inactivation of both transcriptional activating and repressing functions. The partial impairment in DNA binding is not an intrinsic property of the AEC mutants but rather an indirect consequence of aggregation.

Aggregating proteins can inactivate other proteins through coaggregation. Since p63 binds DNA as a tetramer, AEC associated p63 mutant proteins co-aggregate with its wild-type counterpart and with p73, the other member of the p53 family with which it can efficiently form heterotetramers (Gebel et al. 2016), and possibly with other protein partners, acting as a dominant negative and/or a gain of function mutant. One example is p53R175H, a structural mutant with gain-of-function properties that interacts with specific isoforms of p73 and, to a lesser extent, of p63, interfering with their functions. Since p63 is an abundantly expressed transcription factor in keratinocytes, and AEC mutants often show a longer half-life in cells than the wild-type protein (36), mutant p63 may be able to sequester other nuclear proteins. Aggregation between AEC mutants and p73 and/or other p63 protein partners helps explain the severe skin phenotype specifically observed in AEC syndrome and not in other diseases associated with p63 mutations.

### **1.11 Quality control of unfolded proteins**

Protein aggregates can interfere with cellular processes by depleting factors crucial for protein homeostasis (Hipp et al., 2014). The protein quality control (PQC) system plays a crucial role in preventing unfolded protein aggregation by protecting interactive surfaces against aberrant interactions with other not-canonical molecular partners (Fig. 10) (Mayer and Bukau, 2005). The PQC system consists of multiple chaperone and degradation pathways that cooperate to preserve protein homeostasis (or proteostasis) by ensuring a healthy and functional proteome (Sontag et al., 2017; Houck et al., 2012; Jeng et al., 2015).

Molecular chaperones are proteins that transiently interact with newly synthesized polypeptides driving the acquisition of their folded conformation (Kampinga et al., 2010). Chaperone functions are not restricted to the protein folding but include also recognition and sorting of misfolded proteins to the various PQC

compartments, by a cooperation with other cellular structures, such as nuclear membrane, ER network and cytoskeleton (Sontag et al., 2017).

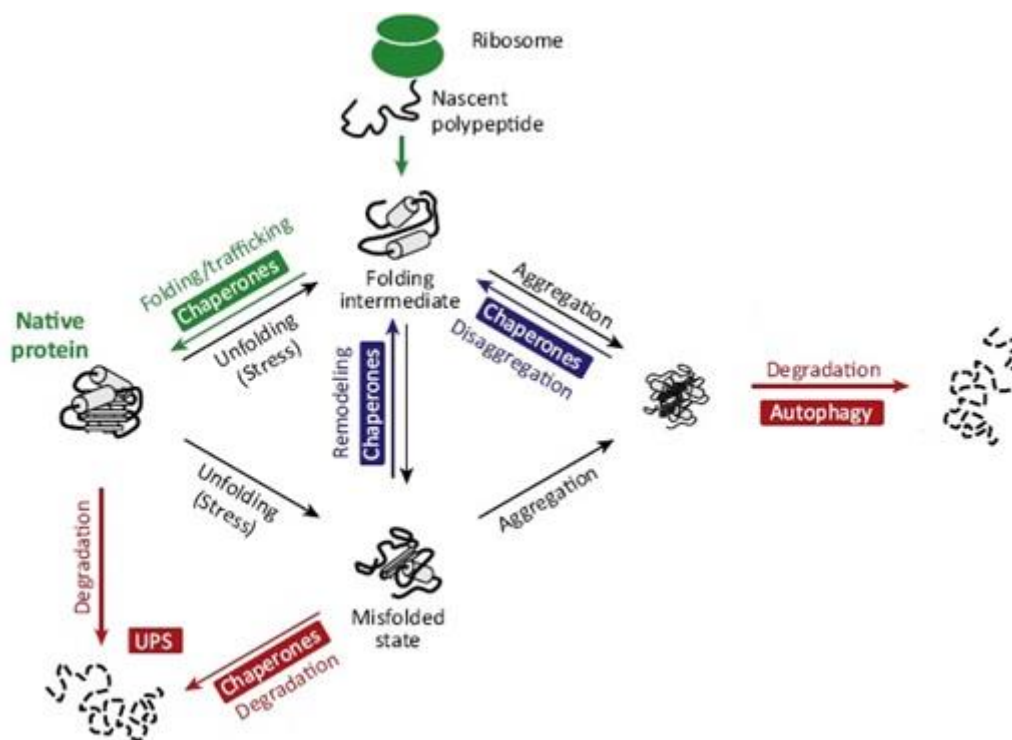


**Figure 10: The proteostasis network (PN).** The PN consists of three branches aimed to the maintenance of protein homeostasis: biogenesis (in green), conformational maintenance (in blue) and degradation (in red). The nascent polypeptide forms a folding intermediate that, if not properly driven to the native state by chaperones, can turn into a prone-aggregation unfolded or misfolded intermediate. This intermediate can be degraded by the ubiquitin-proteasome system (UPS) or can form toxic or less toxic-amorphous aggregates. The aggregates can be dissolved by the disaggregation machinery and proteins can be directed towards either re-folding or degradation via proteasome. Alternatively, not-dissolved aggregates can undergo autophagic clearance (adapted from Hipp et al., 2014).

However, under stress conditions aberrant unfolding proteins may elude the chaperones system control and undergo aggregation. When this happens, cell can respond by different strategies, including disaggregation with recover of the refolded protein or proteasomal degradation and autophagic clearance of protein aggregates (also termed “aggrephagy”; Yamamoto and Simonsen, 2011).

The key component of the disaggregation machinery is the HSP70 chaperone. Heat shock 70 kDa proteins (HSP70s) are ubiquitous molecular chaperones that

function in a myriad of biological processes, including polypeptide folding, degradation, translocation across membranes and protein–protein interactions (Kampinga et al., 2010). Given its ability to play multiple roles HSP70 never works alone, but its activity is driven by a class of cofactors: the J proteins, also known as HSP40s. Historically, J proteins have been divided into three classes (known as DNAJA, DNAJB and DNAJC), although this classification does not reflect either the biochemical function or the mechanism of action of group members, but rather is based on shared domains and motives (Hageman et al., 2009).

Generally, the J proteins orchestrate HSP70 functions by delivering specific client proteins to HSP70 in precise locations in the cell, thus determining their fate. Often multiple J proteins function with a single HSP70, performing different activities. According to the “canonical model” of the HSP70 machinery (Szabo et al., 1994; McCarty et al., 1995; Laufen et al., 1999), J protein initially binds the unfolded client protein preventing its aggregation and delivers it to HSP70, stimulating also HSP70 ATPase activity. Then a nucleotide exchanging factor (NEF) binds to HSP70 causing the release of ADP and the subsequent binding of a new molecule of ATP. ATP binding induces an HSP70 conformational change leading to the release of the client protein and the loading of a new J protein-unfolded client complex and the cycle begins again.

In metazoa, HSP70 exhibits an autonomous disaggregation activity, supported by class A and B-type DNAJ-proteins that enhances loading of HSP70 at the aggregate surface. HSP70 can favor the release of trapped polypeptides from the aggregate applying pulling forces and moving away from the aggregate. Binding of Hsp110, that acts as a NEF, recycles HSP70 to initiate new binding and pulling events (Mogk et al., 2018; Fig.11).

Interestingly, some J proteins localize in precise compartments of the cell where they perform specific functions also in an HSP70-independent manner. More specifically, members of a subclass of the DNAJB family (particularly DNAJB6b and DNAJB8) act as suppressors of aggregation and toxicity of disease-associated polyglutamine proteins and their anti-aggregation activity is performed also in the absence of HSP70 (Fig.11) (Hageman et al., 2010). DNAJB6 is found into two isoforms: the shorter isoform (DNAJB6b) is present in both the nucleus and the cytosol, while the longer isoform (DNAJB6a) is exclusively nuclear (Hanai and

Mashima, 2003) and displays effective anti-aggregation properties only on nuclear aggregates (Hageman et al., 2010).

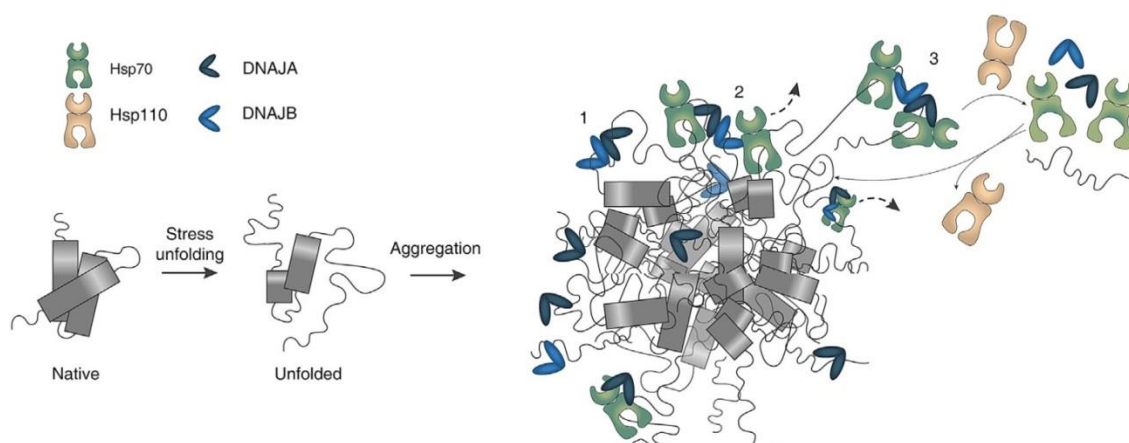


**Figure 11: HSP70 Disaggregation Machinery.** Unfolding stress conditions like heat shock can cause protein unfolding and the formation of amorphous aggregates. A bi-chaperone system formed by Hsp70 and HSP110, with the cooperation of DNAJA and DNAJB co-chaperones, solubilizes aggregated proteins. First, J proteins bind the aggregate (1), then recruit HSP70 at the aggregate surface (2). HSP70 moves away from the aggregate promoting the release and the folding of trapped polypeptides. Finally, HSP110 binds HSP70 and allows its recycle for a new disaggregation event (3) (adapted from Mogk et al., 2018).



## **2. AIM OF THE STUDY**

The aim of my project has been and to understand the molecular mechanism underlying epidermal defects and skin fragility in AEC syndrome using a conditional AEC mouse model as a model. In particular, my study focused on the characterization of molecular pathways involved in the inflammatory state associated with the severe phenotype of AEC conditional mice and the generation and characterization of a novel conditional model for AEC syndrome in a *Tslp* null background.

In addition, I have tested potential therapeutic approaches to treat AEC syndrome based on preventing aggregation and/or enforcing the endogenous protein disaggregation machinery either by an unbiased high-throughput screening of small molecules that may be able to restore the correct folding of the mutant protein, or by genetic manipulations of specific chaperons.

### 3. MATERIALS AND METHODS

#### 3.1 Generation of conditional p63<sup>+/FloxL514F</sup> mouse model

In our laboratory a conditional knock-in model (p63<sup>+/FloxL514F</sup>) was generated, in which the L514F mutation is expressed only in the presence of the CRE recombinase. The knock-in/replacement strategy was designed to replace the wild-type amino acid leucine encoded by codon 514 with a sequence coding for phenylalanine in the p63 protein in murine embryonic stem (ES) cells by homologous recombination. The targeting construct contained two LoxP flanking fused wild-type exons 13 and 14 placed upstream a neomycin resistance cassette flanked by FRT loci and a mutant exon 13 followed by the exon 14 and an immunoeptope tag (3xFlag) at the end of it.

#### 3.2 Mouse genotyping

The conditional knock-in L514F mutant mice p63<sup>+/FloxL514F</sup>, p63<sup>FloxL514F/FloxL514F</sup>, K14Cre;p63<sup>+/FloxL514F</sup> (+/L) and K14Cre;p63<sup>FloxL514F/FloxL514F</sup> (L/L) genotyping was performed by PCR using DNA isolated from mouse tails.

The oligonucleotides primers used for the screening of FloxL514F allele are:

**Forward primer (5'-3'):** CAGCGTATCAAAGAGGAAGGAGA

**Reverse primer (5'-3'):** AGCCAGAATCAGAATCAGGTGAC

A 250bp band is expected for the wild-type mice, a 337bp band for the mutant homozygous mice and both bands for the heterozygous ones.

To screen mice for the presence of Cre-recombinase, the following oligonucleotides primers were used:

**Forward primer (5'-3'):** GGCAGTAAAACTATCCAGCAACA

**Reverse primer (5'-3'):** TAACATTCTCCCACCGTCAGTA

A 300bp band is expected for the K14Cre mice.

### 3.3 RNA isolation and RT-qPCR

Total RNA was extracted from cells using TRIzol reagent (Thermo Fisher Scientific) and retro-transcribed to cDNA using SuperScript Vilo (Thermo Fisher Scientific). RT-qPCR was performed using the SYBR Green PCR master mix (Thermo Fisher Scientific) in an ABI PRISM 7500 (Thermo Fisher Scientific). Target genes were quantified using the following specific oligonucleotide primers and normalized for human RPLP0 expression or for mouse b-actin expression:

#### Oligonucleotide primers used for Real-Time RT-PCR on mouse samples:

Gene	Forward primer (5'-3')	Reverse primer (5'-3')
<b>β-actin</b>	CTAAGGCCAACCGTGAAAA GAT	GCCTGGATGGCTACGTACATG
<b>p63 wt</b>	ACTCTCCATGCCCTCCAC	GAGCAGCCCAACCTTGCT
<b>p63 L514F</b>	ACTCTCCATGCCCTCCAC	GAGCAGCCCAACCTTGCA
<b>Krt5</b>	CAACGTCAAGAAGCAGTGT GC	TTGCTCAGCTTCAGCAATGG
<b>Krt14</b>	ACCACGAGGAGGAAATGGC	TGACGTCTCCACCCACCTG
<b>Dsc3</b>	CCACCGTCTCTCACTACATG GA	TGTCCTGAACTTTCATTATCAGT TTGT
<b>Dsp</b>	CACCGTCAACGACCAGAAC TC	GATGGTGTCTGATTCTGATGT CTAGA
<b>Tslp</b>	GCCAGGGATAGGATTGAGA GTATAGT	GACTGTGAGAGCAAGCCAGCTT
<b>S100a8</b>	AATGACTTCAAGAAAATGGT CACTACTG	ACTATTGATGTCCAATTCTCTGA ACAAG
<b>S100a9</b>	ACAAATGGTGGAAGCACAG TTG	TCATTTATGAGGGCTTCATTTCT CT
<b>Klk5</b>	CTCCTGCCAGGGTGATTCC	CAGGACACAAGGCCCTGTAAC

<b>Klk6</b>	GACATGAAAGAAGGCAACG ATTC	GAGGCGACCCCCACATACTA
<b>Klk7</b>	GCATTCCTGACTCTAAGACC AACA	TTGGAGGGGTGTCGTTGCA
<b>Klk9</b>	AGGCTCTTGCCAGGGTGAC T	CCAGACACTATACCTGCCAAGG T
<b>Klk10</b>	ACGGCCGCACATTGCT	GCAAGTGGTCATCGCCAACCT
<b>NFATc1</b>	CTGGGAGATGGAAGCAAAG ACT	CGGAAAGGTGGTATCTCAACCA

### Oligonucleotide primers for Real Time RT-PCR on human samples

<b>Gene</b>	<b>Forward primer (5'-3')</b>	<b>Reverse primer (5'-3')</b>
<b>RPLP0</b>	GACGGATTACACCTTCCCA CTT	GGCAGATGGATCAGCCAAGA
<b>TSLP</b>	GCTATCTGGTGCCCAGGCT AT	TCTCCTCTTCTTCATTGCCTGAG T
<b>KRT5</b>	CCTCAACAATAAGTTTGCCT CCTT	GCAGCAGGGTCCACTTGGT
<b>KRT14</b>	GGATGACTTCCGCACCAAG T	TCCACACTCATGCGCAGGT
<b>CXCL8</b>	CTGGCCGTGGCTCTCTTG	GCAAAACTGCACCTTCACACA

### 3.4 Primary keratinocytes and cell cultures.

Primary keratinocytes were isolated from the epidermis of newborn mice. 2-3 days old mice were euthanized by hypothermia by placing them in a 100mm Petri Dish and inserted in an ice bucket for 30-45 minutes. Then newborn mice were washed twice with 70% ethanol and twice with water to remove ethanol completely. The skin was removed from each mouse under a tissue culture hood using first sterile surgical scissors to amputate the limbs and the tail and then a sterile scalpel to cut the skin along the dorsal midline from the head to the tail. Using sterile forceps, the whole skin was removed, washed in HBSS and flatten with the dermis down on an empty 6 well dish. Then the skin was incubated overnight at 4°C floating on 2 ml

of Dispase solution (0.80 U/mL Dispase II, 10 mM HEPES, 0.075% sodium bicarbonate, antibiotic/ antimycotic in HBSS) to obtain epidermis-dermis dissociation. The next day the epidermis was peeled away from the dermis with forceps, placed in 2 ml of trypsin solution (0.125% trypsin, 0.1 mM EDTA in HBSS) and cut quickly into very small fragments with scissors to promote the enzymatic and mechanical dissociation of the tissue. The minced epidermis was incubated at 37°C for 5 minutes. Then trypsin was inactivated by adding DMEM medium supplemented with 10% of FBS and the cell suspension was filtered in 70 mm cell strainer to remove undigested tissue and floating fragments. The isolated keratinocytes were plated in collagen coated dishes in high calcium medium to enhance cell attachment. Next day, keratinocytes were washed twice with PBS to remove unattached cells and calcium residuals and grown at 34°C and 8% CO<sub>2</sub> in low calcium medium (0.05 mM CaCl<sub>2</sub>) or treated with 2mM calcium chloride as previously described (Antonini et al., 2010), supplemented with 4% of calcium-chelated Fetal Bovine Serum (FBS) and Epidermal Growth Factor (EGF), changing medium every day.

Human keratinocytes obtained from AEC patients Q11X and T533P (kindly provided by J. Zhou, (Ferone et al., 2013)) and control keratinocytes (Human primary keratinocytes, HK) obtained by unaffected individuals were plated at a density of 10<sup>4</sup> cells/cm<sup>2</sup> and cultured in Epilife medium (Thermo Fisher Scientific) until they reached confluency. Confluent cells were treated with 0.3mM calcium for subsequent analysis.

Normal human epidermal keratinocytes (NHEK-Neo, Lonza; Cat. No. 00192907) were plated at a density of 10<sup>4</sup>cells/cm<sup>2</sup> and cultured in Epilife medium (Thermo Fisher Scientific) until they reach confluence.

H1299 and HEK293T cells were cultured in Dulbecco's Modified Eagle Medium (DMEM) supplemented with 10% FBS.

### **3.5 Skin permeability assay**

Skin permeability of pups at P3 was investigated by toluidine blue dye penetration assay. Small pieces of the embryo tails were cut for genotyping. For toluidine blue

staining, pups were then gently rinsed in PBS and immersed in 25%, 50%, 75%, and 100% methanol for 2 minute each successively. After rehydrated in PBS, pups were placed for 10 min in filtered 0.1% toluidine blue solution for 10 minutes at 4 °C. After staining, pups were rinsed with PBS and photographed using a stereomicroscope (Leica M205FA).

### **3.6 Preparation of CEs**

A defined area of dorsal mouse skin (113 mm<sup>2</sup>) at P3 was incubated at 95°C in CE extraction buffer (100 mM Tris-HCl, pH 8.5, 0.2% SDS, 20 mM DTT, and 5 mM EDTA) under vigorous shaking for 30 min. CEs were collected by centrifugation at 5,000 g. CEs were washed twice at room temperature in CE extraction buffer. Pelleted CEs were dissolved in 0.2% SDS solution and counted using a hemocytometer. The number of intact and altered CEs was counted. The CE suspension was sonicated in a Bioruptor® Sonication System (Diagenode) for 1" at 4 °C. CE aliquots were removed from the sonicator, counted with the hemacytometer, and photographed with a Leica DMI4000B microscope.

### **3.7 Detection of TEWL**

The TEWL on shaved back skin was measured with a Tewameter (TM NANO; Courage and Khazaka).

### **3.8 Serum Na and Cl detection assay**

Blood samples were taken in the morning from isoflurane-anesthetized 7-day-old pups by intra-cardiac puncture and collected into ice-cold microcentrifuge tubes. The sample volume collected was 200 to 300 µL, depending on body mass during final bleeding. Samples were stored at room temperature for 1 to 2 h before being separated by centrifugation. Serum samples were processed immediately after separation or stored at -20° or -80 °C for not more than 1 month before analysis. Serum concentrations of sodium and chloride were analyzed without dilution or diluted 1:2 with deionized water by Integrated Chip Technology (Abbott Diagnostics,

Rome, Italy) with an automated biochemistry analyzer (Architect ci16200 Integrated System, Abbott Diagnostics, Rome, Italy).

### **3.9 RNA-seq analysis**

RNA samples were isolated from epidermis of four mutant versus four wild-type newborn mice at P3 and cleaned using RNase-Free DNase Set (Qiagen). We measured the differential expression of 9198 RNA by QuantSeq technology at TIGEM NGS Facility. The RNA-Seq libraries were sequenced using the Illumina NextSeq 500 to produce 100 bp paired-end reads for each sample. The QuantSeq libraries were prepared using Lexogen's QuantSeq 3' mRNA-Seq Library Prep Kit for Illumina, according to the manufacturer's instructions. The QuantSeq libraries were sequenced using the Illumina NextSeq 500 to produce 100 bp single-end reads for each sample. False Discovery Rate (FDR) correction was performed on the estimated p-value to correct for multiple hypothesis test.

### **3.10 Histology and Immunostaining**

Dorsal skin was dissected, fixed in 4% paraformaldehyde (PFA) and embedded in paraffin or in OCT, from which 7  $\mu$ m sections were cut and stained with Haematoxylin and Eosin (H&E) and immunofluorescence according to standard methods. For paraffin sections, permeabilization for antigen retrieval was performed by microwaving samples in 0.01 M citrate buffer at pH 6.0. The following antibodies were used: keratin 6, keratin 5, keratin 14 (Covance), p63 (4A4, Santa Cruz Biotechnology), E-cadherin (Zymed laboratories-Invitrogen), guinea pig antibody to keratin 15 (a gift from Dr. Langbein), FLAG M2 (Sigma), anti-TSLP antibody (R&D Systems), Col7a1 and Col17aa (a gift from Dr. C. Sitaru), Dsp and Dsc3 (a gift from Dr. H. Thomason) anti-F4/80 (Abcam), anti-CD45 (eBioscience), anti-HMGB1 (a gift from Dr. Marco Bianchi), anti-Ki67 (Dako), NFATc1 (clone 7A6 Santa Cruz Biotechnology), Klk6 (a gift from Dr. Mari Kishibe). The following secondary antibodies were used for immunofluorescence staining: Alexa Fluor® 488 goat anti-mouse (Invitrogen), Alexa Fluor® 594 goat anti-rabbit (Invitrogen), Alexa Fluor® 594 goat anti-rat (Invitrogen). Fluorescent signals were monitored under a Zeiss

Axioskop2 plus image microscope or under a Zeiss confocal microscope LSM510meta. Sections were counterstained with DAPI nuclear stain.

### **1.11 Retroviral preparation**

High-titer retroviruses were produced in HEK293T cells by transient co-transfection of pBABE p63 constructs or pMXs-KLF4 plasmid and amphotropic viral envelope plasmid (pAmpho). Cells were plated on collagen coated-60mm dishes the day before transfection. Subconfluent cells were co-transfected using 6mg of pBABE or pMXs constructs and 6mg of pAmpho plasmid in the presence of 30ul of Lipofectamine 2000 (Thermo Fisher Scientific), according to the manufacturer's instructions. Cell supernatants containing the retroviruses were collected 48 hr after transfection, then fresh medium was added and collected again 72 hr after transfection. Finally, the retrovirus preparation was filtered using 0.45µm filters to remove cell debris.

### **1.12 Retroviral infection**

Mouse primary keratinocytes newly-isolated from wild type mice (C57BL/6 strain) were infected the day after plating at 50% confluence in 35mm dish with retroviruses carrying the GFP (PINCO) or NFATc1 (Porter & Clipstone, 2002), produced as described above, in the presence of 8 µg/ml Polybrene. Cells were incubated in the retrovirus mix for 2 hr at 34°C and 8% CO<sub>2</sub>. Since retroviruses were produced in the high-calcium medium of HEK293T cells, keratinocytes were washed twice with PBS after infection to remove calcium residuals and then low calcium medium was added. Cells were infected for two consecutive days and 48 hr after the second infection were selected with 1µg/ml puromycin. After 48 hr uninfected control keratinocytes were died and infected cells were collected for RT-qPCR and Western blot analysis.



### **1.13 ELISA**

Serum TSLP levels were determined using Quantikine mouse TSLP kit according to manufacturer's instructions (R&D Systems) and was measured with Multiskan™ FC Microplate Photometer (Thermo Fisher Scientific).

### **1.14 Luciferase reporter assay**

Luciferase assays in H1299 cells were performed using the reporter constructs K14 promoter-luc (Candi et al., 2006) or FGFR2 enhancer-luc (Ferone et al., 2012) or BDS2 3X (Hermeking et al., 1997), that carry firefly luciferase gene under the control of Keratin 14 promoter, FGFR2 enhancer and p53 binding site, respectively. 70% confluent cells were co-transfected in 24-well dishes with 100ng of reporter construct and different concentrations (100ng or 200ng) of plasmid encoding wild type or mutated  $\Delta$ Np63 $\alpha$  at a ratio 1:4, using Lipofectamine 2000 (Thermo Fisher Scientific) following the manufacturer's instruction.

Luciferase activities were measured in the same sample 48hr after transfection using the dual-luciferase reporter assay kit (Promega).

### **3.15 BN-PAGE, SDS-PAGE and Western Blot**

For BN-PAGE H1299 cells or mouse primary keratinocytes were scraped on ice in Native lysis buffer (25 mM Tris (pH 7.5), 150 mM NaCl, 2 mM MgCl<sub>2</sub>, 20 mM CHAPS, 1 mM DTT and protease inhibitors), collected and incubated 1h in ice in the presence of benzonase (Merck) for lysis and digestion of nucleic acids. Native lysates were then mixed with 20% Glycerol and 5mM Comassie G-250 and loaded on 3–12% Novex Bis-Tris gradient gel for BN-PAGE (NativePAGE system, Thermo Fisher Scientific), according to the product manuals.

For SDS-PAGE, cells were lysed in Laemmli buffer (10% glycerol, 0.01 % Bromophenol Blue, 0.0625 M Tris-HCl pH 6.8, 3 % SDS, 5 %  $\beta$ -mercaptoethanol), boiled and loaded on denaturing SDS-PAGE gel. To isolate nuclear and cytoplasmic extracts from keratinocytes, the extraction kit "NE-PER™ Nuclear and Cytoplasmic Extraction Reagents" (Thermo Fisher Scientific) was used following the

manufacturer's instruction. Protein concentration was then measured by Bradford assay and 8µg of each extract, nuclear or cytoplasmic, were loaded for SDS-PAGE.

For SDS-PAGE of epidermal extract, epidermis was isolated from dermis by floating skin biopsies, epidermis side up, in a Dispase solution. After isolation from dermis, epidermis was snap frozen in liquid nitrogen and then homogenized with a tissue lyser in sample buffer (10% glycerol, 0.01 % Bromophenol Blue, 0.0625 M Tris-HCl pH 6.8, 3 % SDS, 5 % β-mercaptoethanol) supplemented with phosphatase and protease inhibitors.

For Western Blot, proteins were transferred after run to Immobilon-P transfer membranes (Millipore) and probed with the antibodies diluted in PBS-0.2% Tween-20 with 5% nonfat-dry milk. The primary antibodies used for Western Blot analysis were: anti-p63 (EPR5701), p63 (4A4 Santa Cruz Biotechnology), (Santa Cruz Biotechnology), anti-Keratin 14 (Covance), anti-β-Actin (AC-15, Santa Cruz Biotechnology), anti-HSP70/HSC70 (W27) (Santa Cruz Biotechnology), anti-V5 (Thermo Fisher Scientific), anti-FLAGM2 (Sigma-Aldrich), Cdh1 (BD Bioscience), Krt5, Krt14, Krt1, Krt10, Ivl, Lor (Covance), krt15 (a gift from Dr. Langbein), Notch1 (Santa Cruz Biotechnology), ERK-1 (Santa Cruz Biotechnology), Kik5 and Kik7 (R&D Systems), Kik6 (a gift from Dr. Mari Kishibe). Secondary antibodies donkey anti-rabbit or sheep anti-mouse IgG conjugated to horseradish peroxidase (HRP) (GE Healthcare) were used and revealed by chemiluminescence (ECL, GE Healthcare Sciences).

### **3.16 CHX degradation assay**

H1299 cells were plated 12-wells and co-transfected at 95% confluence the day after plating with 150 ng of pCDNA3.1- DNp63a-myc (wild type or R589L) plasmid and 1.5 mg of pcDNA5-FRT/TO V5 DNAJB2a or DNAJB2b or DNAJB6a or DNAJB6b plasmid, using Lipofectamine 2000 (Thermo Fisher Scientific). After 24hr, cells were treated with 100 µM cycloheximide (CHX) to inhibit protein synthesis. At different time points (0, 6, 12, 18 and 24hr) cells were washed twice with PBS and lysed in 150µL of native lysis buffer (25mM Tris (pH 7.5), 150mM NaCl, 2mM MgCl<sub>2</sub>,

20mM CHAPS, 1mM DTT, and protease inhibitors) and incubated for 1 h on ice in the presence of 0.5 u/μL benzonase (Merck Millipore).

### **3.17 Differentiation and PRIMA-1-Met treatment of human epidermal keratinocytes**

Human keratinocytes were cultured at low density in six-well plates in Epilife medium with Human Keratinocyte Growth Supplement (HKGS). The differentiation process *in vitro* occurred when cells reached the full confluence (covering 100% of the dish area). When keratinocytes became 100% confluent, the Epilife growth medium was switched to Epilife medium supplied with 1.5 mM CaCl<sub>2</sub>, to sustain differentiation, and replaced every two days with fresh medium.

As they became 30% confluent, they were treated with 30 μM PRIMA-1MET, or the vehicle as control, replacing the culture medium with the compound every 48 h until the harvesting. At 100% of confluence, cells underwent differentiation by raising calcium concentration of the medium to 1.5mM. After 10 days of differentiation, cells were lysed in native lysis buffer (25mM Tris (pH 7.5), 150mM NaCl, 2mM MgCl<sub>2</sub>, 20mM CHAPS, 1mM DTT, and protease inhibitors) and incubated for 1 h on ice in the presence of benzonase (Merck Millipore). Protein extracts were loaded on 3–12% Novex Bis-Tris gradient gel for BN-PAGE (Life Technologies) in 20% glycerol and 5mM Coomassie and analyzed by western blotting using p63-specific antibody (anti-p63EPR5701, ab124762, Abcam). Relative quantification of protein band intensity was performed using Image Lab Software (Bio-Rad).

## 4. RESULTS

### 4.1 Epidermal-specific L514F mutation results in severe postnatal epidermal barrier defects

To study the molecular defects occurring after birth in AEC syndrome and to overcome the lethality due to cleft palate of the constitutive AEC mouse model (Ferone et al, 2012), we crossed p63<sup>+/*flox*L514F</sup> mice with Krt14-Cre knock-in mice, in which Cre is highly expressed by Embryonic day 17.5 (E17.5) under the control of the endogenous keratin 14 promoter (Huelsen et al, 2001). In this mouse model, the p63<sup>L514F</sup> mutant protein was expressed only in the presence of the CRE recombinase and it was fused to a 3xFLAG tag at the C-terminus (Fig. 12A). The knock-in strategy was designed to replace the wild-type amino acid leucine encoded by codon 514 with phenylalanine in the p63 protein in murine embryonic stem (ES) cells by homologous recombination.

K14-Cre; p63<sup>+/*flox*L514F</sup> (+/L) newborn mice were indistinguishable from wild type littermates until they reached adulthood when they exhibited a partial and progressive mild hair loss (Fig. 12B). At the histological level, the adult mice (P50) showed epidermal abnormalities characterized by an overall reduction of epidermal thickness with focal hyperplasia and hypercellularized of dermis accompanied with a strong reduction of Fgfr2 in mutant epidermis and in the permanent portion of the hair follicle, similarly to what observed in the constitutive AEC mouse model (Fig.12 C) (Ferone et al., 2012).

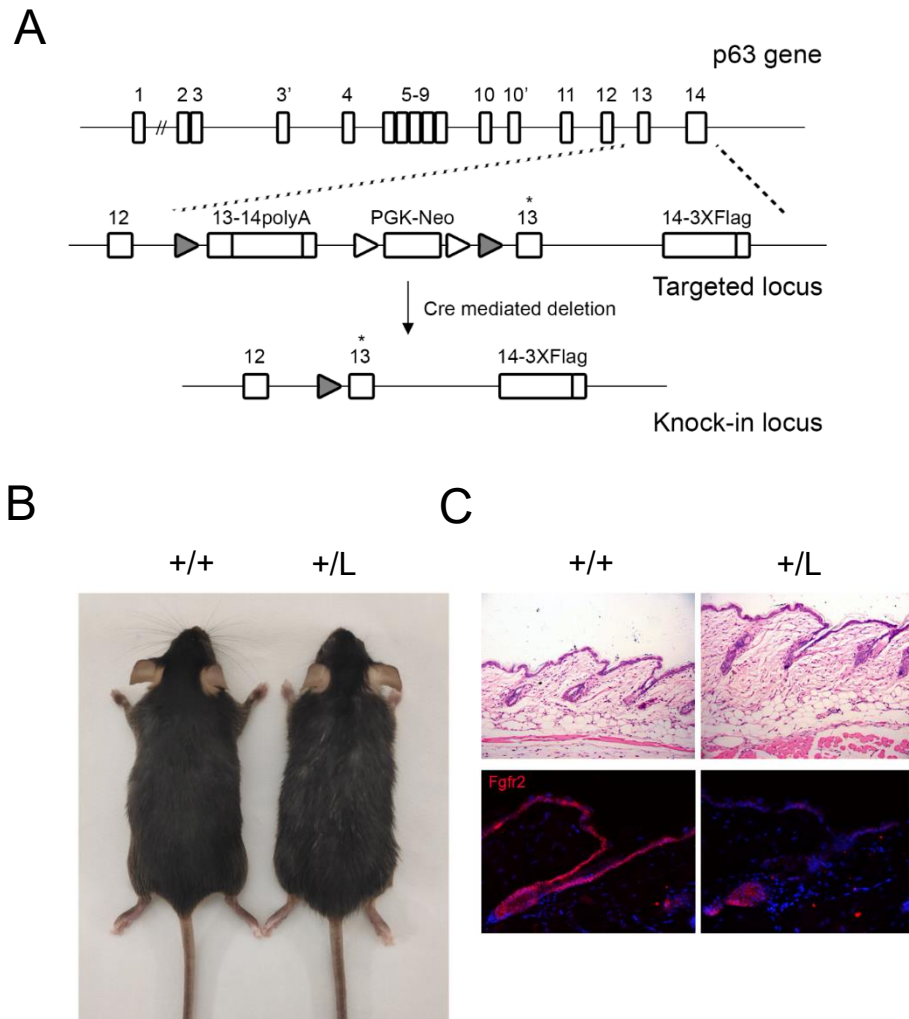


**Figure 12: Generation and characterization of +/L mouse model:** A) Gene targeting strategy used to generate the  $p63^{+/L514F}$  knock-in mice. The L514F mutation is indicated with \* The targeting construct contained two LoxP flanking wild-type exons 13 and 14 fused together and placed upstream a neomycin resistance cassette flanked by FRT loci and a mutant exon 13 followed by the exon 14 and an 3XFLAG epitope tag at the end of it. B) Photographs were taken of +/+ and +/L at 30 days. C) H&E staining of dorsal skin of K14Cre;  $p63^{+/floxL514F}$  (+/L) and control (+/+) mice at P50 reveals focal hyperplasia and hypercellularized of dermis (upper panel). Immunofluorescence analysis of Fgfr2 on dorsal skin of +/L514F and +/+ mice at P50 reveals the reduction of expression of Fgfr2 in the basal layers of the epidermis (lower panel).

Given the relatively mild phenotype which did not reflect the severity of the human disorder, mutant mice were crossed to homozygosity to obtain Krt14-Cre;  $p63^{floxL514F/floxL514F}$  ( $p63^{L/L}$ ) mice. Immunofluorescence analysis with anti-FLAG antibody revealed a uniform expression of the mutant protein in the basal compartment of the interfollicular epidermis at birth, while wild-type  $p63\alpha$  was virtually absent (Fig. 13B). Immunoblot analysis confirmed that by post-natal day 3

(P3) wild-type p63 was virtually absent in L/L epidermis and about 50% expressed in +/L epidermis (Fig. 13A).

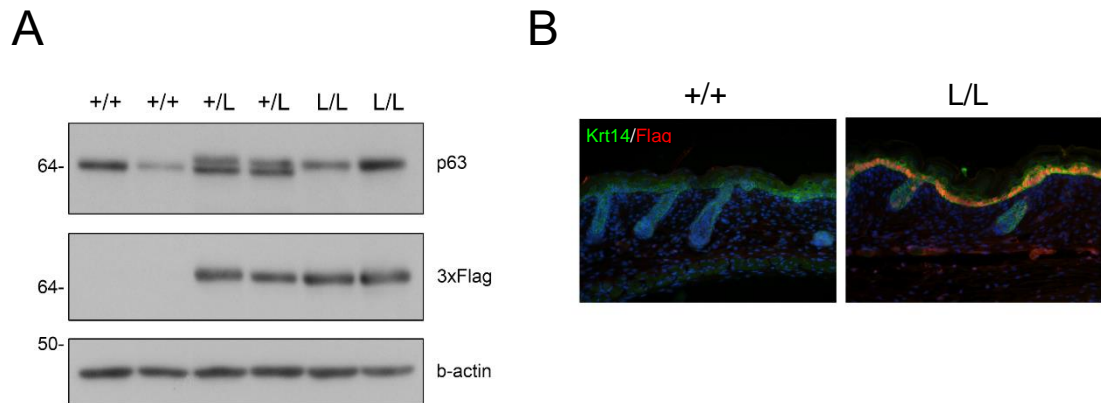


**Figure 13: L514F conditional expression in AEC mutant mice.** A) Immunoblotting of total cell extracts from wild type (+/+), p63<sup>+/L</sup> (+/L) and p63<sup>L/L</sup> (L/L) neonatal epidermis (P3) using antibodies against p63 and cdh1 as loading control. B) Immunofluorescence staining of p63<sup>L/L</sup> and wild type (+/+) skin revealed the expression of the p63<sup>L514F</sup>-3xFLAG protein in the basal layer of the epidermis and hair follicle at P3 in mutant skin compared to wild-type mice. Nuclei are stained with DAPI.

At birth p63<sup>L/L</sup> mutant mice had no evident skin defects and they were indistinguishable from their wild-type littermates. However, ~14% of newborn mice died before P5 and macroscopic epidermal defects became evident with dry scaly skin and large areas of skin erosion (Fig. 14A-B). Starting at P3, all p63<sup>L/L</sup> mutant mice developed a progressively severe phenotype, characterized by skin erosions and exfoliative erythroderma, associated with stunted growth, and died within 15 days after birth (median survival 9 days) (Fig. 14C), suggesting a compromised epidermal barrier in p63<sup>L/L</sup> mutant mice. A significant reduction of body weight was observed at P7 (Fig. 14D).

Epidermal barrier defects lead to water loss, weight loss, electrolyte imbalances, and loss of skin turgor (Shwayder and Akland, 2005). The p63<sup>L/L</sup> mutant mice showed a significant reduction of body weight at P7 and significantly increased serum sodium concentration levels compared with control mice (Fig. 14E). The combination of hypernatremia, hyperchloremia and weight loss suggested dehydration as the underlying cause of death in p63<sup>L/L</sup> mutant mice.

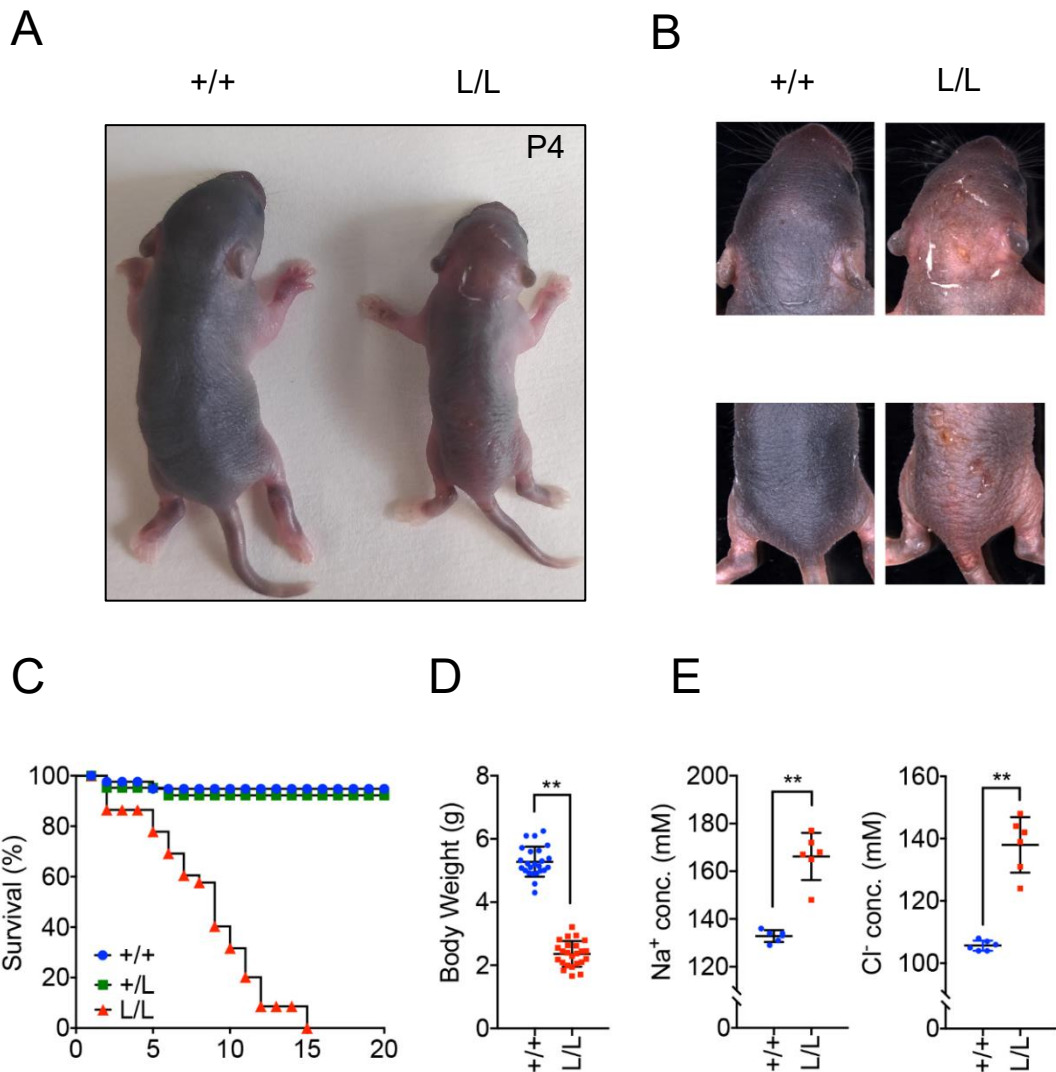


**Figure 14: Phenotype of AEC mutant mice:** A) Photographs are taken from wild type and  $p63^{L/L}$  mice at P4. B) From P3  $p63^{L/L}$  mice showed a progressively strong phenotype characterized by shallow skin erosions, skin crusting, hair loss and ulcerations that worsen throughout their life. C) Survival curve of  $p63^{L/L}$  (L/L red line),  $p63^{+/L}$  (+/L green line) and wild type (+/+ blue line) mice ( $n=110$ ). D) Body weight at P7 of  $p63^{L/L}$ ,  $p63^{+/L}$  and wild type mice ( $n=72$ ). E) Serum  $\text{Na}^+$  and  $\text{Cl}^-$  concentrations. Serum samples were taken from P7 mice and were analyzed for  $\text{Na}^+$  ( $166.7 \pm 4.03$  ( $n=6$ ) vs  $135.30 \pm 0.95$  ( $n=12$ ), P value  $< 0.0001$ ) and  $\text{Cl}^-$  ( $138.00 \pm 3.64$  ( $n=6$ ) vs  $106.00 \pm 0.46$  ( $n=12$ ), P value  $< 0.0001$ ). Results: mean  $\pm$  SD. Student's t test: \*,  $P < 0.05$ ; \*\*,  $P < 0.01$ ; \*\*\*,  $P < 0.001$

To test the hypothesis that the progressive dehydration observed in AEC mutant mice may be due to at least partially impaired integrity of the epidermal barrier, we performed a dye penetration assay to examine the integrity of the skin barrier. The epidermis of mice at E17.5 was completely resistant to toluidine blue penetration (data not shown), whereas newborn mutant mice (P3) showed dye permeability with

focal gaps in the mechanically stressed areas, including in snout and dorsal skin, consistent with the focal skin blistering observed at histological level (Fig. 15A-B).

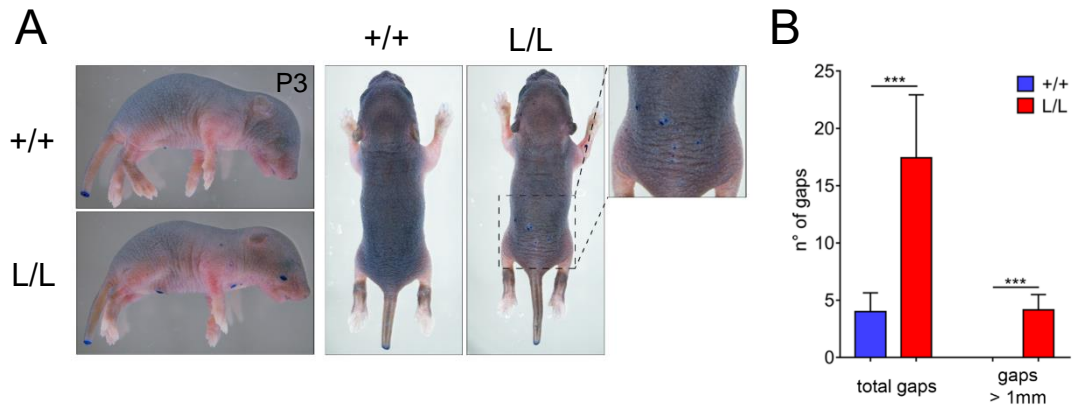


**Figure 15: Impaired skin barrier function.** A) Barrier assay at P3 on L514F and control mice (WT) revealed the presence of focal gaps in mutant mice. B) Representation of number of total gaps and gaps with diameter > 1mm in p63<sup>L/L</sup> mice compared to wild type mice (n= 7). Results: mean  $\pm$  SD. Student's t test: \*, P<0.05; \*\*<0.01; \*\*\*, P<0.001.

Transepidermal water loss (TEWL) of the skin surface was higher in p63<sup>L/L</sup> mutant mice than in wild type mice at P3, P5 and P8, indicating severe inside-out barrier defects and that weight loss in p63<sup>L/L</sup> mutant mice was caused by elevated body water loss (Fig. 16A). Because epidermal lipids are crucial to form the protective barrier of the skin in the stratum corneum we stained P3 skin sections with the lipophilic dye Nile Red (Fig. 16B). No significant differences in epidermal lipid content and distribution were observed dye Nile Red. No significant differences in epidermal lipid content and distribution were observed.

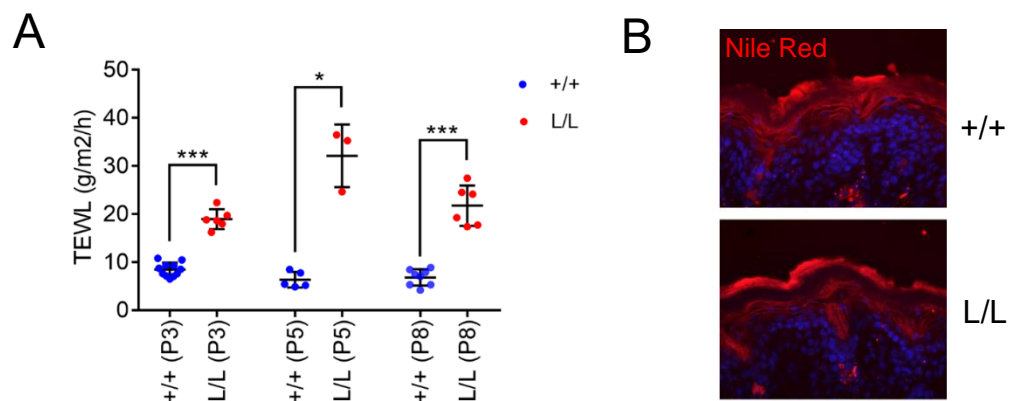


**Figure 16: Inside-out barrier defects** A) TEWL from p63<sup>L/L</sup> mice compared with wild type mice at P3, P5 and P19 (n $\geq$ 3). Results: mean  $\pm$  SD. Student's t test: \*, P<0.05; \*\*<0.01; \*\*\*, P<0.001. B) Fluorescent images of skin slices treated with NR (2.5  $\mu$ g/ml) for NR dye for about 10'.



Since, impaired integrity of the cornified envelope (CE) has been linked to skin barrier defects (Sevilla et al., 2007), we analyzed CE preparations derived from dorsal skin of P3 mice. This analysis revealed a reduction of integrity in mutant versus control preparations (Fig. 17A-B).

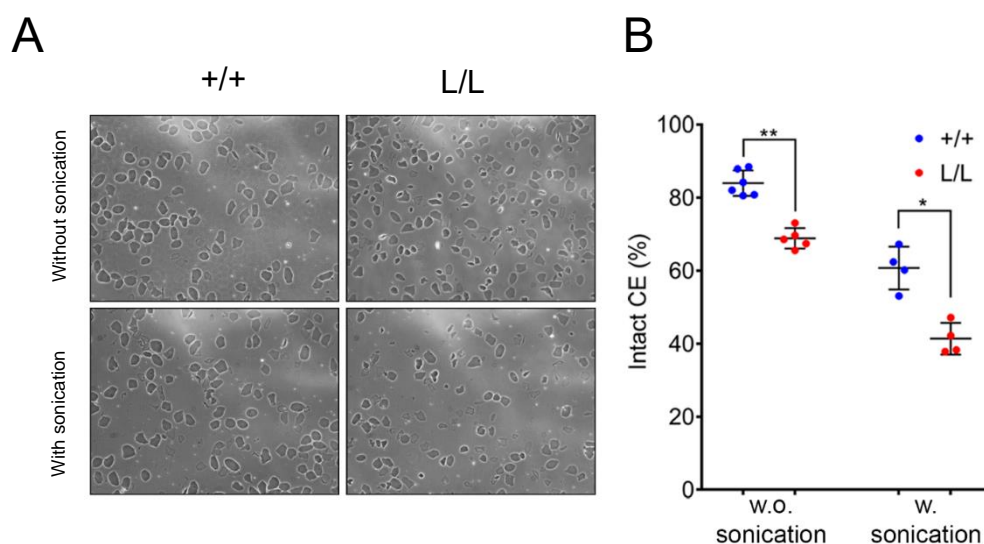


**Figure 17: Fragility of mutant CE.** (A and B) wild type (+/+) and  $p63^{L/L}$  (L/L) CE at P3 were isolated and treated with ultrasound for 1". 15% of CEs were disrupted in wild type (+/+) compared with 30% in  $p63^{L/L}$  (L/L) before sonication ( $n \geq 5$ ). 33% of CEs were disrupted in wild type (+/+) compared with 58% in  $p63^{L/L}$  (L/L) before sonication ( $n \geq 4$ ). Results: mean  $\pm$  SD. Student's *t* test: \*,  $P < 0.05$ ; \*\*,  $P < 0.01$ ; \*\*\*,  $P < 0.001$ .

#### 4.2 Dysregulated epidermal differentiation markers and defective adhesion molecules in AEC mice

To obtain a global view of changes in gene expression of AEC mutant mice, we performed a comparison of gene expression profiling of mutant versus wild-type epidermis at P3 using RNA-seq. Analysis of the data revealed that a subset of genes, known to be p63 target genes, is down-regulated by L514F mutation. Among the p63 targets affected in mutant epidermis we found the two fibroblast growth factor receptors *Fgfr2* and *Fgfr3* and *Krt15* (Ferone et al., 2012), *Col17a1* and *Dst*, two genes encoding for hemidesmosome components (Carroll et al., 2006), *Ddit4* gene, also called *Redd1*, a developmentally regulated transcriptional target of p63 and p53, involved in DNA damage (Ellisen et al., 2002), and *Notch1* and *Jag2*, two key components of the Notch signaling pathway (Nguyen et al., 2006)(Fig. 18A).

In contrast, AEC mutant epidermis displayed increased focal expression of some keratins, including *Keratin 16 (Krt6)* and *Keratin 16 (Krt16)* that were essential to maintain keratinocyte integrity in wounded epidermis, and *Keratin 8 (Krt8)* and *Keratin 18 (Krt18)*, simple epithelial keratins, that for their nature could participate to intermediate filaments but did not confer strong mechanical resistance to the epithelium. Also kallikreins, enzymes with serine protease activity that regulate the desquamation of the epidermis (Candi et al., 2005) were strongly up-regulated thus indicating an altered equilibrium in epidermis structure (Fig. 18B and B).

Surprisingly, we found a strong up-regulation of inflammatory genes. In particular, we found an up-regulation of one hundred fold of *Tslp*, an IL-7-like cytokine produced by epithelial cells, including keratinocytes that was highly expressed in the epidermis of atopic dermatitis and asthmatic patients (Ziegler and Artis, 2010) (Fig. 18C). In addition to *Tslp* induction, our microarray data revealed us also the induction of damage-associated molecular pattern molecules (DAMPs) that initiate the inflammatory response in the event of a disruption of the epidermal barrier, such as the inflammatory complex of calprotectin (*S100a8/ S100a9* complex), and -to a lesser extent- antimicrobial peptides, *Defb4* and *Defb6* (Fig. 18C).

A		B		C	
p63 target genes		Terminal differentiation genes		Biological processes	
Gene Symbol	Fold +/-ctr	Gene Symbol	Fold +/-ctr	Gene Symbol	Fold +/-ctr
Fgfr2	0.43	Klk10	3.36	Defb4	2.58
Fgfr3	0.36	Klk5	1.20	Defb6	2.31
Krt15	0.30	Klk6	5.12	S100a8	9.03
Col17a1	0.44	Klk7	1.42	S100a9	7.81
Dst	0.57	Klk9	1.56	Tslp	112.93
Ddit4	0.49			Krt6a	11.09
Notch1	0.44			Krt6b	14.18
Jag2	0.63			Krt16	9.24

**Figure 21. Gene expression analysis.** A) RNA-seq data confirmed that a subset of known p63 target genes are affected in the epidermis of L/L mice at P3 compared to wild-type controls. B-C) RNA-seq data indicated that a subset of genes involved in different biological processes were down-regulated and up-regulated consistently with what we observed in AEC mutant mice.

The skin morphology of the wild type and p63<sup>L/L</sup> mutant mice was examined by hematoxylin and eosin staining. Histological analysis of the back skin revealed a mild epidermal hypoplasia at P0 in AEC mutant mice with apparently normal upper

layers and an intact cornified layer (Fig. 19A). Interestingly, histological analysis of the back skin at P3, showed epidermal hyperplasia (acanthosis), irregularity in the basal layer and increased number of infiltrates in the dermis (Fig. 19B). Epidermis of p63<sup>L/L</sup> mutant mice showed skin blistering localized both between the basal and suprabasal layers and among cells of the basal layer consistent with previous observations in the AEC constitutive mouse model and in agreement with a crucial role of p63 in cell-cell adhesion (Fig. 19C) (Ferone et al., 2013; Ferone et al., 2015).

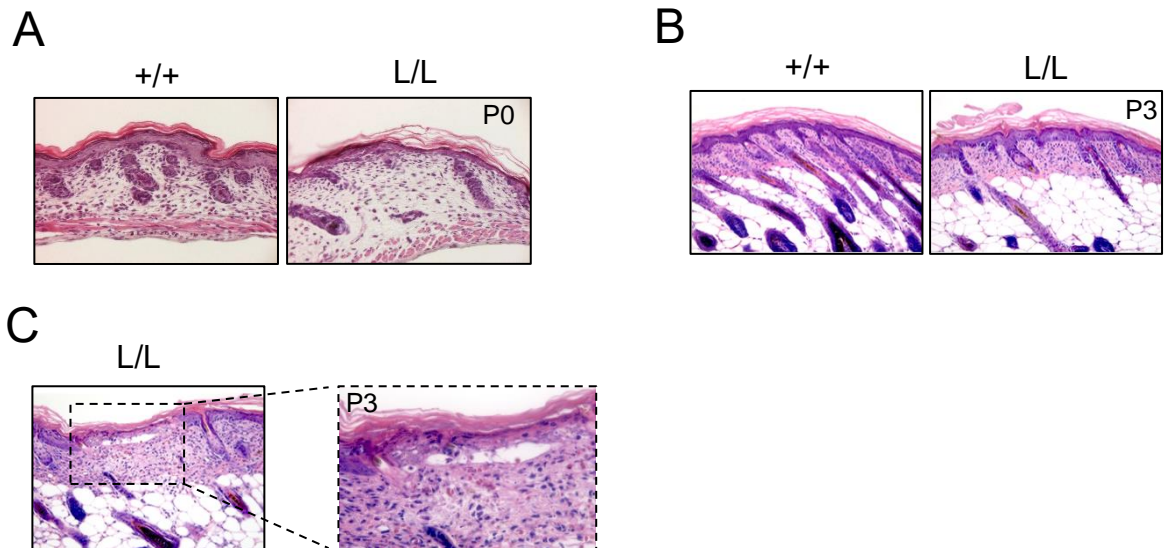


**Figure 19: Epidermal blistering and skin fragility in AEC mutant mice.** A) H&E staining of dorsal skin of L/L mice at P0. Mutant epidermis was thinner. B-C) H&E staining of dorsal skin of L/L mice at P3. Mutant epidermis was hyperplastic, with less developed hair follicles and focal gaps were visible in L/L epidermis.

The attachment of basal cells to the extracellular matrix is of crucial importance in the maintenance of tissue structure and integrity. Importantly, skin blistering in p63<sup>L/L</sup> mice was also observed underneath the basal cell compartment consistent with a defect in cell-matrix adhesion. Two crucial components of cell-matrix adhesion between the basal layer and the basement membrane are collagen VII (Col7a1) and collagen XVII (Col17a1), which are mutated in different forms of epidermolysis bullosa. Immunostaining analysis showed a strong reduction in Col7a1 expression, and somewhat reduced and delocalized of Col17a1 (Fig. 20A). Real time qPCR analysis of Col7a1 and Col17a1 confirmed a dramatic reduced expression of both in epidermis of p63<sup>L/L</sup> mutant mice (Fig. 20B).

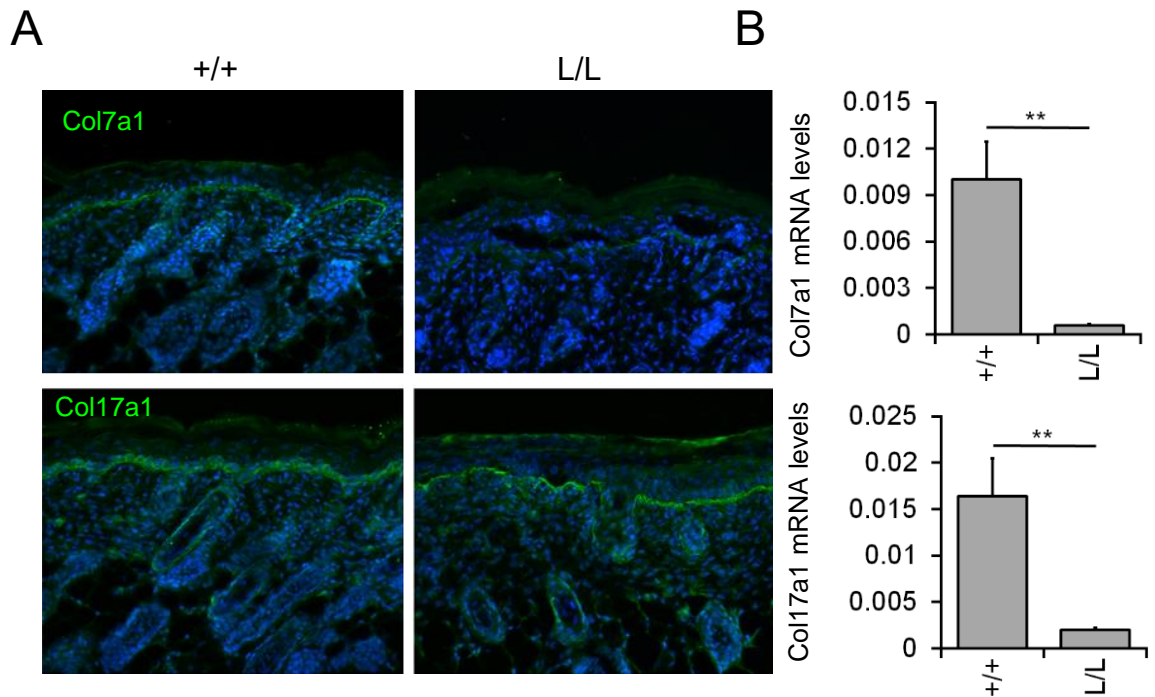


**Figure 20: Skin blistering in the AEC mouse model.** A) Immunofluorescence on frozen section of dorsal skin at P3 for Collagen VII revealed a strong reduction of the protein in p63<sup>L/L</sup> mutant epidermis respect to the controls, whereas for Collagen XVII revealed reduction and delocalization of the protein. B) real time qPCR analysis of Col7a1 and Col17a1 revealed reduction of expression in p63<sup>L/L</sup> mutant epidermis respect to the control (n=4). Results: mean ± SD. Student's *t* test: \*, P<0.05; \*\*<0.01; \*\*\*, P<0.001.

Interestingly, other cell surface or extracellular components involved in basal cell-to-basement membrane adhesion, such as Itgb5, Dst, Frem2, Lamb3 and Fras1 were strongly reduced at the mRNA levels in epidermis of p63<sup>L/L</sup> mice compared to wild type mice (Fig. 21A). Among them expression of Dst (also named BP230 or BPAG1 for Bullous pemphigoid antigen), a crucial hemidesmosome component together with Col17a1 (BP180 or BPAG2 for Bullous pemphigoid antigen 2) was severely compromised. Therefore, reduced expression of these crucial genes is likely to significantly contribute to the formation of subepidermal blistering in response to minor trauma.

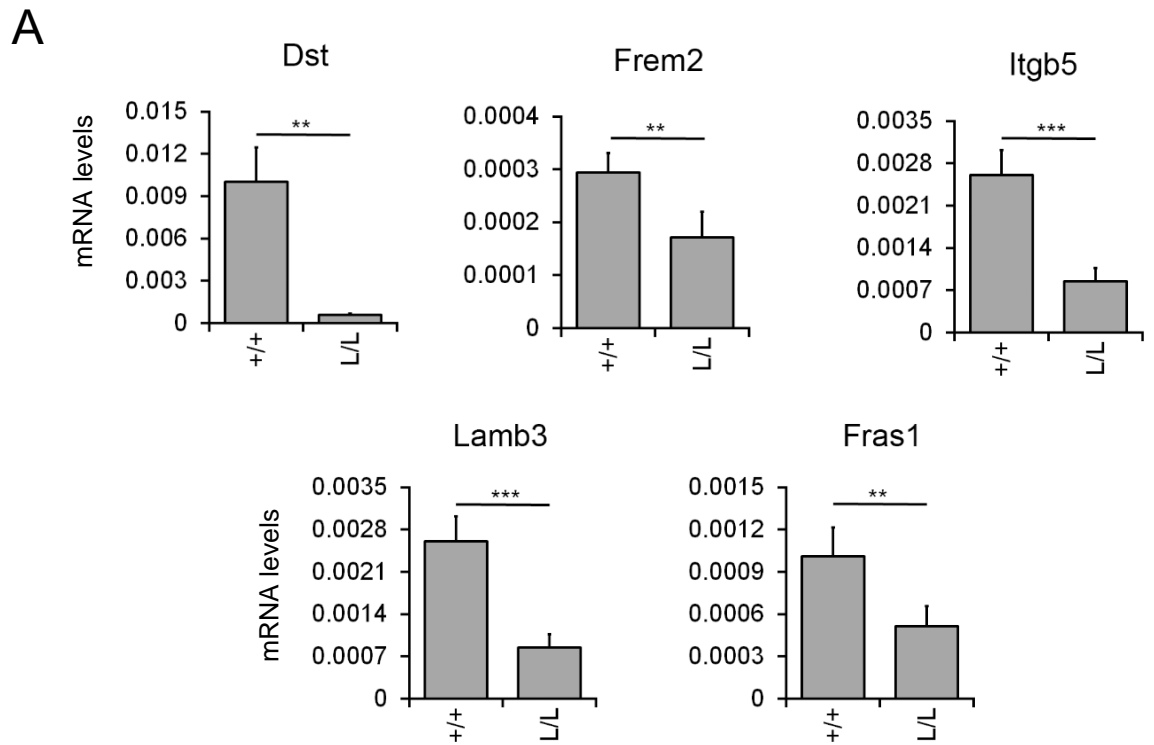


**Figure 21: Hemidesmosomal constituents are down-regulated in AEC skin.** A) real time qPCR analysis of Dst, Frem2, Itgb5, Lamb3 and Fras1 revealed reduction of expression in p63<sup>L/L</sup> mutant epidermis respect to the control (n=4). Results: mean  $\pm$  SD. Student's t test: \*, P<0.05; \*\*<0.01; \*\*\*, P<0.001.

In addition, immunostaining for basal keratin Krt14 revealed that epidermal blisters were not only accompanied by reduced cohesion between keratinocytes (acantholysis), and between keratinocytes and basement membrane, but also by basal cell disruption (cytolysis) (Fig. 22A).

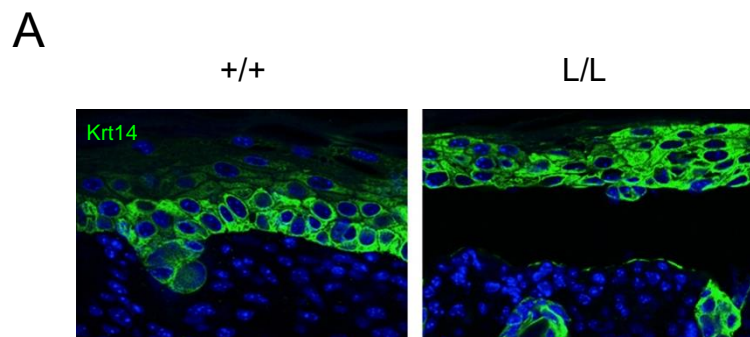


**Figure 22: Cell disruption in keratinocytes of basal layer.** A) Immunofluorescence analysis of dorsal skin for Krt14 revealed that in L/L skin focal blistering were accompanied by acantholysis and cytolysis.

In epidermal cells, keratins constitute intermediate filaments (IF) that are crucial to protect epithelial cells from mechanical stresses that cause cell rupture and death (Coulombe et al, 2009). Previous evidence from our laboratory indicated that keratin 15 (Krt15), a keratin expressed in the basal layer and in the hair follicle buldge, is downregulated in AEC syndrome (Ferone et al 2012). While Krt15 is expressed at relatively lower levels, IF in the basal layer are mainly composed by keratin 5 (Krt5) and keratin (Krt14) that pair to form a strong structure. The expression level analysis of keratins in epidermis of p63<sup>L/L</sup> mutant and wild type mice confirmed reduced levels of Krt15, but also revealed a strong reduction in expression of Krt5 and Krt10, a marker of the spinous layer (Fig. 23A). In contrast, the analysis of the late differentiation markers, such as loricrin and involucrin, revealed that are normally expressed in mutant mice (data not shown).

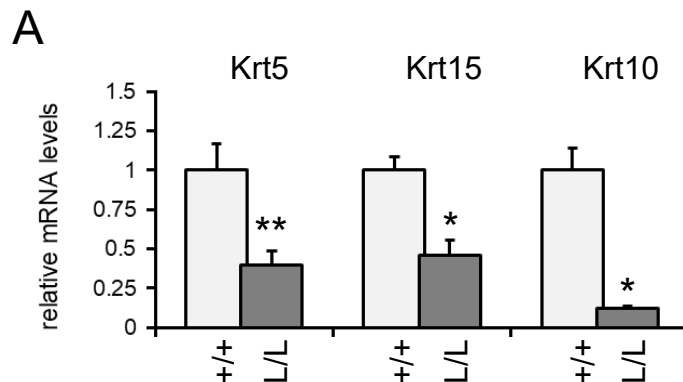


**Figure 231: Expression of keratins in the AEC mouse model** A) real time qPCR analysis of Krt5, Krt15 and Krt10 revealed reduction of expression in p63<sup>L/L</sup> mutant epidermis respect to the control (n=4). Results: mean ± SD. Student's t test: \*, P<0.05; \*\*<0.01; \*\*\*, P<0.001.

In agreement with the alteration of keratins of the basal layer, ultrastructural analysis obtained by transmission electron microscopy demonstrated reduces keratin bundles in the basal layer of the epidermis of mutant mice compared to controls (Fig. 24A).

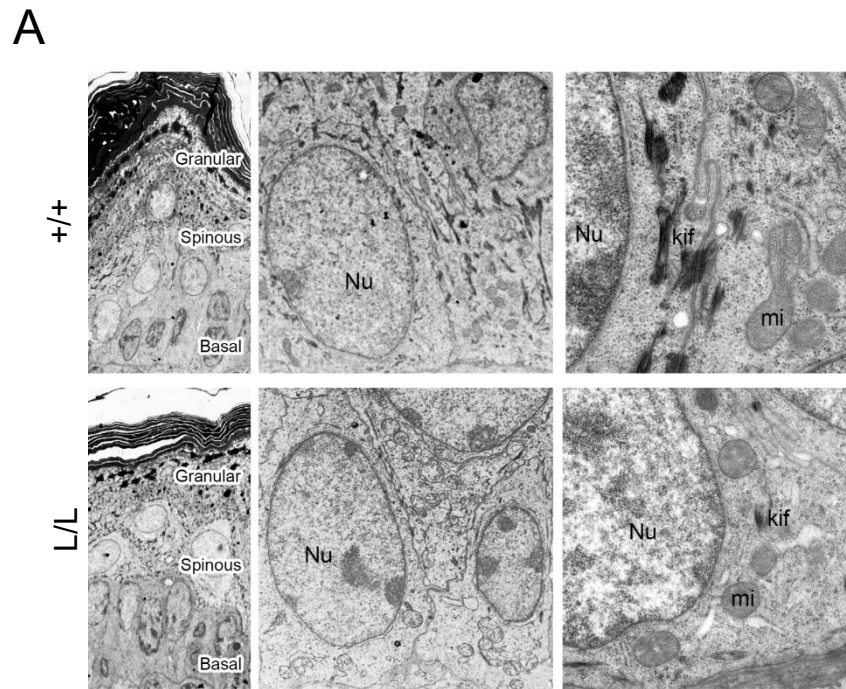


**Figure 24: TEM analysis in AEC skin.** A) Tissue-electron microscopy (TEM) of newborn skin.

In conclusion these data indicate that the skin phenotype observed in AEC mutant mice is likely due to reduced mechanical strength of the lower layers of the epidermis, due to reduced expression of IF, cell-to-cell adhesion and cell-to-matrix components, causing skin blistering and erosions. In addition, a focal impairment in the epidermal barrier was observed.

### 4.3 Inflammation in AEC mouse model

Few days after birth (P3), skin of mutant mice progressively became hyperplastic with signs of inflammation, consisting in acanthosis of the epidermis with multifocal hyperkeratosis (Fig. 25A). In addition, we observed a massive inflammatory infiltrate in the dermis and the epidermis associated with spongiosis in the basal layers and hypercellularization of the dermis. A marker of perturbed differentiation, Krt6 was massively expressed throughout all layers of mutant epidermis, indicating an altered balance between proliferation and differentiation (Fig. 25B). Immunostaining for leukocytes, macrophages and mast cells revealed increased skin infiltration (data not shown).



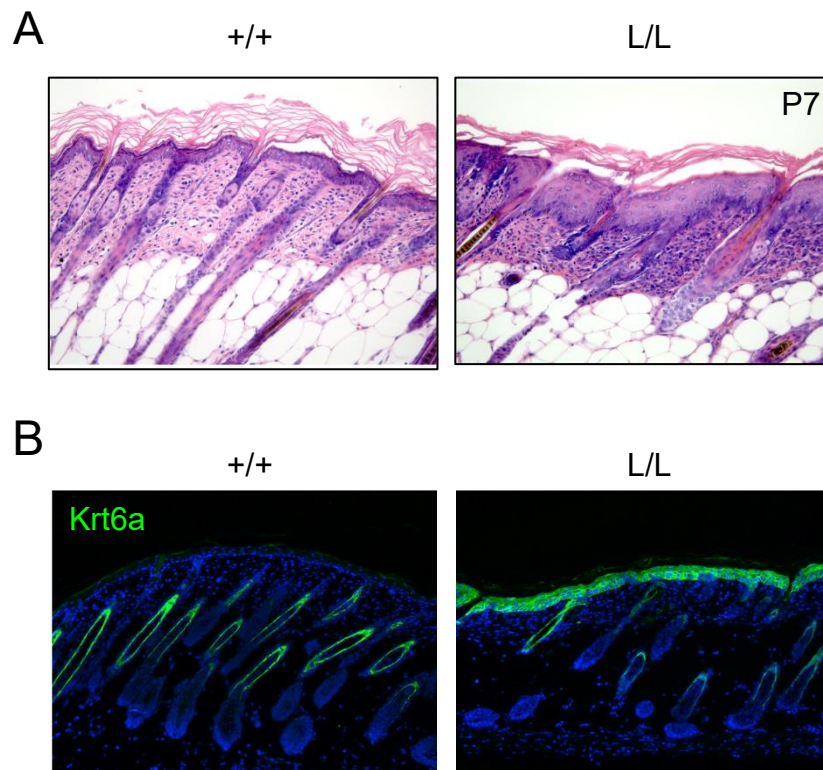


**Figure 25: Clear signs of inflammation in L514F mice.** A) H&E staining of dorsal skin of L/L mice at P3. Mutant epidermis was hyperplastic, with progressive signs of inflammation. B) Immunofluorescence analysis for Krt6 in skin at P3 reveals a strong up-regulation in mutant epidermis respect to the wild type.

The presence of infiltrating inflammatory cells in the dermis and the up-regulation of Krt6 in the epidermis of mutant mice suggested that an inflammatory response may be implicated in the development of the severe skin phenotype observed in the newborn mice.

Mechanical stress leads to uncontrolled necrosis characterized by loss of plasma membrane integrity and cellular collapse and release of intracellular content, causing an inflammatory response. Consistent with severe cell damage, antimicrobial peptides S100a8 and S100a9, Danger-Associated Molecular Patterns (DAMPs) often induced in epidermal inflammation and in keratin dysfunction (Lessard et al., 2013; Roth et al., 2012; Hammad and Lambrecht, 2015), were strongly upregulated at the RNA level in newborn p63<sup>L/L</sup> epidermis (respectively 22x and 21x) (Fig. 26A). The high mobility group box 1 protein (Hmgb1), another crucial DAMP molecule that translocate from the nucleus to the cytoplasm and is released



into the extracellular space by damaged cells {Lu, 2012 #46}, was selectively lost in the nuclei of basal p63<sup>L/L</sup> epidermal cells, whereas nuclear staining was retained in the suprabasal layers, consistent with cell damage occurring primarily in the basal layer (Fig. 26B).

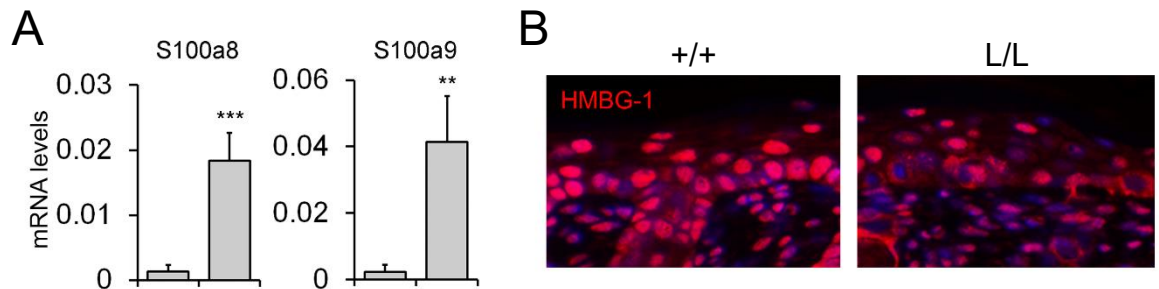


**Figure 26: Inflammation in AEC mouse model.** A) Real time RT-PCR for S100A8 and S100A9 in mouse epidermis derived from p63<sup>L/L</sup> mice and wild type at P3. mRNA expression of the analyzed genes was strongly up-regulated in mutant skin as compared to controls (n=7). Data are normalized for  $\beta$ -actin mRNA levels. Results: mean  $\pm$  SD. Student's t test: \*,  $P < 0.05$ ; \*\*,  $P < 0.01$ ; \*\*\*,  $P < 0.001$ . B) Immunofluorescence analysis for HMBG-1 in skin at P3 reveals a nuclear-cytoplasm translocation of the protein in mutant epidermis compared to controls.

To further characterize the molecules involved in the early steps of inflammation in p63<sup>L/L</sup> mutant mice, we performed a global gene expression comparison between p63<sup>L/L</sup> mutant and wild-type epidermis at P3. As expected, a number of well-characterized p63 target genes were downregulated in mutant epidermis, whereas selected genes encoding for inflammatory molecules were upregulated. Global gene expression profiling revealed that thymic stromal lymphopoietin (Tslp) is the most induced gene in mutant epidermis compared to controls. qRT-PCR analysis in epidermis of mutant mice at P3 confirmed that Tslp mRNA expression was up-regulated 788x fold in mutant epidermis (Fig. 27A). Thymic stromal lymphopoietin (Tslp) is able to activate dendritic cells to promote adaptive Th2 cell immunity, and license the innate type 2 cell response by activation of lymphoid cells, basophils, eosinophils, and mast cells (Hammad & Lambrecht, 2015).

Tslp has been reported to be aberrantly expressed in the suprabasal compartment as a consequence of defects in epidermal barrier (such as in atopic dermatitis and in Netherton syndrome) (Ziegler et al., 2010; Briot et al., 2009; Yoo et al., 2005). Interestingly, in p63<sup>L514F/L514F</sup> mutant skin Tslp protein expression was specifically detected in the basal and -to a lesser extent- the spinous layers of mutant epidermis (Fig. 27B), suggesting that Tslp induction was unlikely to be due to a canonical defect in epidermal barrier.

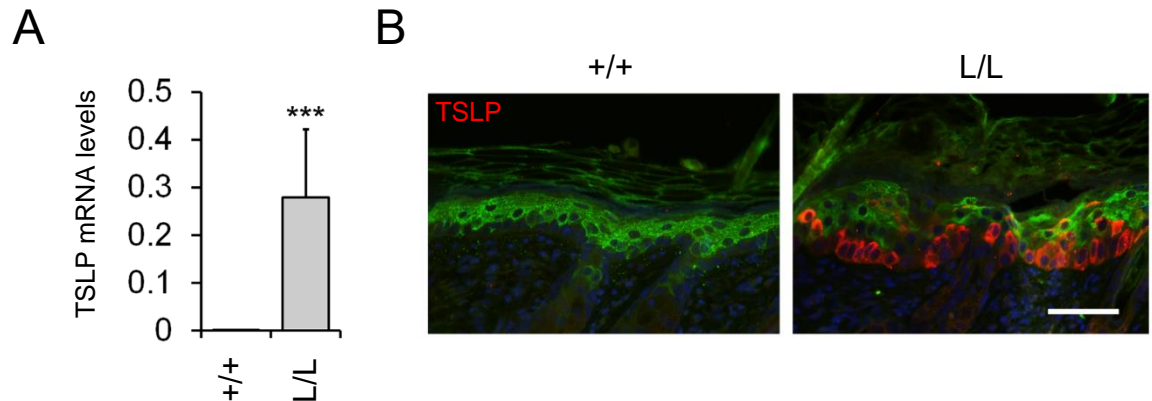


**Figure 27: Tslp levels in AEC conditional mouse model.** A) RNA-seq data showed that a subset of genes involved in different biological processes were up-regulated consistently with what we observed in AEC mutant mice. B) Real time RT-PCR for TSLP in mouse epidermis derived from p63<sup>L/L</sup> mice and wild type at P3. mRNA expression of TSLP was strongly up-regulated in mutant skin as compared to controls (n=15). Data are normalized for  $\beta$ -actin mRNA levels. Results: mean  $\pm$  SD. Student's t test: \*, P<0.05; \*\*, P<0.01; \*\*\*, P<0.001. C) Immunofluorescence analysis for Tslp and Krt10 at P7 reveals a strong expression in basal and suprabasal mutant epidermis respect to controls.

Being AEC syndrome a rare disorder with variable penetrance, extensive studies in patients have not been performed. However, using a set of RNA isolated from non-lesional epidermis, *TSLP* expression was significantly increased in AEC patients as compared to control individuals (data not shown). Thus, cytolysis of basal layer cells and epidermal fragility are associated with massive induction of Tslp expression in the lower layers of the epidermis in AEC syndrome.

Since Tslp was able to reach the bloodstream to arrive in different body districts, we evaluated its expression also in blood serum derived from AEC mutant and control mice. ELISA assays revealed that TSLP levels >3500-fold above the normal levels in sera from mutant mice at P10 (Fig. 28A). Interestingly, also in human AEC patients we observed an induction of Tslp, thus indicating that Tslp may be involved

in AEC syndrome and could be the cause of the progressive severe phenotype that characterized the AEC mutant mice.

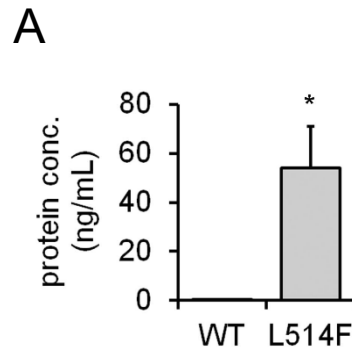


**Figure 28: Tslp levels in AEC conditional mouse model:** A) Systemic accumulation of Tslp protein (ng/ml) in blood serum of mutant mice at P10 measured by ELISA (\*P-value=0.04; n=6).

#### 4.4 Kiks/PAR2/NFAT pathway regulates Tslp expression in AEC syndrome

Given the key role of Tslp in the progression of the inflammatory process and its massive up-regulation in the epidermis of AEC mice, we investigated the molecular pathways underlying TSLP induction. It is known that the cleavage and activation of PAR2, mediated by extracellular serine proteases, leads to induction of Tslp expression in keratinocytes.

Calcineurin/NFAT signaling has been implicated in Tslp expression downstream of the PAR2 receptor (Wilson et al, 2013). The cleavage of PAR2 receptor on plasma membrane by serine proteases triggers the influx of  $Ca^{2+}$  and the activation of calcineurin, causing the transcription factor NFAT nuclear translocation. To detect serine proteases, we measured the proteolytic activity in p63<sup>L/L</sup> mutant and control skin. An overall induction of proteolytic activity was observed in p63<sup>L/L</sup> mutant epidermis by performing an *in situ* zymography and it was localized in the spinous layer of the epidermis and in the hair follicle (Fig. 29A; in collaboration with A. Hovnanian).

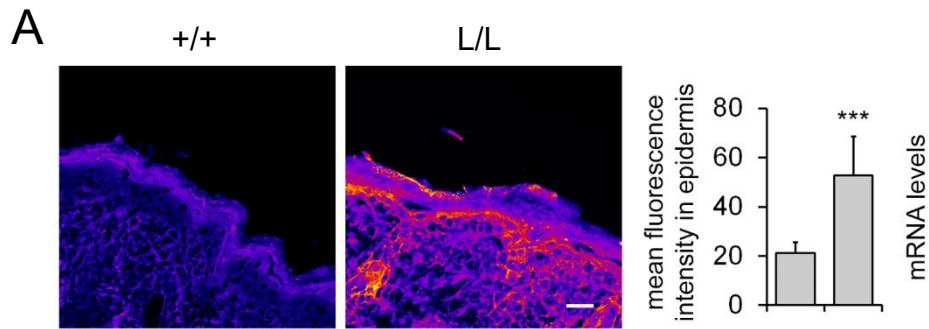


**Figure 29: Figure 31. Proteolytic activity in AEC mutant epidermis.** In situ gel zymography with casein as substrate demonstrate a strong induction of serine-protease protein activity in p63<sup>L/L</sup> mutant mice at P3.

Our RNA-seq data showed that kallikreins, enzymes with serine protease activity that regulate desquamation of the epidermis (Candi et al, 2005) were strongly up-regulated at P3 thus indicating an altered equilibrium in epidermis structure. In particular, Klk6 is the proteases most induced in AEC mutant mice compared to wild type. Interestingly we tested the expression of several KLKs in AEC mutant and wild-type epidermis at P3 and we confirmed the RNA-seq data (Fig. 30A). Klk5 and Klk7 protein levels were expressed equally in L514F mouse epidermis and relative controls (Fig. 30B). Klk6 was poorly expressed in wild-type epidermis, consistently with a previous report, while a strong expression was observed in AEC mutant epidermis both at the RNA and protein levels. Interestingly, Klk6 expression was localized in the spinous layer (Fig. 30C).

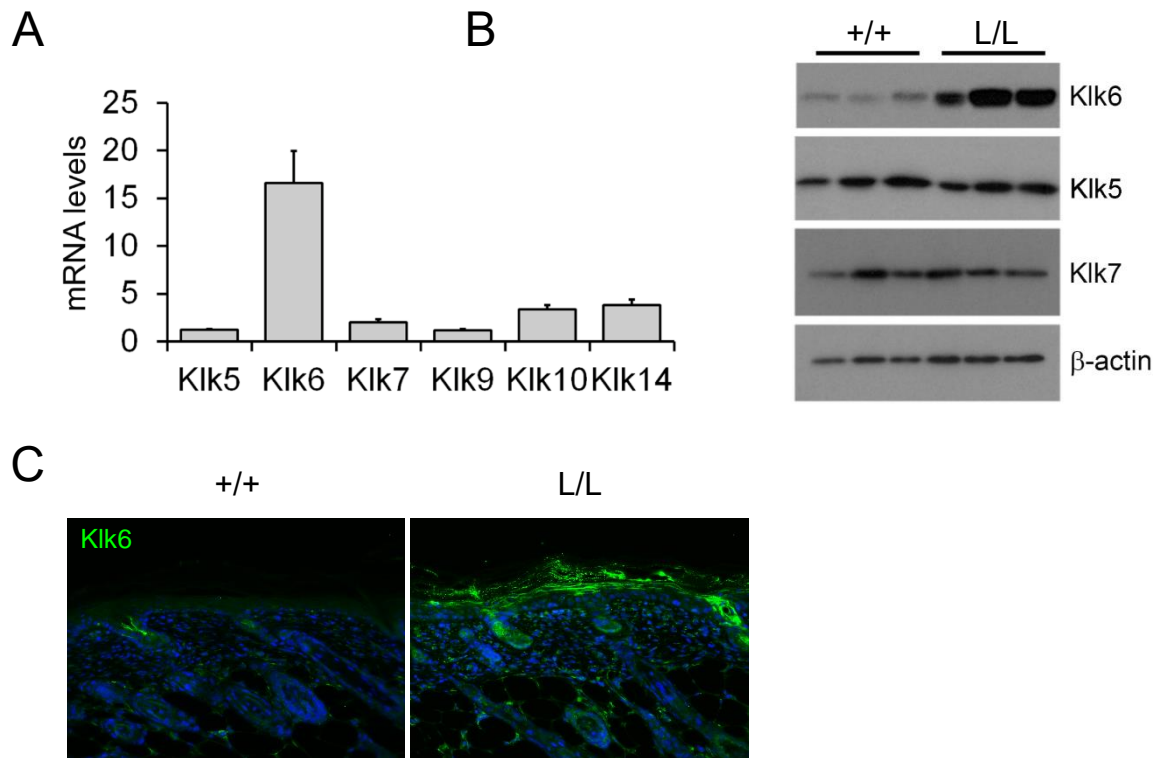


**Figure 30: Klk6 upregulation in AEC mice.** A) RNA-seq data showed that a subset of genes belonging to Kik family were up-regulated consistently with what we observed in AEC mutant mice. B) Relative mRNA expression of the indicated kallikreins shows a strong upregulation of Klk6 in the epidermis of  $p63^{L/L}$  mutant mice at P3. C) Immunoblotting analysis for the indicated proteins in cell extracts of mouse epidermis derived from mutant and control mice at P3. Data are normalized for  $\beta$ -actin protein expression. D) Immunofluorescence analysis for Klk6 in skin at P3 shows the strong upregulation of Klk6 in the stratum corneum of the epidermis of  $p63^{L/L}$  mutant mice compared to control animals.

Among the serine proteases, KLK5, KLK6, KLK7 and KLK14 have been reported to cleave PAR2 in the epidermis. Given the strong upregulation in AEC mice epidermis of Klk6, and localization in the spinous layer, in contrast to the other KLK expressed in the granular layer, we considered a possible correlation between p63 mutation and Klk6 induction. We found that p63 may directly regulate Klk6 since p63 depletion in keratinocytes leads to increase Klk6 expression (Fig. 31A), and p63 binds on the promoter of the Klk6 gene. *In vivo*, in AEC mutant epidermis we observed at P3 that NFAT is highly expressed compared to wild-type (Fig. 31C). NFAT overexpression triggers Tslp induction in mouse keratinocytes (Fig. 31B).

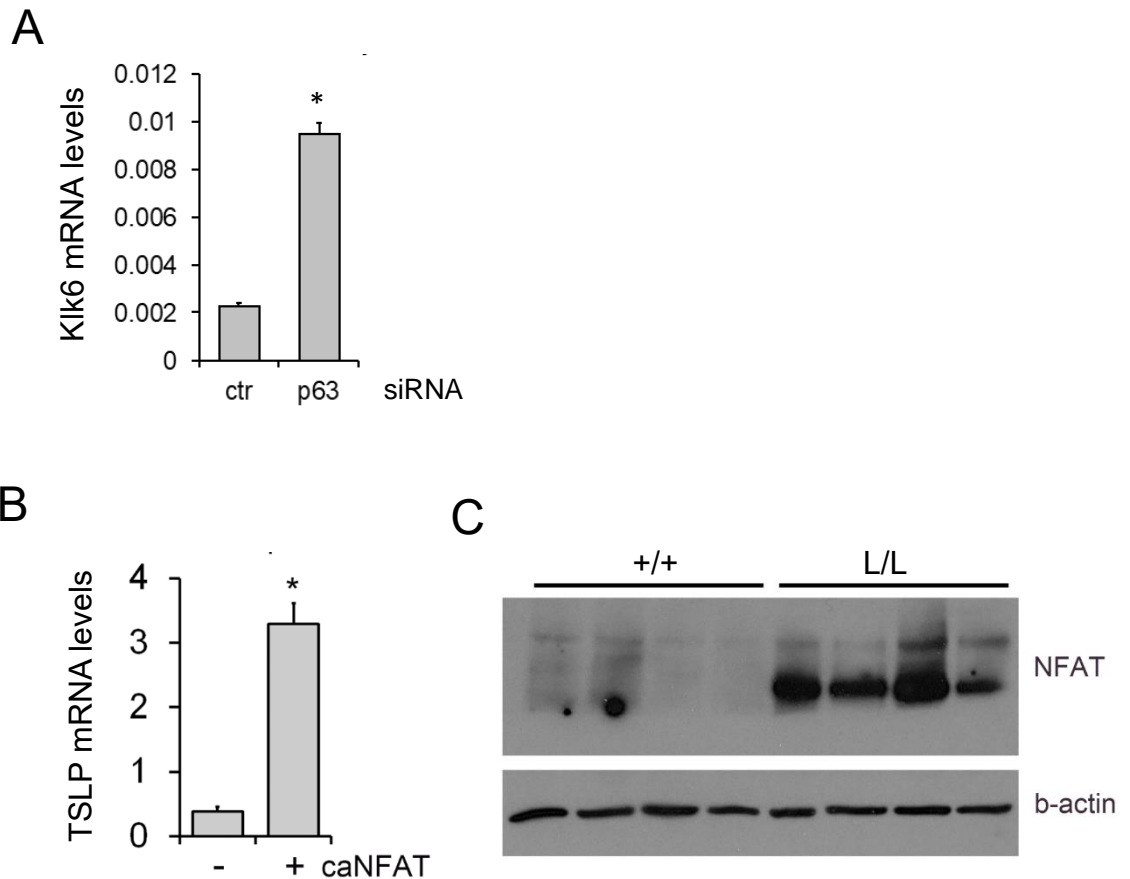


**Figure 31: Klk6 upregulation in L514F mice.** A) *Klk6* mRNA levels is upregulated upon p63 depletion ( $n=8$ ). B) *Tslp* mRNA is induced by a constitutive active form of NFAT ( $n=5$ ). Data are normalized for  $\beta$ -actin mRNA levels. Results: mean  $\pm$  SD. Student's *t* test: \*,  $P<0.05$ ; \*\*,  $P<0.01$ ; \*\*\*,  $P<0.001$ . C) Immunoblotting analysis for NFAT in skin at P3 showed an up-regulation of NFAT in the epidermis of  $p63^{L/L}$  mice compared to control animals.

Take together these data support the hypothesis that the axis KLK/PAR2/NFAT signaling may be involved in aberrant overexpression of TSLP in AEC syndrome.

#### 4.5 KLK6 activates TSLP expression through NFAT and NF- $\kappa$ B signaling in human keratinocytes

To test the hypothesis that in  $p63^{L/L}$  mice KLK6 may be involved in aberrant overexpression of Tslp causing a proinflammatory cascade independently of exogenous proteases, such as those derived from the microbiome, mouse primary keratinocytes were treated with an active form of recombinant human Klk6, proKlk6 R80Q, and Tslp mRNA expression was evaluated. Interestingly, Klk6 treatment

strongly induced *Tslp* mRNA expression, thus indicating that Klk6 may be involved in *Tslp* induction (Fig. 32A).

NFAT-dependent TSLP induction has already been associated with cleavage and activation of PAR2. To evaluate the involvement of PAR2/NFAT signaling activation by KLK6 on TSLP induction, normal human primary keratinocytes (NHKs) were treated with an active form of recombinant human Klk6, proKlk6 R80Q, in the presence or in the absence of two different calcineurin antagonists, CsA and Vivit, and *Tslp* mRNA expression was evaluated. In KLK6-treated NHKs, *TSLP* mRNA was significantly increased (Fig. 32B). In addition, we assessed whether interleukin *IL8*, a well-characterized target gene for PAR2 cleavage in cultured keratinocytes, could be directly regulated by KLK6. Administration of recombinant human KLK6 in the medium led to an increase of *IL8* mRNA in NHKs (Fig. 32C). The production of these inflammatory mediators suggests a role for KLK6 in the cleavage and activation of PAR2 receptor.

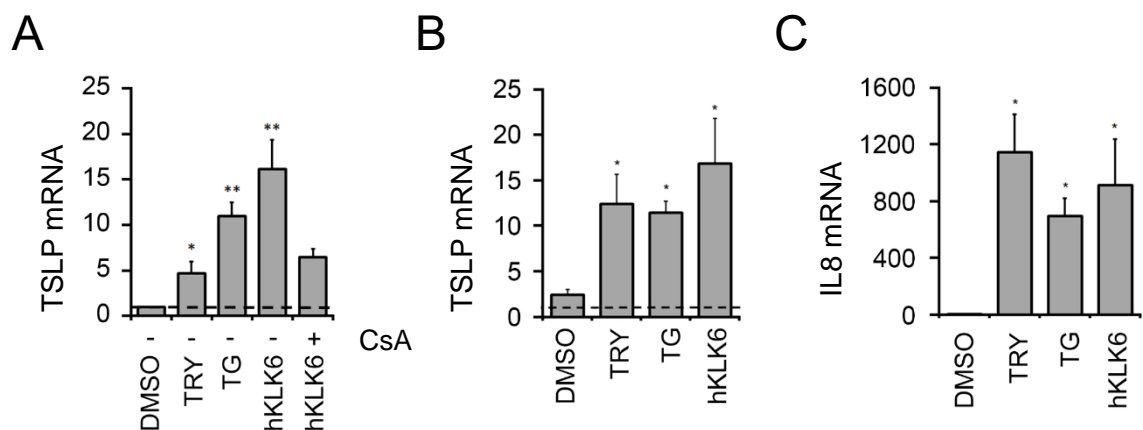


**Figure 32: KLK6 up-regulates TSLP and proinflammatory molecules in keratinocytes.** A) NHKs were stimulated with 300nM Trypsin, 500nM Thapsigargin or recombinant KLK6 for 3 h. TSLP transcripts are increased by five-, five-, twelve-, and fifteen-fold, respectively ( $n = 5$ ). Data are normalized for  $\beta$ -actin mRNA levels. Results: mean  $\pm$  SD. Student's  $t$  test: \*,  $P < 0.05$ ; \*\*,  $P < 0.01$ ; \*\*\*,  $P < 0.001$ . B-C) NHKs were stimulated with 300nM Trypsin, 500nM Thapsigargin or recombinant KLK6 for 3 h. TSLP and IL8 transcripts are strongly increased ( $n = 5$ ). Data are normalized for RPLP0 mRNA levels. Results: mean  $\pm$  SD. Student's  $t$  test: \*,  $P < 0.05$ ; \*\*,  $P < 0.01$ ; \*\*\*,  $P < 0.001$ .

Induction of *Tslp* and *IL-8* in response to KLK6 treatment in NHK was suppressed by both calcineurin antagonists, CsA and Vivit, indicating that these cytokines are transcriptionally regulated by the calcineurin-NFAT pathway (Fig. 33A-B).

Interestingly, Tslp induction by PAR2 activation was only partially inhibited by CsA and Vivit. We speculate that this partial reduction of mRNA expression level may reflect the possibility that additional NFAT-independent mechanisms activated by PAR2 signaling contribute to drive Tslp induction.

Previous studies have shown that up-regulation of TSLP by PAR2 signaling was also mediated by NF- $\kappa$ B pathway (Briot et al., 2008). We next tested the hypothesis that KLK6 may also modulate TSLP and IL8 expression through NF- $\kappa$ B signaling. To this purpose, we treated human primary keratinocytes with hKLK6 in the presence or in the absence of CAPE (Caffeic Acid Phenethyl Ester), a specific inhibitor of the NF- $\kappa$ B pathway. Treatment of NHK with CAPE decreased the effect of KLK6 on *TSLP* and *IL8* mRNA expression, whereas a MAPK kinase inhibitor, PD 098059, did not indicating that KLK6 does not act via the MAPK kinase pathway to induce TSLP in this model (Fig. 33A-B).

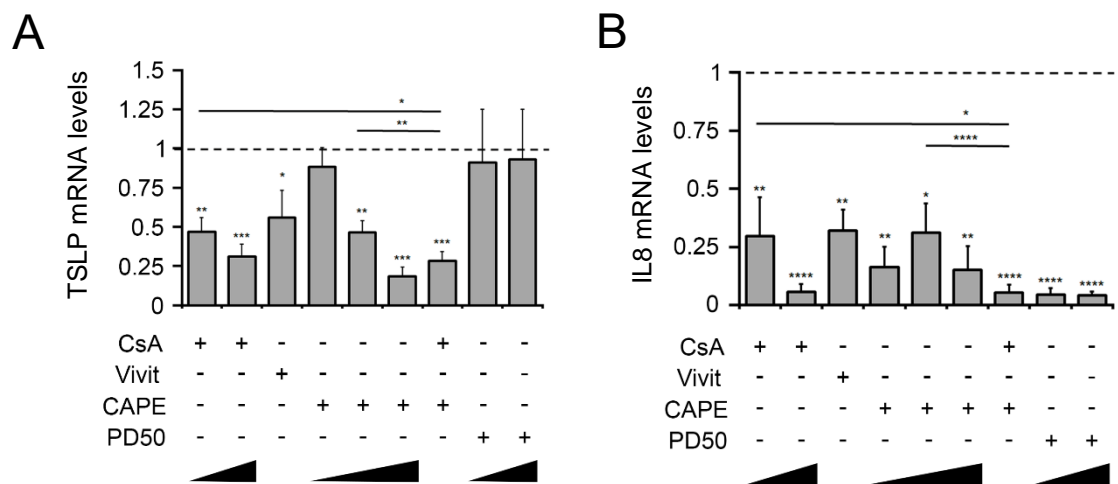


**Figure 33: KLK6 up-regulates TSLP and proinflammatory molecules in keratinocytes.** A) NHKs were stimulated with recombinant KLK6 for 3 h in the absence or presence of the CsA (40 and 60 $\mu$ M), Vivit (10 $\mu$ M), CAPE (25, 35 and 50 $\mu$ M) and PD50 (50 and 75 $\mu$ M) alone or in combination ( $n = 5$ ). Data are normalized for RPLP0 mRNA levels. Results: mean  $\pm$  SD. Student's  $t$  test: \*,  $P < 0.05$ ; \*\* $< 0.01$ ; \*\*\* $< 0.001$ .

Based on these results, we propose a model for TSLP regulation in keratinocytes in which the cleavage of PAR2 receptor by KLK6 causes the activation and the cytoplasm to nucleus translocation of the transcription factor NFAT, which promotes the expression of TSLP and IL8 genes in conjunction with NF- $\kappa$ B pathway.



## 4.6 Generation of AEC conditional mouse model in a *Tslp* null background

To evaluate whether the absence of *Tslp* in AEC conditional mouse model may lead to a reduced inflammatory state, AEC mice (L514F) were crossed with *Tslp*<sup>floxL2/floxL2</sup> conditional null mice (*Tslp* epidermal Knock-out (*Tslp*<sup>eKO</sup>)) (Li et al, 2009). RT-PCR analysis confirmed the deletion of TSLP in epidermal of *p63*<sup>L/L</sup>;*TSLP*<sup>eKO</sup> mice at P3. General health conditions were ameliorated with no erosion or crusting, although a progressive hair loss was observed (Fig. 34A). Accordingly, more than 40% of *p63*<sup>L/L</sup>;*TSLP*<sup>eKO</sup> mice survived up to P15, and a significant rescue in body weight was observed in the *p63*<sup>L/L</sup>;*TSLP*<sup>eKO</sup> as compared to *p63*<sup>L/L</sup> (Fig. 34B-C). To confirm the association between weight loss and dehydration, we analyzed sodium and chlorine serum concentration in *p63*<sup>L/L</sup>;*TSLP*<sup>eKO</sup> mice at P7. We observed a significantly lower sodium and chloride in *p63*<sup>L514F/L514F</sup>;*TSLP*<sup>eKO</sup> mice compared to *p63*<sup>L/L</sup> mutant mice (Fig. 34D).

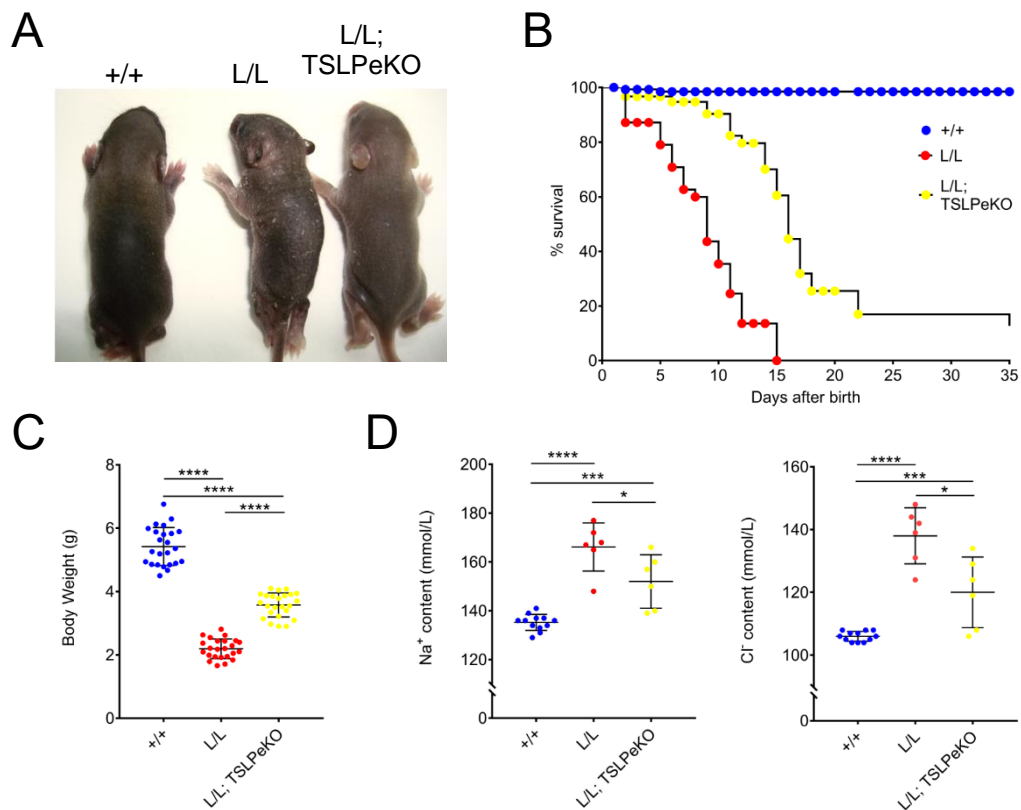


**Figure 34: Phenotype of *p63*<sup>L/L</sup>; *TSLP*<sup>eKO</sup> mutant mice:** A) Photographs are taken from wild type, *p63*<sup>L/L</sup>, *p63*<sup>L/L</sup>;*TSLP*<sup>eKO</sup> mice at P3. B) Survival curve of *p63*<sup>L/L</sup> (L/L red line), *p63*<sup>L/L</sup>;*TSLP*<sup>eKO</sup> (+/L yellow line) and wild type (+/+ blue line) mice (n=110). C) Body weight at P7 of *p63*<sup>L/L</sup>, *p63*<sup>+L</sup> and wild type mice (n= 72). D) Serum Na<sup>+</sup> and Cl<sup>-</sup> concentrations. Serum samples were taken from P7 mice and were analyzed for Na<sup>+</sup> (152.00 ± 4.48 (n=6) vs 166.7 ± 4.03 (n=6), P value = 0.0001) and Cl<sup>-</sup> (120.00

$\pm 4.60$  ( $n=6$ ) vs  $138.00 \pm 3.64$  ( $n=6$ ),  $P$  value = 0.0005) levels compared to  $p63^{L/L}$  mutant mice. Results: mean  $\pm$  SD. Student's  $t$  test: \*,  $P < 0.05$ ; \*\*,  $P < 0.01$ ; \*\*\*,  $P < 0.001$ .

Together, partial rescue of hypernatremia, hyperchloremia and weight loss suggests that ablation of *Tslp* gene in  $p63^{L/L};TSLP^{eKO}$  mice could partially improve the epidermal barrier defect reducing and/or delaying the intensity of proinflammatory process in skin.

To test whether *Tslp* depletion may reduce skin inflammation, the skin morphology was examined by hematoxylin and eosin staining. Histological analysis showed an improvement of skin phenotype of  $p63^{L/L};TSLP^{eKO}$ , with a reduction of hyperplasia and dermal cellularity compared with  $p63^{L/L}$  mice (Fig. 35A).

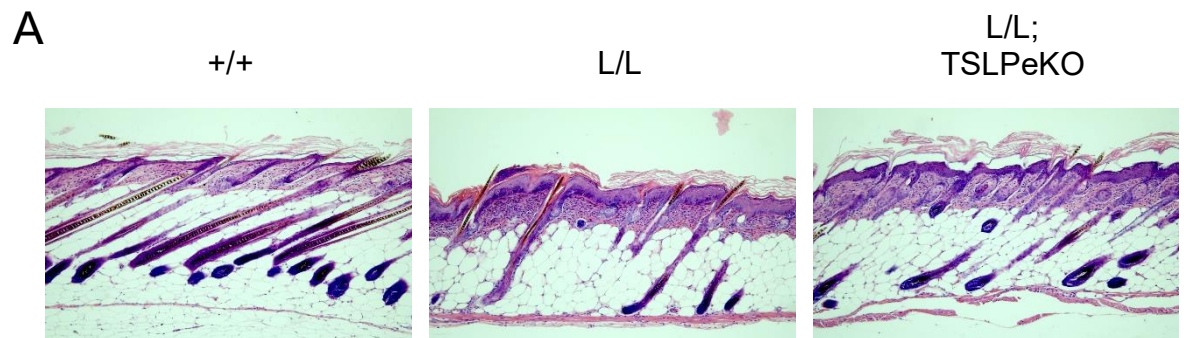


**Figure 35: Rescue of the inflammatory state in L514F mice with a *Tslp* null background A)** H&E staining of dorsal skin wild type,  $p63^{L/L}$ ,  $p63^{L/L};TSLP^{eKO}$  mice at P7.

Accordingly, we observed reduced signs of hyperproliferation in  $p63^{L/L};TSLP^{eKO}$  skin and expression of *Krt6* limited to few cells of the basal and suprabasal layers in contrast to the massive expression seen in  $p63^{L/L}$  skin (Fig. 36A). Immunostaining for leukocytes, macrophages and mast cells revealed reduced infiltration (data not shown).

At the histological level newborn  $p63^{L/L};TSLP^{eKO}$  mice were characterized by a similar reduction of *Krt5*, *Krt15* and to a lesser *Krt10* at mRNA levels (Fig. 36B), indicating that *Tslp* ablation did not interfere with the skin fragility observed in L514F mice at early stages.

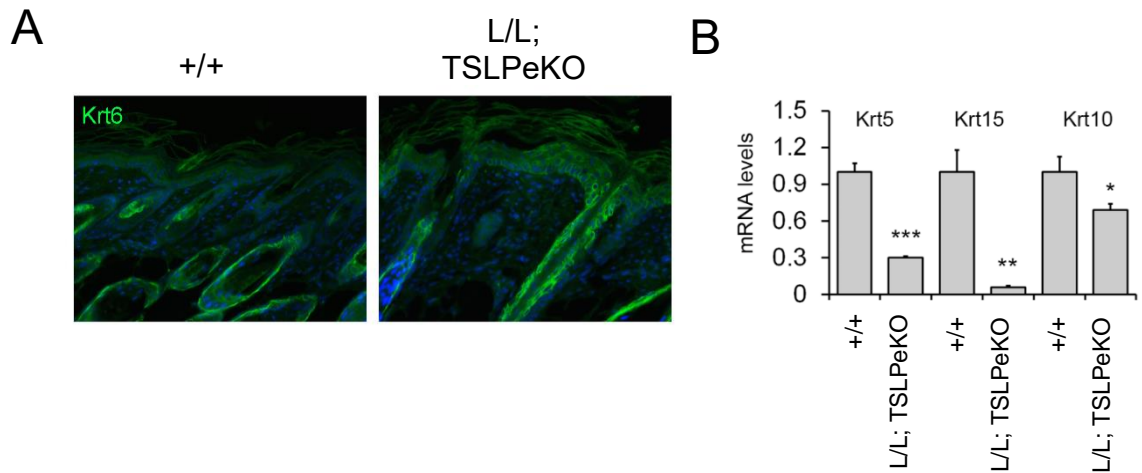


**Figure 36: Rescue of the inflammatory state in L514F mice with a Tslp null background.** A) Immunofluorescence analysis for Krt6 in skin at P8 revealed its properly localization in  $p63^{L/L};TSLPeKO$  epidermis. B) real time qPCR analysis of Krt5, Krt15 and Krt10 revealed reduction of expression in  $p63^{L/L};TSLPeKO$  mutant epidermis respect to the control (n=4). Results: mean  $\pm$  SD. Student's t test: \*,  $P < 0.05$ ; \*\*,  $P < 0.01$ ; \*\*\*,  $P < 0.001$

Therefore, the strong reduction of infiltrating inflammatory cells as well as of inflammatory mediators in the skin indicates that the inflammatory response may be driven by Tslp in  $p63^{L/L}$  mice and that, by ablating Tslp in L514F background the severe skin inflammatory phenotype observed is rescued to a large extent.

#### 4.7 AEC-associated p63 mutants interact with specific molecular chaperones involved in protein disaggregation

Protein folding is mediated by synergistic cooperation among different members of molecular chaperones (Nillegoda et al., 2015). The multifunctionality of HSP70 is often driven by DNAJ co-chaperones, which deliver specific unfolded client proteins to HSP70 stimulating its ATPase activity (Kampinga et al., 2010). Chaperone functions are not restricted to the protein folding but include also recognition and sorting of misfolded proteins to the various Protein Quality Control (PQC) compartments (Sontag et al., 2017). In addition, a subclass of the DNAJB family, particularly DNAJB6a, DNAB6b and DNAJB8, can display also anti-aggregating HSP70-independent functions (Hageman et al., 2010).

In this context, we tested the hypothesis that by reducing protein aggregation, transactivation functions may be at least partially restored. A collection of thirty-five members of the HSP70 (HSPA), HSPB (small HSP), HSP110 (HSPH), and HSP40 (DNAJs) chaperone and co-chaperone families (provided by Dr. H.H. Kampinga, Depart. of Cell Biology, Groningen University, The Netherlands) were tested for their efficacy to prevent or suppress AEC mutant p63 aggregation and restore p63 transcription activity by co-transfection with  $\Delta$ Np63 $\alpha$ WT or  $\Delta$ Np63 $\alpha$ R598L in heterologous H1299 cells devoid of all p53 family members, in the presence of the protein synthesis inhibitor cycloheximide.

We found that five members of HSP40 (DNAJs) family, DNAJA1, DNAJB2a, DNAJB2b, DNAJB6a and DNAJB6d, but not other such as DNAJC7 for which no degradation functions are known, preferentially promote the degradation of mutant proteins in co-transfected H1299 cells in the presence of the protein synthesis inhibitor cycloheximide (Fig. 37A-B). Preliminary data obtained in our laboratory, indicated that AEC mutant, and not wild type p63, specifically interacts with DNAJA1, DNAJB6a and DNAJB6b co-chaperones when co-overexpressed in heterologous cells (data not shown).

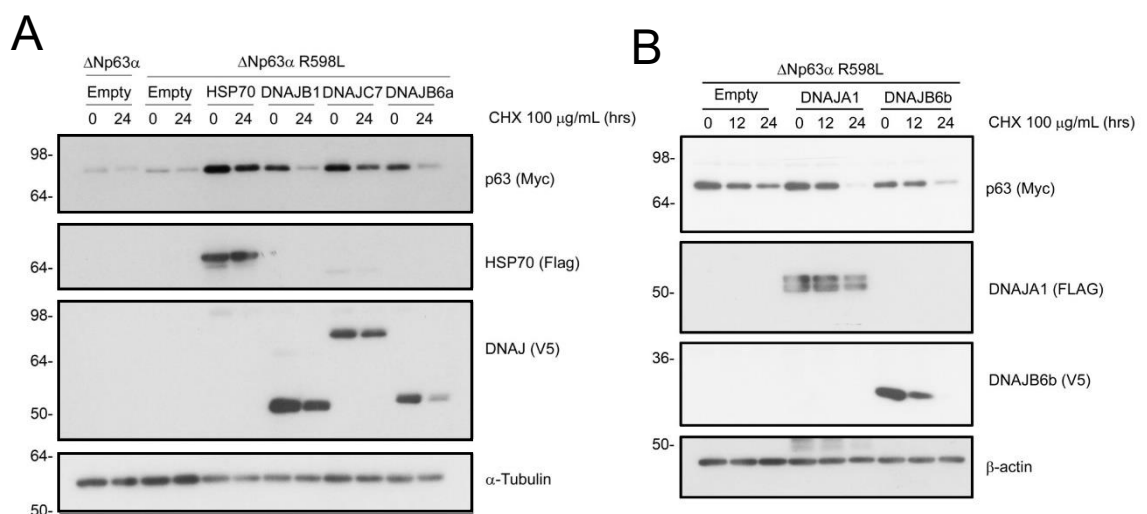


**Figure 37: Co-chaperones reduce preferentially the half-life of the p63<sup>L/L</sup> protein.** A)  $\Delta$ Np63 $\alpha$ R598L was expressed in H1299 cells, with co-expression of Flag-tagged HSP70 or V5-tagged DNAJB1, DNAJC7 or DNAJB6a. Twenty-four hours after transfection, cells were incubated with cycloheximide (20  $\mu$ g/mL), and, at the indicated time points, cells were harvested, lysed, and analyzed for p63 levels by using an anti-Myc antibody. In all cases,  $\beta$ -actin levels were measured as a loading control. B)  $\Delta$ Np63 $\alpha$ R598L was expressed in H1299 cells, with co-expression of Flag-tagged DNAJA1 or V5-tagged DNAJB6b. Twenty-four hours after transfection, cells were incubated with

cycloheximide (20  $\mu\text{g}/\text{mL}$ ), and, at the indicated time points, cells were harvested, lysed, and analyzed for p63 levels by using an anti-Myc antibody. In all cases,  $\beta$ -actin levels were measured as a loading control.

Importantly, both DNAJB2a, DNAJB6a and DNAJB6b isoforms act in the nucleus, where p63 aggregates accumulate, whereas DNAJA1 is normally localized in the cytosol, and DNAJB2b isoform is associated to the endoplasmic reticulum where it participates in ER-associated degradation (ERAD).

Subsequently, we evaluated the capacity of DNAJB6a to dispose of p63 aggregate in H1299 cells co-transfected with  $\Delta\text{Np63}\alpha\text{L514F}$  or  $\Delta\text{Np63}\alpha\text{R598L}$  by BN-PAGE followed by Western blot for p63. Consistently with the results of degradation experiment, for the L514F and R598L mutants, aggregation was progressively alleviated in the presence of DNAJB6a and DNAJB6b (Fig. 38A).

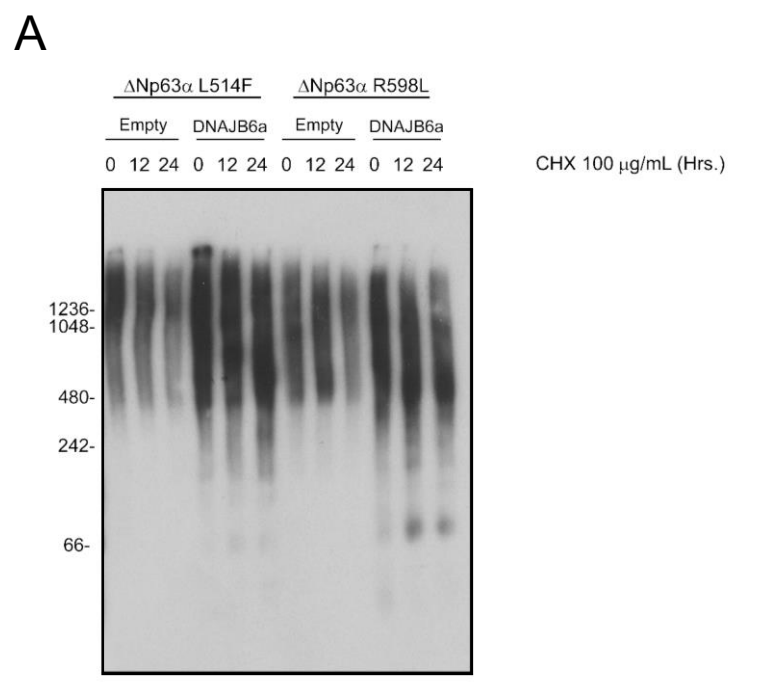


**Figure 38: Disaggregation activity of DNAJB6a on AEC-associated p63 mutants in H1299 cells.** A) BN-PAGE followed by Western blot for p63 in H1299 co-transfected with  $\Delta\text{Np63}\alpha\text{L514F}$  or  $\Delta\text{Np63}\alpha\text{R598L}$  and V5-tagged DNAJB6a. Twenty-four hours after transfection, cells were incubated with cycloheximide (20  $\mu\text{g}/\text{mL}$ ), and, at the indicated time points, cells were harvested, lysed, and analyzed for p63 levels by using an anti-Myc antibody.

Taken together these data indicate that AEC mutants are bound by molecular chaperones involved in disaggregation functions which are selective for p63 mutant protein and may help to resolve the aggregates.

#### **4.8 p63 aggregation is not reduced by PRIMA-1<sup>MET</sup>**

The preliminary data shown above open new avenues to counteract aggregation and hopefully to rescue the skin defects in AEC syndrome, based on targeting the molecular chaperones that specifically interact with AEC mutants to potentiate their anti-aggregation activity.

Alternatively, a chemical approach could be used to deal with protein aggregation.

As a first attempt, we recently tested the effect of APR-246 (also known as PRIMA-1-Met), a small compound which binds covalently to thiols and reactivates apoptotic functions of mutant p53 in human cancer cells (Bykov et al., 2002) and is currently used in anti-cancer clinical trials. Furthermore, it has been demonstrated that PRIMA-1Met is able to partially rescue keratinocyte differentiation of keratinocyte derived from EEC patients (Shen et al., 2013), targeting EEC-associated mutant p63.

Based on the structural homology between p53 and p63, Prof. Daniel Aberdam (INSERM, Paris, France) and co-workers evaluated the effects of the treatment with PRIMA-1-Met on the differentiation of human keratinocytes derived from two AEC patients carrying the p63 mutation I576T and I549T. After treatment with PRIMA-1-Met, AEC keratinocytes showed a partial rescue for specific differentiated epidermal markers, such as Krt1, ZNF750 and TGM1. On the basis of the in vitro results, two AEC patients were treated daily with a topic formulation of PRIMA-1MET, allowing re-epithelialization of the eroded skin and improving their quality of life (data not shown).

In collaboration with Prof. Aberdam, we tested whether PRIMA-1MET amelioration of the phenotype could be due to reduced protein aggregation. AEC mutant and normal human epidermal keratinocytes (NHEK) keratinocytes were

treated with PRIMA-1-Met 30 mM every other day, and kept in culture for 10 days after they reached 100% confluency to induce differentiation in the presence of 1.5 mM CaCl<sub>2</sub> (Fig. 39A). At the end of treatment, AEC mutant and normal human epidermal keratinocytes (NHEK) were lysed in native conditions for total protein extraction. We normalized the samples for p63 amount by Western blot analysis (Fig. 39C). We performed BN-PAGE on keratinocytes lysates, followed by Western blot analysis for p63. Protein aggregation was detected in AEC-differentiated cells and not in WT cells, as expected. However, while PRIMA-1-MET was able to rescue epidermal differentiation, it did not reduce p63 protein aggregation, suggesting that PRIMA-1-MET targets cell differentiation and not p63 activity directly (Fig. 39B).

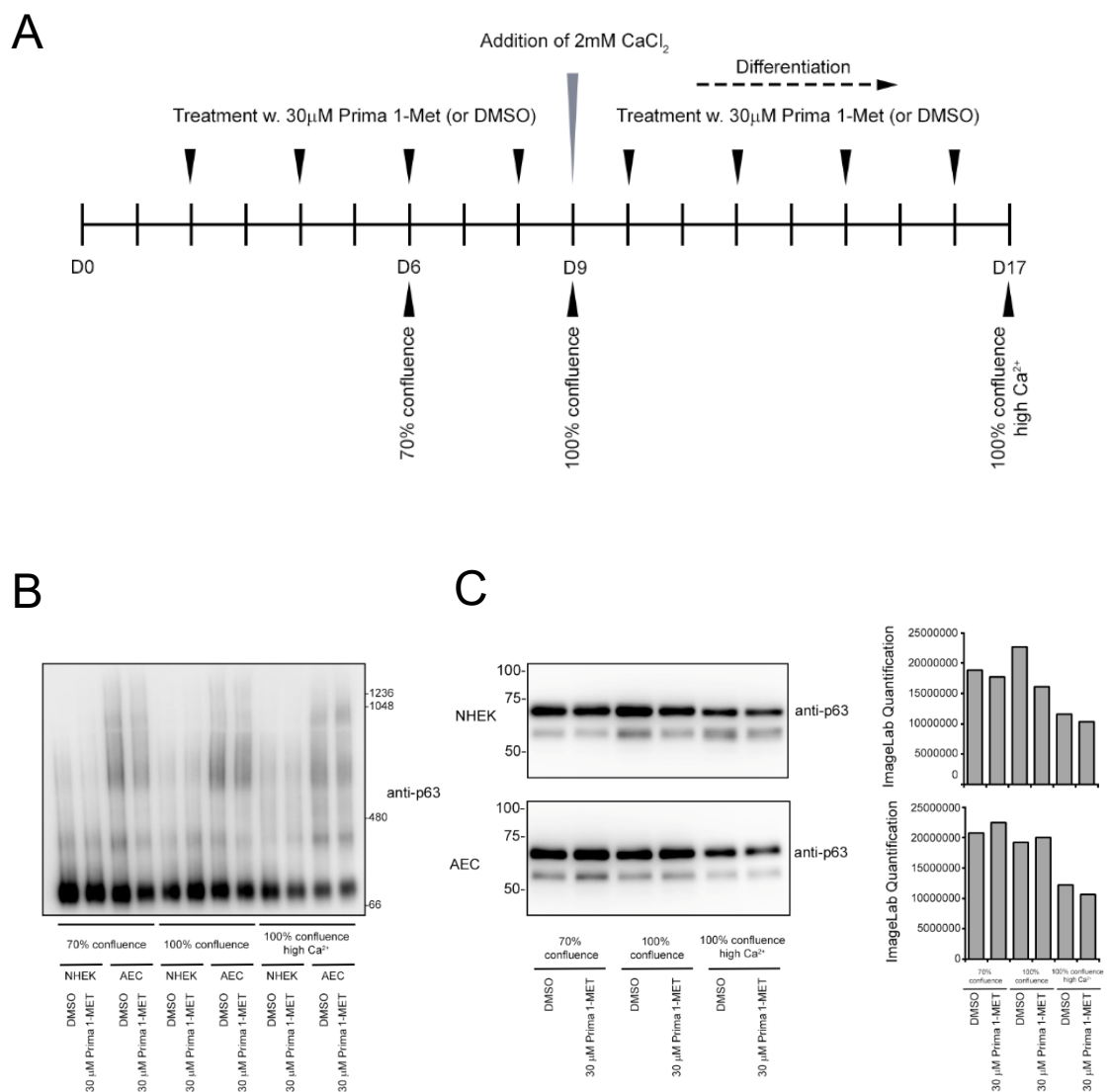


**Figure 39: Protein aggregation is not reduced by PRIMA-1MET.** A) Protein extracts were collected from WT and patient 1 KCs (AEC) at different confluences and after 10 days of differentiation and loaded on BN-PAGE followed by Western blot for p63 C) SDS-PAGE followed by

*Western blot for p63 of the samples shown in (A). Quantification of the bands. Equivalent amount of protein was loaded for each condition.*

These preliminary data indicate that PRIMA-1-Met rescued the differentiated morphology of AEC keratinocytes but it did not abolish protein aggregation driven by the mutant p63 molecule.

#### **4.9 Doxorubicin and epirubicin rescue mutp63 transactivation function**

Since AEC p63 mutants act in a dominant-negative fashion through hetero-oligomerization with wtp63, in order to identify other therapeutic strategies for AEC syndrome it is crucial to determine the specific mechanisms underlying mutp63 stabilization/degradation and to identify compounds able to selectively destabilize mutp63 without altering wtp63 levels.

To identify small compounds capable to disaggregate or deplete specifically mutp63, a luciferase reporter-based HTS was performed in H1299 (p63null) cell line. Preliminary data have been obtained to prove the feasibility of this screening, using a reporter constructs BDS2 3X- or K14-Luc that carry firefly luciferase gene under the control of p53-responsive element (highly responsive to p63) and Keratin 14 promoter.

We screened chemical libraries comprising of 2,000 compounds in H1299 cells transfected with two plasmid vectors constitutively expressing  $\Delta$ Np63 $\alpha$ WT and  $\Delta$ Np63 $\alpha$ L514F (ratio 1:1) by performing luciferase assays and identified 11 compounds that increased luciferase activity compared with dimethylsulfoxide (DMSO).

Next, H1299 cell expressing a combination of  $\Delta$ Np63 $\alpha$ WT and  $\Delta$ Np63 $\alpha$ L514F,  $\Delta$ Np63 $\alpha$ WT alone or empty vector were used to establish a dose-response relationship and to eliminate false positives including luciferase activators and general transcription/translation activators (Fig. 40A). The top three compounds showing dose-dependent induction of luciferase activity in H1299 cells were examined further for their effects on toxicity in human keratinocytes (HK) (Fig. 40B).



The remaining two compounds (doxorubicin and epirubicin) belong to a class of cytotoxic antineoplastic antibiotics called anthracyclines that are used in the therapy of several forms of lymphoma, leukemia, sarcoma and solid organ cancers.

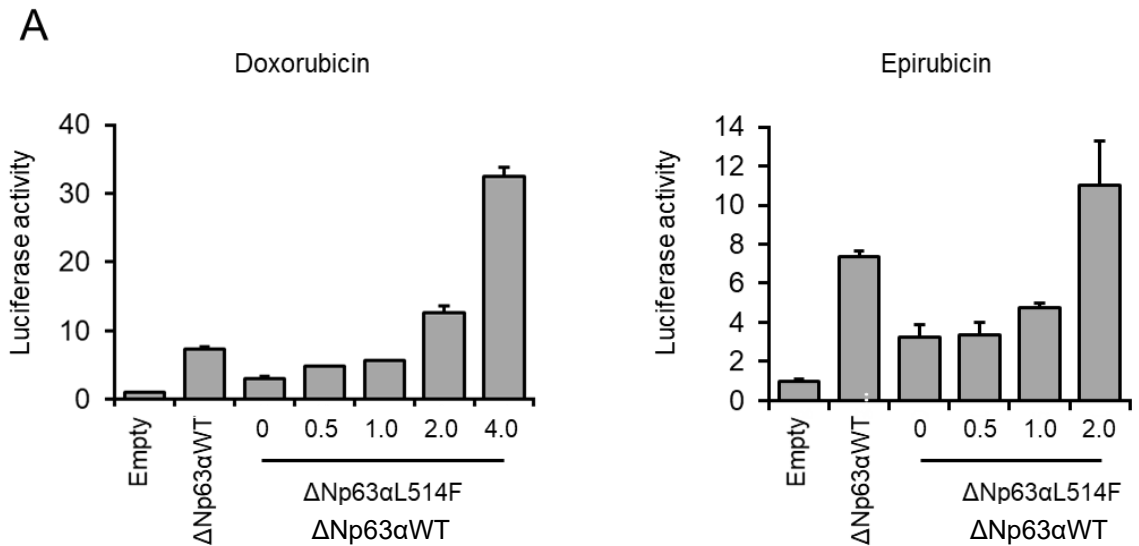


**Figure 40: Transactivation activity of AEC-associated p63 mutants with or without mutations or deletions that prevent their aggregation.** A) Luciferase reporter assay in H1299 cells co-transfected with a combination of  $\Delta Np63\alpha WT$  and  $\Delta Np63\alpha L514F$ ,  $\Delta Np63\alpha WT$  alone or empty vector and the BDS2 3X promoter-luc vector. Twenty-four hours after transfection, cells were incubated with doxorubicin or epirubicin at different concentration and after twenty-four hours after treatment cells were harvested, lysed, and analyzed for luciferase activity.

To test the effects of doxorubicin and epirubicin on the rescue of transcriptional activity of p63L514F mutant protein in a more physiological context, we will use a recently developed protocol to convert human dermal fibroblasts (HDFs) into induced keratinocyte-like cells (iKCs) by co-expression of  $\Delta Np63\alpha$  and the reprogramming factor Krüppel-like factor 4 (KLF4) (Chen et al., 2014). More specifically, we will test the ability of wild type p63 and p63L514F to induce the expression of keratinocyte-specific p63 target genes, such as KRT14 and IRF6, thus leading to the conversion, after treatment with doxorubicin and epirubicin. HDFs will be co-infected with retroviruses carrying wild type or p63L514F and KLF4 and collect after eighteen days, required for the conversion into iKCs, for real time RT-PCR and Western blot analysis.

## 5. Discussion

Little is known about the pathogenetic mechanisms underlying AEC skin atrophy and skin erosions, and possible treatments. We recently reported that skin atrophy and delayed wound healing is associated with a reduced number of epidermal stem cells due to a defective Fibroblast Growth Factor (FGF) signaling in embryogenesis (Ferone et al., 2012). However, the constitutive mouse models did not allow to study the skin phenotype after birth.

Since this disorder is rare and it is complicated to have patient material, we generated a conditional mouse model for AEC syndrome to study the evolution of the molecular defects occurring after birth, and to test future *in vivo* treatments. In humans the disorder is due to heterozygous mutations in p63. In mice, we found that heterozygous mice have a subtle phenotype. Since the K14-Cre that was used to activate the mutation is expressed from E17.5 (Huelsen et al, 2001), we hypothesized that a number of biological processes that require p63 are not affected because they happen when the mutation is still not expressed. Another possibility is that heterozygous mutations in mice may not be sufficient to recapitulate the human skin phenotype. Importantly, alteration of the p63 target genes in the conditional homozygous model is comparable to the constitutive heterozygous mutant in spite of nearly complete absence of the wild-type copy by P0, thus indicating that the L/L model is comparable to the constitutive one. In addition, the phenotype of the homozygous mice resembles at least some of the characteristic typical of AEC syndrome in humans.

Several studies including our own indicated that p63 is a crucial transcriptional regulator of genes involved in cell-matrix adhesion and cell-cell adhesion genes (Ferone et al., 2013; Mollo et al., 2014; Ferone, 2015, Richardson, Plos Genetics 2017). Skin erosions in AEC syndrome are likely to be caused by cell adhesion defects and reduced mechanical resistance. Here, we confirmed these hypotheses and further extended them by demonstrating that not only desmosomes are affected by AEC syndrome, but also this disorder leads to impairment in cell-matrix adhesion due to downregulation of several hemidesmosome and basal membrane components. In addition, reduced mechanical resistance is caused by downregulation of crucial basal and suprabasal keratins (namely Krt5 and Krt10),

the intermediate filaments required to withstand mechanical traumas in epidermis. This is an agreement with the similarity between skin blistering in AEC patients and EB patients, as several types of EB are caused by mutations in genes encoding for cell-cell adhesion, cell-matrix adhesion molecules and keratins.

The severe skin phenotype is associated to reduced body weight and survival, caused by dehydration as a consequence of skin erosions and/or focal epidermal barrier defect. Analyses of in situ dye permeability and of TEWL in newborn mouse skin at P3 clearly reveal that the development of the skin barrier and its patterning is totally defective in p63<sup>+L514F</sup> mice. This result suggests that the impaired skin barrier function of p63<sup>+L514F</sup> mice is due to defective development of the skin barrier at neonatal stage. During development, permeability barrier needs prior expression of loricrin, the major component of the CE. However, no delay or decrease in loricrin and in other late differentiation markers expression was evident in developing p63<sup>+L514F</sup> mouse skin. Sonication experiments showed that purified p63<sup>+L514F</sup> CEs were reduced to small fragments under conditions in which wild-type CEs remained largely intact. This suggests that the biomechanical properties of the stratum corneum are compromised, making it more susceptible to physical stress.

In stratified epithelia, such as in skin, multiprotein complexes called hemidesmosomes are involved in promoting the stable adhesion of basal epithelial cells to the underlying basement membrane. The attachment of cells to the extracellular matrix is of crucial importance in the maintenance of tissue structure and integrity. Their importance has become apparent in clinical conditions, in which defects in the hemidesmosomal proteins or other components mediating cell-to-matrix adhesion result in devastating blistering diseases of the skin. In the AEC mouse model, we find that the expression of the hemidesmosome proteins Col17a1, Dst, the integrin Itgb5, and the extracellular components Col7A1, Lamb3, Frem2, and Fras1 is disrupted, thus supporting the idea that epidermal blistering in AEC mouse model may be due to alteration in different structures that regulate adhesion processes. In support of this hypothesis, a transcriptomic profile of AEC patients skin showed defects in *FRAS1* and *COL7A1* expression (Clements et al., 2012). Type VII collagen is a major component of anchoring fibrils and mutations in this gene are associated with both the autosomal dominant and recessive forms of dystrophic epidermolysis bullosa (DEB) (Dang and Murrell, 2008).

The structural integrity of epidermal keratinocytes is maintained also by a filamentous network made up of keratins (Magin et al., 2000). The keratin intermediate filament cytoskeleton is essential for the maintenance of epithelial integrity by virtue of its unique biochemical and biophysical properties, its interaction with cell adhesion complexes (Herrmann and Aebi, 2004). The basal layer of the epidermis is characterized by heteropolymers of Krt5 and Krt14. It is well established that mechanically induced blistering disorders of the epidermis involve mutations in keratins and often the severity of these diseases seems to correlate with the degree to which the keratin mutants perturb IF assembly in vitro (Bonifas et al., 1991; Coulombe et al., 1991). Ultrastructural analysis demonstrated reduced keratin bundles in the basal layer of the epidermis, accompanied by reduced expression of several keratins, of which Krt5 and Krt15 are the most severely affected, in spite of a normal amount of Krt14. Importantly reduced Krt5 and Krt15 are observed also in human samples derived from AEC patients at the RNA and protein levels. These results reinforce the idea that in AEC syndrome the impairment of intermediate filaments network may be responsible for epidermal fragility and skin blistering. These results reinforce the idea that in AEC syndrome the impairment of intermediate filaments network may be responsible for epidermal fragility and skin blistering.

The severe skin phenotype observed in AEC mice is associated to reduced body weight and survival, caused by dehydration as a consequence of skin erosions and/or focal epidermal barrier defect. Analyses of in situ dye permeability and of TEWL in newborn mouse skin at P3 clearly revealed that the skin barrier and its patterning is partially defective in L/L mice. During development, permeability barrier needs prior expression of loricrin, the major component of the CE. However, no delay or decrease in loricrin and in other late differentiation markers expression was evident in developing p63+/L514F mouse skin. Sonication experiments showed that purified p63+/L514F CEs were reduced to small fragments under conditions in which wild-type CEs remained largely intact. This suggests that the biomechanical properties of the stratum corneum are compromised, making it more susceptible to physical stress.

Few days after the first biochemical sign of inflammation, AEC mutant epidermis becomes hyperplastic and hyperkeratotic with neutrophils accumulation in the epidermis, Krt6 induction and massive infiltration of macrophages and mast cells in

the dermis (Fig. 4). Blister healing often involves the induction of keratins related to Krt5 (Krt6a and Krt6b) suggesting a partial and selective compensation (Coulombe et al., 2009). Concomitant with Krt6, we observed significant induction of damage-associated molecular pattern molecules (DAMPs) that initiate the inflammatory response in the event of a disruption of the epidermal barrier, such as the inflammatory complex calprotectin (S100a8/ S100a9 complex). In addition, we observed a strong induction of thymic stromal lymphopoietin (Tslp), an interleukin 7-like cytokine produced by epidermal cells, that is markedly elevated in lesioned skin of atopic dermatitis and asthmatic patients (Ziegler and Artis, 2010). TSLP is produced by epithelial cells and causes a polarization of dendritic cells to drive T helper (Th) 2 cytokine production. TSLP also directly promotes T-cell proliferation in response to T-cell receptor activation and Th2 cytokine production, and supports B-cell expansion and differentiation. TSLP further amplifies Th2 cytokine production by mast cells and natural killer T cells.

To evaluate whether the absence of Tslp in AEC mice may lead to a reduction of inflammatory state, AEC mice were crossed with TSLP conditional null mice (Li et al., 2009). General health conditions of AEC Tslp<sup>eKO</sup> are mildly ameliorated with reduction of erosion and crusting, with significantly increasing survival, body weight and reducing water loss and skin inflammation. Taken together these data indicate that Tslp is likely to be a crucial mediator of skin and systemic inflammation in AEC syndrome.

Interestingly, Tslp is implicated in different disorders beyond allergic inflammation including atopic dermatitis (AD), a chronic inflammatory skin disease in which Tslp protein is highly expressed in acute and chronic lesions (Ziegler and Artis, 2010). In mice, overexpression of Tslp specifically in the skin was sufficient to induce a disease phenotype characterized by all the hallmark features of AD (Yoo et al., 2005). Tslp is also overexpressed in the skin of individuals with Netherton syndrome (NS), a severe skin disease characterized by AD-like lesions as well as other allergic manifestations that result from mutations in the serine peptidase inhibitor Kazal-type 5 (SPINK5) gene (Briot et al., 2008). SPINK5 regulates a biological cascade in which unregulated kallikrein (KLK) 5 directly activates PAR2 receptor and induces NF- $\kappa$ B-mediated overexpression of TSLP, tumor TNF $\alpha$ , and IL8.

Global gene expression profile of AEC mutant epidermis reveals an upregulation of Klk5, Klk6, Klk7 and Klk10, serin-protease named kallikreins that coordinate the desquamation mechanism, a process that lead to the shedding of the outer epidermis. The correct balance between these proteases and their inhibitors preserve epidermal homeostasis and provide an environmental barrier (Candi et al., 2005). In AEC mouse epidermis at P3 Klk6 mRNA (and to a lesser extent Klk10) is strongly upregulated as compared to controls. We demonstrated that p63 might directly regulate Klk6 since p63 depletion in keratinocytes leads to increase Klk6 expression. In agreement with Klk6 upregulation, protease activity is induced in AEC mouse skin as determined by in situ zymography.

In addition to NF- $\kappa$ B, other pathways may be responsible for Tslp induction downstream of mutant p63. Calcineurin/NFAT signaling has been recently implicated in Tslp expression downstream of the PAR2 receptor (Wilson et al., 2013). PAR2 activation by serine proteases leads to calcineurin-dependent nuclear translocation of the transcription factor NFAT. Furthermore, we observed that NFAT overexpression triggers Tslp induction in mouse keratinocytes, supporting the hypothesis that the KLK/PAR2/NFAT axis may be involved in aberrant overexpression of TSLP in AEC syndrome. To investigate the involvement of NF- $\kappa$ B and calcineurin/NFAT in the regulation of Tslp expression levels mediated by Klk6, we treated primary keratinocytes with an active form of human Klk6, in presence or in absence of specific NF- $\kappa$ B or/and calcineurin/NFAT inhibitors. The treatments showed that TSLP regulation in keratinocytes in which the cleavage of PAR2 receptor by KLK6 causes the activation and the cytoplasm to nucleus translocation of the transcription factor NFAT, which promotes the expression of TSLP and IL8 genes in conjunction with NF- $\kappa$ B pathway.

Our data shows that TSLP plays an important role in the progression of inflammatory response associated to AEC syndrome and suggest that treatments with pharmacological Tslp inhibitors or specific inhibitors of upstream pathways could be used to significantly improve the health conditions of AEC patients. Recently, TSLP neutralizing antibody (TSLP-Ab) were developed and used in the treatment of TDI-induced asthma obtaining a significantly reduction of inflammatory process of the airway (Yu et al., 2019).

Our laboratory has recently demonstrated that AEC syndrome is a protein aggregation disorder as AEC-associated p63 mutations lead to protein misfolding and aggregation, a defect observed in keratinocytes isolated from an AEC patient and from a novel conditional knock-in mouse model for the disorder (Russo et al., 2018). AEC mutant proteins exhibit impaired transcriptional activity, leading to dominant negative and gain-of-function effects due to coaggregation with wild-type p63 and with other protein partners. p63 variants that abolish aggregation of the mutant proteins are able to rescue p63's transcriptional function. Based on this knowledge, I tested three potential therapeutic approaches to treat AEC syndrome based on 1) preventing aggregation and/or enforcing the endogenous protein disaggregation machinery 2) treating with PRIMA-1-Met that has shown to be efficacious for p53 mutations 3) unbiased high-throughput screening of small molecules that may be able to restore the correct folding of the mutant protein or by genetic manipulations of specific chaperons.

The Protein Quality Control (PQC) system responds to protein aggregation by different mechanisms to target aggregating proteins and assist their disaggregation. These mechanisms often involve the HSP70 molecular chaperone, which is provided of a standalone disaggregase activity supported by specific co-chaperones (Kampinga et al., 2010; Nillegoda et al., 2017). The multifunctionality of HSP70 is often driven by DNAJ proteins co-chaperones, which deliver specific unfolded client proteins to HSP70 stimulating also its ATPase activity (Kampinga et al., 2010). In addition, a subclass of the DNAJB family, particularly DNAJB6a, DNAB6b and DNAJB8, can display also anti-aggregating HSP70-independent functions (Hageman et al., 2010). Interestingly, we found that AEC mutant L514F, and not wild type p63, is specifically degraded by DNAJB6a and DNAJB6b co-chaperones when co-overexpressed in H1299 cells. Importantly, both isoforms DNAJB6a and DNAJB6b act in the nucleus, where p63 aggregates accumulate. Other two members of DNAJB family, DNAJB2a and DNAJB2b, and a member of DNAJA family, DNAJA1, showed the same preferential effect on AEC mutant L514F.

Taken together, these data provide novel elements to design a targeted strategy aimed to prevent the aggregation of AEC-associated p63 mutant proteins, by selectively modulating the activity of AEC mutant interactors involved in the PQC system.

Alternatively, a chemical approach could be used to deal with protein aggregation. Previous published studies demonstrated that some small molecules may be able to assist the correct folding and rescue the function of mutant p53 in cancer (Bykov et al., 2016, Bykov et al., 2002, Zache et al., 2008; Lambert et al., 2009). One of these molecules is PRIMA-1-Met (or APR-246) that is converted to the Michael acceptor methylene quinuclidinone (MQ), which binds covalently to cysteines in p53. MQ modification of cysteine residues enhances p53 core domain thermostability, leading to refolding and restoration of its wild type function (Lambert et al., 2009, Zhang et al., 2018). MQ also targets oxidative stress by inhibiting thioredoxin reductase (TrxR1) and depleting glutathione (Bykov et al., 2016, Tessoulin Blood 2014, Ogiwara et al., 2019). Therefore, PRIMA-1-Met induces tumor cell death through both reactivation of mutant p53 and inhibition of cellular thiol-dependent redox systems inducing ROS dependent cell death (Tessoulin et al., 2019) PRIMA-1-Met is currently in clinical trials (phase I- III) for solid and hematological tumors.

Interestingly, corneal epithelial lineage commitment is partially restored by PRIMA-1-Met treatment in iPS derived from EEC patients (Shalom-Feuerstein et al., 2013). Similarly, PRIMA-1-Met partially rescues morphological features and gene expression of EEC-derived human keratinocytes (Shen et al., 2013). These positive effects on EEC mutant keratinocytes are independent on p63 aggregation since EEC mutations do not lead to aggregation in p63 (Russo et al., 2018). Consistently, the main p63 target genes are not rescued in EEC mutant keratinocytes, indicating that PRIMA-1-Met may be acting on epidermal differentiation rather than directly on p63. Based on these studies, in collaboration with Dr. Aberdam (INSERM, Paris, France) we tested the effects of PRIMA-1-Met on epidermal keratinocytes derived from an AEC patient carrying the p63 mutation T537P (Aberdam et al, 2020). We found that AEC keratinocytes displayed an impaired epidermal differentiation *in vitro* compared to normal keratinocytes and this impairment was morphologically rescued by the treatment with PRIMA-1-Met. However, this partial phenotypic rescue was not associated with disaggregation of the p63 mutant protein. Further investigation will be required to clarify the molecular mechanisms underlying PRIMA-1-MET effects on keratinocyte differentiation.

Therefore, in a broader search for compounds that may specifically reactivate p63, we are currently performing an HTS screening in collaboration with Dr.



Mandinova (MGH-Harvard, Boston, USA) to identify chemical compounds that may reduce accumulation of mutant protein, prevent aggregation, and/or reactivate p63 functions. After the initial screening of FDA-approved drugs, we isolated two compounds able to rescue p63L514F mutant transactivation ability, doxorubicin and epirubicin. These compounds are anticancer drugs with antimetabolic and cytotoxic activity that intercalate DNA leading to topoisomerase II inhibition thereby stopping DNA replication. Their action on DNA can also lead to inhibition of DNA helicase activity, and histone removal from transcriptionally active chromatin. Doxorubicin induces cellular toxicity via a mechanism that involves the synthesis of ceramide followed by activation of a transcription factor called CREB3L1, which drives the transcription of genes that inhibit cellular proliferation (Denard et al., 2012). Different strategies have been proposed to attenuate doxorubicin toxicity, including combined therapy with bioactive compounds, such as vitamins (A, C, E), minerals (selenium) and n-3 polyunsaturated fatty acids (Sung et al., 2007). Furthermore, doxorubicin is capable to interfere with function of a member of PQC system, Hsp60, promoting Hsp60/p53 complex dissociation, both causing an increase in the levels of free p53, which can then activate the p53-dependent pathway toward cell senescence (Marino Gammazza et al., 2016). A dose-dependent curve was performed to test the potency of each active compound. Doxorubicin and epirubicin will be tested for their toxicity and for the ability to rescue p63 activity and reduce p63 mutant aggregation in human and mouse keratinocytes.

In conclusion, an important goal of this study is to obtain novel insights into the mechanisms that can disentangle p63 aggregates. Targeting disaggregation activity could be by itself of therapeutic value. In addition, these two complementary approaches may lead to significant improvement of the understanding of this and other protein aggregation diseases.

## 6. REFERENCES

- Antonini D, Rossi B, Han R, Minichiello A, Di Palma T, Corrado M, Banfi S, Zannini M, Brissette JL, Missero C. 2006. An autoregulatory loop directs the tissue-specific expression of p63 through a long-range evolutionarily conserved enhancer. *Mol Cell Biol* 26:3308-3318.
- Antonini D, Russo MT, De Rosa L, Gorrese M, Del Vecchio L, Missero C. 2010. Transcriptional repression of miR-34 family contributes to p63-mediated cell cycle progression in epidermal cells. *J Invest Dermatol* 130:1249-1257.
- Astrakhan A, Omori M, Nguyen T, Becker-Herman S, Iseki M, Aye T, Hudkins K, Dooley J, Farr A, Alpers CE, Ziegler SF, Rawlings DJ (2007) Local increase in thymic stromal lymphopoietin induces systemic alterations in B cell development. *Nature immunology* 8: 522-531
- Barrow LL, van Bokhoven H, Daack-Hirsch S, Andersen T, van Beersum SE, Gorlin R, Murray JC. 2002. Analysis of the p63 gene in classical EEC syndrome, related syndromes, and non-syndromic orofacial clefts. *J Med Genet* 39:559-566.
- Bertola DR, Kim CA, Albano LM, Scheffer H, Meijer R, van Bokhoven H. 2004. Molecular evidence that AEC syndrome and Rapp-Hodgkin syndrome are variable expression of a single genetic disorder. *Clin Genet* 66:79-80.
- Bykov VJ, Issaeva N, Shilov A, Hultcrantz M, Pugacheva E, Chumakov P, Bergman J, Wiman KG, Selivanova G. 2002. Restoration of the tumor suppressor function to mutant p53 by a low-molecular-weight compound. *Nat Med* 8:282–288.
- Bykov VJ, Zhang Q, Zhang M, Ceder S, Abrahmsen L, Wiman KG. 2016. Targeting of Mutant p53 and the Cellular Redox Balance by APR-246 as a Strategy for Efficient Cancer Therapy. *Front. Oncol.* 6:21
- Candi E, Rufini A, Terrinoni A, Dinsdale D, Ranalli M, Paradisi A, De Laurenzi V, Spagnoli LG, Catani MV, Ramadan S, Knight RA, Melino G. 2006. Differential roles of p63 isoforms in epidermal development: selective genetic complementation in p63 null mice. *Cell Death Differ* 13:1037-1047.
- Candi E, Rufini A, Terrinoni A, Giamboi-Miraglia A, Lena AM, Mantovani R, Knight R, Melino G. 2007. DeltaNp63 regulates thymic development through enhanced expression of FgfR2 and Jag2. *Proc Natl Acad Sci U S A* 104:11999-12004.
- Candi E, Schmidt R, Melino G. 2005. The cornified envelope: a model of cell death in the skin. *Nat Rev Mol Cell Biol* 6:328-340.

- Carroll DK, Carroll JS, Leong CO, Cheng F, Brown M, Mills AA, Brugge JS, Ellisen LW. 2006. p63 regulates an adhesion programme and cell survival in epithelial cells. *Nat Cell Biol* 8:551-561.
- Celli J, Duijf P, Hamel BC, Bamshad M, Kramer B, Smits AP, Newbury-Ecob R, Hennekam RC, Van Buggenhout G, van Haeringen A, Woods CG, van Essen AJ, de Waal R, Vriend G, Haber DA, Yang A, McKeon F, Brunner HG, van Bokhoven H. 1999. Heterozygous germline mutations in the p53 homolog p63 are the cause of EEC syndrome. *Cell* 99:143-153.
- Chapiro E, Russell L, Lainey E, Kaltenbach S, Ragu C, Della-Valle V, Hanssens K, Macintyre EA, Radford-Weiss I, Delabesse E, Cave H, Mercher T, Harrison CJ, Nguyen-Khac F, Dubreuil P, Bernard OA (2010) Activating mutation in the TSLPR gene in B-cell precursor lymphoblastic leukemia. *Leukemia* 24: 642-645
- Chen Y, Mistry DS, Sen GL (2014) Highly rapid and efficient conversion of human fibroblasts to keratinocyte-like cells. *J Invest Dermatol* 134:335–344.
- Chi SW, Ayed A, Arrowsmith CH. 1999. Solution structure of a conserved C-terminal domain of p73 with structural homology to the SAM domain. *EMBO J* 18:4438-4445.
- Clements SE, Techanukul T, Lai-Cheong JE, Mee JB, South AP, Pourreyaon C, Burrows NP, Mellerio JE, McGrath JA (2012) Mutations in AEC syndrome skin reveal a role for p63 in basement membrane adhesion, skin barrier integrity and hair follicle biology. *The British journal of dermatology* 167: 134-144
- Coulombe PA, Hutton ME, Letai A, Hebert A, Paller AS, Fuchs E. 1991. Point mutations in human keratin 14 genes of epidermolysis bullosa simplex patients: genetic and functional analyses. *Cell* 66:1301-1311.
- De Moerlooze L, Spencer-Dene B, Revest JM, Hajihosseini M, Rosewell I, Dickson C. 2000. An important role for the IIIb isoform of fibroblast growth factor receptor 2 (FGFR2) in mesenchymal-epithelial signalling during mouse organogenesis. *Development* 127:483-492.
- Della Gatta G, Bansal M, Ambesi-Impiombato A, Antonini D, Missero C, di Bernardo D. 2008. Direct targets of the TRP63 transcription factor revealed by a combination of gene expression profiling and reverse engineering. *Genome Res* 18:939-948.
- Demehri S, Liu Z, Lee J, Lin MH, Crosby SD, Roberts CJ, Grigsby PW, Miner JH, Farr AG, Kopan R. 2008. Notch-deficient skin induces a lethal systemic B-lymphoproliferative disorder by secreting TSLP, a sentinel for epidermal integrity. *PLoS Biol* 6:e123.
- Demehri S, Morimoto M, Holtzman MJ, Kopan R. 2009. Skin-derived TSLP triggers progression from epidermal-barrier defects to asthma. *PLoS Biol* 7:e1000067.

- Denard B, Lee C, Ye J. 2012. Doxorubicin blocks proliferation of cancer cells through proteolytic activation of CREB3L1. *eLife* 1:e00090.
- Deutsch GB, Zielonka EM, Coutandin D, Weber TA, Schafer B, Hannewald J, Luh LM, Durst FG, Ibrahim M, Hoffmann J, Niesen FH, Senturk A, Kunkel H, Brutschy B, Schleiff E, Knapp S, Acker-Palmer A, Grez M, McKeon F, Dotsch V. 2011. DNA damage in oocytes induces a switch of the quality control factor TAp63alpha from dimer to tetramer. *Cell* 144:566-576.
- Dohn M, Zhang S, Chen X. 2001. p63alpha and DeltaNp63alpha can induce cell cycle arrest and apoptosis and differentially regulate p53 target genes. *Oncogene* 20:3193-3205.
- Duijf PH, Vanmolkot KR, Propping P, Friedl W, Krieger E, McKeon F, Dotsch V, Brunner HG, van Bokhoven H. 2002. Gain-of-function mutation in ADULT syndrome reveals the presence of a second transactivation domain in p63. *Hum Mol Genet* 11:799-804.
- Dumortier A, Durham AD, Di Piazza M, Vauclair S, Koch U, Ferrand G, Ferrero I, Demehri S, Song LL, Farr AG, Leonard WJ, Kopan R, Miele L, Hohl D, Finke D, Radtke F. 2010. Atopic dermatitis-like disease and associated lethal myeloproliferative disorder arise from loss of Notch signaling in the murine skin. *PLoS One* 5:e9258.
- Eissa A, Diamandis EP, Human tissue kallikreins as promiscuous modulators of homeostatic skin barrier functions, *Biol. Chem.* 389 (6) (2008) 669–680.
- Eissa A, Amodeo V, Smith CR, Diamandis EP, Kallikrein-related peptidase-8 (KLK8) is an active serine protease in human epidermis and sweat and is involved in a skin barrier proteolytic cascade, *J. Biol. Chem.* 286 (1) (2011) 687– 706.
- Ferone G, Mollo MR, Missero C. 2015. Epidermal cell junctions and their regulation by p63 in health and disease. *Cell Tissue Res.*
- Ferone G, Mollo MR, Thomason HA, Antonini D, Zhou H, Ambrosio R, De Rosa L, Salvatore D, Getsios S, van Bokhoven H, Dixon J, Missero C. 2013. p63 control of desmosome gene expression and adhesion is compromised in AEC syndrome. *Hum Mol Genet* 22:531-543.
- Ferone G, Thomason HA, Antonini D, De Rosa L, Hu B, Gemei M, Zhou H, Ambrosio R, Rice DP, Acampora D, van Bokhoven H, Del Vecchio L, Koster MI, Tadini G, Spencer-Dene B, Dixon M, Dixon J, Missero C. 2012. Mutant p63 causes defective expansion of ectodermal progenitor cells and impaired FGF signalling in AEC syndrome. *EMBO Mol Med* 4:192-205.

- Friend SL, Hosier S, Nelson A, Foxworthe D, Williams DE, Farr A (1994) A thymic stromal cell line supports in vitro development of surface IgM+ B cells and produces a novel growth factor affecting B and T lineage cells. *Experimental hematology* 22: 321-328
- Fuchs E, Green H. 1980. Changes in keratin gene expression during terminal differentiation of the keratinocyte. *Cell* 19:1033-1042.
- Furio L, Pampalakis G, Michael IP, Nagy A, Sotiropoulou G, Hovnanian A (2015) KLK5 Inactivation Reverses Cutaneous Hallmarks of Netherton Syndrome. *PLoS genetics* 11: e1005389.
- Marino Gammazza A, Campanella C, Barone R, Caruso Bavisotto C, Gorska M, Wozniak M, Carini F, Cappello F, D'Anneo A, Lauricella M, Zummo G, Conway de Macario E, Macario AJ, Di Felice V. 2016. Doxorubicin anti-tumor mechanisms include Hsp60 post-translational modifications leading to the Hsp60/p53 complex dissociation and instauration of replicative senescence. *Cancer Lett.* 28;385:75-86.
- Ghioni P, Bolognese F, Duijf PH, Van Bokhoven H, Mantovani R, Guerrini L. 2002. Complex transcriptional effects of p63 isoforms: identification of novel activation and repression domains. *Mol Cell Biol* 22:8659-8668.
- Hageman J and Kampinga HH. (2009) Computational analysis of the human HSPH/HSPA/DNAJ family and cloning of a human HSPH/HSPA/DNAJ expression library. *Cell Stress Chaperones* 14, 1–21
- Hageman J, Rujano MA, van Waarde MA, Kakkar V, Dirks RP, Govorukhina N, Oosterveld-Hut HM, Lubsen NH, Kampinga HH. (2010) A DNAJB chaperone subfamily with HDAC-dependent activities suppresses toxic protein aggregation. *Mol Cell.* 12;37(3):355-69.
- Hammad H, Lambrecht BN (2015) Barrier Epithelial Cells and the Control of Type 2 Immunity. *Immunity* 43: 29-40
- Hanai R and Mashima K. (2003) Characterization of two isoforms of a human DnaJ homologue, HSJ2. *Mol. Biol. Rep.* 30, 149–153.
- Harder J, Schroder JM (2005) Antimicrobial peptides in human skin. *Chemical immunology and allergy* 86: 22-41
- Hay RJ, Wells RS. 1976. The syndrome of ankyloblepharon, ectodermal defects and cleft lip and palate: an autosomal dominant condition. *Br J Dermatol* 94:277-289.
- Helton ES, Zhu J, Chen X. 2006. The unique NH2-terminally deleted (DeltaN) residues, the PXXP motif, and the PPXY motif are required for the transcriptional activity of the DeltaN variant of p63. *J Biol Chem* 281:2533-2542.
- Hipp MS, Park SH., and Hartl FU. (2014) Proteostasis impairment in protein-misfolding and -aggregation diseases. *Trends Cell Biol.* 24, 506–514.

- Houck SA, Singh S, Cyr DM. (2012) Cellular responses to misfolded proteins and protein aggregates. *Methods Mol. Biol.* 832:455–61
- Huelsken J, Vogel R, Erdmann B, Cotsarelis G, Birchmeier W. 2001. beta-Catenin controls hair follicle morphogenesis and stem cell differentiation in the skin. *Cell* 105:533-545.
- Hutton E, Paladini RD, Yu QC, Yen M, Coulombe PA, Fuchs E. 1998. Functional differences between keratins of stratified and simple epithelia. *J Cell Biol* 143:487-499.
- Ikoma A, Steinhoff M, Stander S, Yosipovitch G, Schmelz M (2006) The neurobiology of itch. *Nature reviews Neuroscience* 7: 535-547
- Iseki M, Omori-Miyake M, Xu W, Sun X, Takaki S, Rawlings DJ, Ziegler SF (2012) Thymic stromal lymphopoietin (TSLP)-induced polyclonal B-cell activation and autoimmunity are mediated by CD4+ T cells and IL-4. *International immunology* 24: 183-195
- Ishida-Yamamoto A, Simon M, Kishibe M, Miyauchi Y, Takahashi H, Yoshida S, O'Brien TJ, Serre G, Iizuka H, Epidermal lamellar granules transport different cargoes as distinct aggregates, *J. Invest. Dermatol.* 122 (5) (2004) 1137–1144.
- Jeng W, Lee S, Sung N, Lee J, Tsai FT. (2015) Molecular chaperones: guardians of the proteome in normal and disease states. *F1000Research* 4:1448
- Julapalli MR, Scher RK, Sybert VP, Siegfried EC, Bree AF. 2009. Dermatologic findings of ankyloblepharon-ectodermal defects-cleft lip/palate (AEC) syndrome. *Am J Med Genet A* 149A:1900-1906.
- Kampinga HH, Craig EA. (2010) The HSP70 chaperone machinery: J proteins as drivers of functional specificity. *Nat Rev Mol Cell Biol.* Aug;11(8):579-92.
- Kantaputra PN, Hamada T, Kumchai T, McGrath JA. 2003. Heterozygous mutation in the SAM domain of p63 underlies Rapp-Hodgkin ectodermal dysplasia. *J Dent Res* 82:433-437.
- Kashyap M, Rochman Y, Spolski R, Samsel L, Leonard WJ (2011) Thymic stromal lymphopoietin is produced by dendritic cells. *Journal of immunology* 187: 1207-1211
- Kerr JB, Hutt KJ, Michalak EM, Cook M, Vandenberg CJ, Liew SH, Bouillet P, Mills A, Scott CL, Findlay JK, Strasser A. 2012. DNA damage-induced primordial follicle oocyte apoptosis and loss of fertility require TAp63-mediated induction of Puma and Noxa. *Mol Cell* 48:343-352.
- Kim S, Choi IF, Quante JR, Zhang L, Roop DR, Koster MI. 2009. p63 directly induces expression of Alox12, a regulator of epidermal barrier formation. *Exp Dermatol* 18:1016-1021.

- Komatsu N, Takata M, Otsuki N, Toyama T, Ohka R, Takehara K, Saijoh K, Expression and localization of tissue kallikrein mRNAs in human epidermis and appendages, *J. Invest. Dermatol.* 121 (3) (2003) 542–549.
- Kopan R. 2012. Notch signaling. *Cold Spring Harb Perspect Biol* 4.
- Koster MI, Dai D, Marinari B, Sano Y, Costanzo A, Karin M, Roop DR. 2007. p63 induces key target genes required for epidermal morphogenesis. *Proc Natl Acad Sci U S A* 104:3255-3260.
- Koster MI, Dinella J, Chen J, O'Shea C, Koch PJ. 2014. Integrating animal models and in vitro tissue models to elucidate the role of desmosomal proteins in diseases. *Cell Commun Adhes* 21:55-63.
- Koster MI, Roop DR. 2004. The role of p63 in development and differentiation of the epidermis. *J Dermatol Sci* 34:3-9.
- Koster MI, Roop DR. 2007. Mechanisms regulating epithelial stratification. *Annu Rev Cell Dev Biol* 23:93-113.
- Kouwenhoven EN, van Heeringen SJ, Tena JJ, Oti M, Dutilh BE, Alonso ME, de la Calle-Mustienes E, Smeenk L, Rinne T, Parsaulian L, Bolat E, Jurgelenaite R, Huynen MA, Hoischen A, Veltman JA, Brunner HG, Roscioli T, Oates E, Wilson M, Manzanares M, Gomez-Skarmeta JL, Stunnenberg HG, Lohrum M, van Bokhoven H, Zhou H. 2010. Genome-wide profiling of p63 DNA-binding sites identifies an element that regulates gene expression during limb development in the 7q21 SHFM1 locus. *PLoS Genet* 6:e1001065.
- Lambert JM, Gorzov P, Veprintsev DB, Söderqvist M, Segerbäck D, Bergman J, Fersht AR, Hainaut P, Wiman KG, Bykov VJ. 2009. PRIMA-1 reactivates mutant p53 by covalent binding to the core domain. *Cancer Cell* 5;15(5):376-88
- Laufen T, Mayer MP, Beisel C, Klostermeier D, Mogk A, Reinstein J, Bukau B. (1999) Mechanism of regulation of Hsp70 chaperones by DnaJ cochaperones. *Proc. Natl Acad. Sci. USA* 96, 5452–5457
- Laurikkala J, Mikkola ML, James M, Tummers M, Mills AA, Thesleff I. 2006. p63 regulates multiple signalling pathways required for ectodermal organogenesis and differentiation. *Development* 133:1553-1563.
- Leoyklang P, Siriwan P, Shotelersuk V. 2006. A mutation of the p63 gene in non-syndromic cleft lip. *J Med Genet* 43:e28.
- Levin SD, Koelling RM, Friend SL, Isaksen DE, Ziegler SF, Perlmutter RM, Farr AG (1999) Thymic stromal lymphopoietin: a cytokine that promotes the development of IgM+ B cells in vitro and signals via a novel mechanism. *Journal of immunology* 162: 677-683

- Liu YJ, Soumelis V, Watanabe N, Ito T, Wang YH, Malefyt Rde W, Omori M, Zhou B, Ziegler SF (2007) TSLP: an epithelial cell cytokine that regulates T cell differentiation by conditioning dendritic cell maturation. *Annual review of immunology* 25: 193-219
- Lundwall A, Brattsand M, Kallikrein-related peptidases, *Cell. Mol. Life Sci.* 65 (13) (2008) 2019–2038.).
- Magin TM, Kaiser HW, Leitgeb S, Grund C, Leigh IM, Morley SM, Lane EB. 2000. Supplementation of a mutant keratin by stable expression of desmin in cultured human EBS keratinocytes. *J Cell Sci* 113 Pt 23:4231-4239.
- Mayer MP, and Bukau B. (2005) Hsp70 chaperones: cellular functions and molecular mechanism. *Cell. Mol. Life Sci.* 62, 670–684.
- McCarty JS, Buchberger A, Reinstein J and Bukau B. (1995) The role of ATP in the functional cycle of the DnaK chaperone system. *J. Mol. Biol.* 249, 126–137
- McDade SS, Henry AE, Pivato GP, Kozarewa I, Mitsopoulos C, Fenwick K, Assiotis I, Hakas J, Zvelebil M, Orr N, Lord CJ, Patel D, Ashworth A, McCance DJ. 2012. Genome-wide analysis of p63 binding sites identifies AP-2 factors as co-regulators of epidermal differentiation. *Nucleic Acids Res* 40:7190-7206.
- McGrath JA, Duijf PH, Doetsch V, Irvine AD, de Waal R, Vanmolkot KR, Wessagowitz V, Kelly A, Atherton DJ, Griffiths WA, Orlow SJ, van Haeringen A, Ausems MG, Yang A, McKeon F, Bamshad MA, Brunner HG, Hamel BC, van Bokhoven H. 2001. Hay-Wells syndrome is caused by heterozygous missense mutations in the SAM domain of p63. *Hum Mol Genet* 10:221-229.
- McGregor L, Makela V, Darling SM, Vrontou S, Chalepakis G, Roberts C, Smart N, Rutland P, Prescott N, Hopkins J, Bentley E, Shaw A, Roberts E, Mueller R, Jadeja S, Philip N, Nelson J, Francannet C, Perez-Aytes A, Megarbane A, Kerr B, Wainwright B, Woolf AS, Winter RM, Scambler PJ. 2003. Fraser syndrome and mouse blebbed phenotype caused by mutations in FRAS1/Fras1 encoding a putative extracellular matrix protein. *Nat Genet* 34:203-208.
- Mills AA, Zheng B, Wang XJ, Vogel H, Roop DR, Bradley A. 1999. p63 is a p53 homologue required for limb and epidermal morphogenesis. *Nature* 398:708-713.
- Mogk A, Bukau B, Kampinga HH. (2018) Cellular Handling of Protein Aggregates by Disaggregation Machines. *Mol Cell.* Jan 18;69(2):214-226.
- Mollo MR, Antonini D, Mitchell K, Fortugno P, Costanzo A, Dixon J, Brancati F, Missero C. 2014. p63-dependent and independent mechanisms of nectin-1 and -4 regulation in the epidermis. *Exp Dermatol.*



- Moon PD, Choi IH, Kim HM (2011) Naringenin suppresses the production of thymic stromal lymphopoietin through the blockade of RIP2 and caspase-1 signal cascade in mast cells. *European journal of pharmacology* 671: 128-132
- Moretti F, Marinari B, Lo Iacono N, Botti E, Giunta A, Spallone G, Garaffo G, Vernersson-Lindahl E, Merlo G, Mills AA, Ballaro C, Alema S, Chimenti S, Guerrini L, Costanzo A. 2010. A regulatory feedback loop involving p63 and IRF6 links the pathogenesis of 2 genetically different human ectodermal dysplasias. *J Clin Invest* 120:1570-1577.
- Moriyama M, Durham AD, Moriyama H, Hasegawa K, Nishikawa S, Radtke F, Osawa M. 2008. Multiple roles of Notch signaling in the regulation of epidermal development. *Dev Cell* 14:594-604.
- Murthy A, Shao YW, Narala SR, Molyneux SD, Zuniga-Pflucker JC, Khokha R. 2012. Notch activation by the metalloproteinase ADAM17 regulates myeloproliferation and atopic barrier immunity by suppressing epithelial cytokine synthesis. *Immunity* 36:105-119.
- Nguyen BC, Lefort K, Mandinova A, Antonini D, Devgan V, Della Gatta G, Koster MI, Zhang Z, Wang J, Tommasi di Vignano A, Kitajewski J, Chiorino G, Roop DR, Missero C, Dotto GP. 2006. Cross-regulation between Notch and p63 in keratinocyte commitment to differentiation. *Genes Dev* 20:1028-1042.
- Nicolas M, Wolfer A, Raj K, Kummer JA, Mill P, van Noort M, Hui CC, Clevers H, Dotto GP, Radtke F. 2003. Notch1 functions as a tumor suppressor in mouse skin. *Nat Genet* 33:416-421.
- Nillegoda NB, Stank A, Malinverni D, Alberts N, Szlachcic A, Barducci A, De Los Rios P, Wade RC and Bukau B. (2017) Evolution of an intricate J-protein network driving protein disaggregation in eukaryotes. *eLife* 6, <https://doi.org/10.7554/eLife.24560>.
- Ogiwara H, Takahashi K, Sasaki M, Kuroda T, Yoshida H, Watanabe R, Maruyama A, Makinoshima H, Chiwaki F, Sasaki H, Kato T, Okamoto A, Kohno T. 2019. Targeting the Vulnerability of Glutathione Metabolism in ARID1A-Deficient Cancers. *Cancer Cell*. 11;35(2):177-190.e8.
- Petiot A, Conti FJ, Grose R, Revest JM, Hodivala-Dilke KM, Dickson C. 2003. A crucial role for Fgfr2-IIIb signalling in epidermal development and hair follicle patterning. *Development* 130:5493-5501.
- Powers ET, Morimoto RI, Dillin A, Kelly JW, Balch WE. (2009) Biological and chemical approaches to diseases of proteostasis deficiency. *Annu Rev Biochem*. 2009;78:959-91.

- Prassas I, Eissa A, Poda G, Diamandis EP (2015) Unleashing the therapeutic potential of human kallikrein-related serine proteases. *Nature reviews Drug discovery* 14: 183-202
- Qiao F, Bowie JU. 2005. The many faces of SAM. *Sci STKE* 2005:re7.
- Reardon C, Lechmann M, Brustle A, Gareau MG, Shuman N, Philpott D, Ziegler SF, Mak TW (2011) Thymic stromal lymphopoietin-induced expression of the endogenous inhibitory enzyme SLPI mediates recovery from colonic inflammation. *Immunity* 35: 223-235
- Reche PA, Soumelis V, Gorman DM, Clifford T, Liu M, Travis M, Zurawski SM, Johnston J, Liu YJ, Spits H, de Waal Malefyt R, Kastelein RA, Bazan JF (2001) Human thymic stromal lymphopoietin preferentially stimulates myeloid cells. *Journal of immunology* 167: 336-343
- Rice R, Spencer-Dene B, Connor EC, Gritli-Linde A, McMahon AP, Dickson C, Thesleff I, Rice DP. 2004. Disruption of Fgf10/Fgfr2b-coordinated epithelial-mesenchymal interactions causes cleft palate. *J Clin Invest* 113:1692-1700.
- Rinne T, Bolat E, Meijer R, Scheffer H, van Bokhoven H. 2009. Spectrum of p63 mutations in a selected patient cohort affected with ankyloblepharon-ectodermal defects-cleft lip/palate syndrome (AEC). *Am J Med Genet A* 149A:1948-1951.
- Rinne T, Brunner HG, van Bokhoven H. 2007. p63-associated disorders. *Cell Cycle* 6:262-268.
- Rinne T, Clements SE, Lamme E, Duijf PH, Bolat E, Meijer R, Scheffer H, Rosser E, Tan TY, McGrath JA, Schalkwijk J, Brunner HG, Zhou H, van Bokhoven H. 2008. A novel translation re-initiation mechanism for the p63 gene revealed by amino-terminal truncating mutations in Rapp-Hodgkin/Hay-Wells-like syndromes. *Hum Mol Genet* 17:1968-1977.
- Roll JD, Reuther GW (2010) CRLF2 and JAK2 in B-progenitor acute lymphoblastic leukemia: a novel association in oncogenesis. *Cancer research* 70: 7347-7352
- Romano RA, Ortt K, Birkaya B, Smalley K, Sinha S. 2009. An active role of the DeltaN isoform of p63 in regulating basal keratin genes K5 and K14 and directing epidermal cell fate. *PLoS One* 4:e5623.
- Romano RA, Smalley K, Magraw C, Serna VA, Kurita T, Raghavan S, Sinha S. 2012. DeltaNp63 knockout mice reveal its indispensable role as a master regulator of epithelial development and differentiation. *Development* 139:772-782.
- Russo C, Osterburg C, Sirico A, Antonini D, Ambrosio R, Würz JM, Rinnenthal J, Ferniani M, Kehroesser S, Schäfer B, Güntert P, Sinha S, Dötsch V, Missero C. (2018)

- Protein aggregation of the p63 transcription factor underlies severe skin fragility in AEC syndrome. *Proc Natl Acad Sci USA* 115(5):E906-E915
- Senoo M, Pinto F, Crum CP, McKeon F. 2007. p63 Is essential for the proliferative potential of stem cells in stratified epithelia. *Cell* 129:523-536.
- Sevilla LM, Nachat R, Groot KR, Klement JF, Uitto J, Djian P, Maatta A, Watt FM. 2007. Mice deficient in involucrin, envoplakin, and periplakin have a defective epidermal barrier. *J Cell Biol* 179:1599-1612.
- Shen Q, Jin H, Wang X. 2013. Epidermal stem cells and their epigenetic regulation. *Int J Mol Sci* 14:17861-17880.
- Simpson CL, Patel DM, Green KJ. 2011. Deconstructing the skin: cytoarchitectural determinants of epidermal morphogenesis. *Nat Rev Mol Cell Biol* 12:565-580.
- Sims JE, Williams DE, Morrissey PJ, Garka K, Foxworthe D, Price V, Friend SL, Farr A, Bedell MA, Jenkins NA, Copeland NG, Grabstein K, Paxton RJ (2000) Molecular cloning and biological characterization of a novel murine lymphoid growth factor. *The Journal of experimental medicine* 192: 671-680
- Sinha S, Degenstein L, Copenhaver C, Fuchs E. 2000. Defining the regulatory factors required for epidermal gene expression. *Mol Cell Biol* 20:2543-2555.
- Sontag EM, Samant RS, Frydman J. (2017) Mechanisms and Functions of Spatial Protein Quality Control. *Annu Rev Biochem.* Jun 20;86:97-122.
- Soumelis V, Reche PA, Kanzler H, Yuan W, Edward G, Homey B, Gilliet M, Ho S, Antonenko S, Lauerma A, Smith K, Gorman D, Zurawski S, Abrams J, Menon S, McClanahan T, de Waal-Malefyt Rd R, Bazan F, Kastelein RA, Liu YJ (2002) Human epithelial cells trigger dendritic cell mediated allergic inflammation by producing TSLP. *Nature immunology* 3: 673-680
- Straub WE, Weber TA, Schafer B, Candi E, Durst F, Ou HD, Rajalingam K, Melino G, Dotsch V. 2010. The C-terminus of p63 contains multiple regulatory elements with different functions. *Cell Death Dis* 1:e5.
- Su X, Chakravarti D, Cho MS, Liu L, Gi YJ, Lin YL, Leung ML, El-Naggar A, Creighton CJ, Suraokar MB, Wistuba I, Flores ER. 2010. TAp63 suppresses metastasis through coordinate regulation of Dicer and miRNAs. *Nature* 467:986-990.
- Suh EK, Yang A, Kettenbach A, Bamberger C, Michaelis AH, Zhu Z, Elvin JA, Bronson RT, Crum CP, McKeon F. 2006. p63 protects the female germ line during meiotic arrest. *Nature* 444:624-628.
- Sung, L., Tomlinson, G.A., Greenberg, M.L., Koren, G., Judd, P., Ota, S., Feldman, B.M., 2007. Serial controlled N-of-1 trials of topical vitamin E as prophylaxis for chemotherapy-induced oral mucositis in paediatric patients. *Eur. J. Cancer* 43, 1269–1275.

- Szabo A, Langer T, Schröder H, Flanagan J, Bukau B and Hartl FU. (1994) The ATP hydrolysis-dependent reaction cycle of the Escherichia coli Hsp70 system DnaK, DnaJ, and GrpE. *Proc. Natl Acad. Sci. USA* 91,10345–10349
- Tachibana K, Nakanishi H, Mandai K, Ozaki K, Ikeda W, Yamamoto Y, Nagafuchi A, Tsukita S, Takai Y. 2000. Two cell adhesion molecules, nectin and cadherin, interact through their cytoplasmic domain-associated proteins. *J Cell Biol* 150:1161-1176.
- Tasian SK, Loh ML (2011) Understanding the biology of CRLF2-overexpressing acute lymphoblastic leukemia. *Critical reviews in oncogenesis* 16: 13-24.
- Tessoulin B, Descamps G, Dousset C, Amiot M, and Pellat-Deceunynck C. 2019. Targeting Oxidative Stress with Auranofin or Prima-1Met to Circumvent p53 or Bax/Bak Deficiency in Myeloma Cells. *Front Oncol* 9: 128.
- Thomason HA, Zhou H, Kouwenhoven EN, Dotto GP, Restivo G, Nguyen BC, Little H, Dixon MJ, van Bokhoven H, Dixon J. 2010. Cooperation between the transcription factors p63 and IRF6 is essential to prevent cleft palate in mice. *J Clin Invest* 120:1561-1569.
- Truong AB, Kretz M, Ridky TW, Kimmel R, Khavari PA. 2006. p63 regulates proliferation and differentiation of developmentally mature keratinocytes. *Genes Dev* 20:3185-3197.
- van Bokhoven H, Brunner HG. 2002. Splitting p63. *Am J Hum Genet* 71:1-13.
- van Bokhoven H, Hamel BC, Bamshad M, Sangiorgi E, Gurrieri F, Duijf PH, Vanmolkot KR, van Beusekom E, van Beersum SE, Celli J, Merckx GF, Tenconi R, Fryns JP, Verloes A, Newbury-Ecob RA, Raas-Rotschild A, Majewski F, Beemer FA, Janecke A, Chitayat D, Crisponi G, Kayserili H, Yates JR, Neri G, Brunner HG. 2001. p63 Gene mutations in eec syndrome, limb-mammary syndrome, and isolated split hand-split foot malformation suggest a genotype-phenotype correlation. *Am J Hum Genet* 69:481-492.
- Vauclair S, Nicolas M, Barrandon Y, Radtke F. 2005. Notch1 is essential for postnatal hair follicle development and homeostasis. *Dev Biol* 284:184-193.
- Vigano MA, Lamartine J, Testoni B, Merico D, Alotto D, Castagnoli C, Robert A, Candi E, Melino G, Gidrol X, Mantovani R. 2006. New p63 targets in keratinocytes identified by a genome-wide approach. *EMBO J* 25:5105-5116.
- Watanabe N, Hanabuchi S, Soumelis V, Yuan W, Ho S, de Waal Malefyt R, Liu YJ (2004) Human thymic stromal lymphopoietin promotes dendritic cell-mediated CD4+ T cell homeostatic expansion. *Nature immunology* 5: 426-434

- Williams MR, Nakatsuji T, Sanford JA, Vrbanac AF, Gallo RL, Staphylococcus aureus induces increased serine protease activity in keratinocytes, *J. Invest. Dermatol.* 137 (2) (2017) 377–384
- Yamamoto A and Simonsen A. (2011) The elimination of accumulated and aggregated proteins: a role for autophagy in neurodegeneration. *Neurobiol. Dis.* 43, 17–28.
- Yamamoto K, Sato T, Matsui T, Sato M, Okada T, Yoshida H, Harada A and Mori K. (2007) Transcriptional induction of mammalian ER quality control proteins is mediated by single or combined action of ATF6a and XBP1. *Dev. Cell* 13, 365–376.
- Yang A, Kaghad M, Caput D, McKeon F. 2002. On the shoulders of giants: p63, p73 and the rise of p53. *Trends Genet* 18:90-95.
- Yang A, Kaghad M, Wang Y, Gillett E, Fleming MD, Dotsch V, Andrews NC, Caput D, McKeon F. 1998. p63, a p53 homolog at 3q27-29, encodes multiple products with transactivating, death-inducing, and dominant-negative activities. *Mol Cell* 2:305-316.
- Yang A, Schweitzer R, Sun D, Kaghad M, Walker N, Bronson RT, Tabin C, Sharpe A, Caput D, Crum C, McKeon F. 1999. p63 is essential for regenerative proliferation in limb, craniofacial and epithelial development. *Nature* 398:714-718.
- Yang A, Walker N, Bronson R, Kaghad M, Oosterwegel M, Bonnin J, Vagner C, Bonnet H, Dikkes P, Sharpe A, McKeon F, Caput D. 2000. p73-deficient mice have neurological, pheromonal and inflammatory defects but lack spontaneous tumours. *Nature* 404:99-103.
- Yang A, Zhu Z, Kapranov P, McKeon F, Church GM, Gingeras TR, Struhl K. 2006. Relationships between p63 binding, DNA sequence, transcription activity, and biological function in human cells. *Mol Cell* 24:593-602.
- Yang XH, Mirchev R, Deng X, Yacono P, Yang HL, Golan DE, Hemler ME. 2012. CD151 restricts the alpha6 integrin diffusion mode. *J Cell Sci* 125:1478-1487.
- Yousef GM, Chang A, Scorilas A, Diamandis EP, Genomic organization of the human kallikrein gene family on chromosome 19q13.3-q13.4, *Biochem. Biophys. Res. Commun.* 276 (1) (2000) 125–133.
- Yu G, Zhang Y, Wang X, Sai L, Bo C, Yeo AJ, Lavin MF, Peng C, Jia Q, Shao H. Thymic stromal lymphopoietin (TSLP) and Toluene-diisocyanate-induced airway inflammation: Alleviation by TSLP neutralizing antibody. *Toxicology Letters.* 10.1016/j.toxlet.2019.09.021
- Zhang Q, Bykov VJN, Wiman KG, Zawacka-Pankau J. 2018. APR-246 reactivates mutant p53 by targeting cysteines 124 and 277. *Cell Death Dis.* 1;9(5):439.

Ziegler SF, Artis D. 2010. Sensing the outside world: TSLP regulates barrier immunity.  
Nat Immunol 11:289-293.